

# Dynamical Systems

Bernard Deconinck  
Department of Applied Mathematics  
University of Washington  
Campus Box 352420  
Seattle, WA, 98195, USA

June 4, 2009



## Prolegomenon

These are the lecture notes for Amath 575: Dynamical Systems. This is the first year these notes are typed up, thus it is guaranteed that these notes are full of mistakes of all kinds, both innocent and unforgivable. Please point out these mistakes to me so they may be corrected for the benefit of your successors. If you think that a different phrasing of something would result in better understanding, please let me know.

These lecture notes are not meant to supplant the textbook used with this course. The main textbook is Steven Wiggins' "Introduction to Applied Nonlinear Dynamical Systems and Chaos" (2nd edition, 2003) (Springer Texts in Applied Mathematics 2).

These notes are not copywrited by the author and any distribution of them is highly encouraged, especially without express written consent of the author.



# Contents

<b>1</b>	<b>Resources</b>	<b>1</b>
1.1	Internet . . . . .	1
1.2	Software . . . . .	1
1.3	Books . . . . .	1
1.4	Other . . . . .	2
<b>2</b>	<b>Introduction</b>	<b>3</b>
2.1	Continuous time systems: flows . . . . .	3
2.2	Discrete time systems: maps . . . . .	4
2.3	So, what's the theory of dynamical systems all about? . . . . .	6
<b>3</b>	<b>Equilibrium solutions</b>	<b>9</b>
3.1	Equilibrium solutions of flows . . . . .	9
3.2	Equilibrium solutions of maps . . . . .	10
3.3	The stability of trajectories. Stability definitions . . . . .	12
3.4	Investigating stability: linearization . . . . .	13
3.5	Stability of equilibrium solutions . . . . .	15
<b>4</b>	<b>Invariant manifolds</b>	<b>17</b>
4.1	Linear, autonomous vector fields . . . . .	17
4.2	Nonlinear, autonomous systems . . . . .	20
4.3	Transverse intersections . . . . .	27
4.4	The Center manifold reduction . . . . .	27
4.5	Center manifolds with parameters . . . . .	31
<b>5</b>	<b>Periodic solutions</b>	<b>35</b>
5.1	Bendixson' theorem . . . . .	35
5.2	Vector fields possessing an integral . . . . .	36
<b>6</b>	<b>Properties of flows and maps</b>	<b>39</b>
6.1	General properties of autonomous vector fields . . . . .	39
6.2	Liouville's theorem . . . . .	40
6.3	The Poincaré recurrence theorem . . . . .	42

6.4	The Poincaré-Bendixson theorem . . . . .	43
<b>7</b>	<b>Poincaré maps</b>	<b>49</b>
7.1	Poincaré maps near periodic orbits . . . . .	49
7.2	Poincaré maps of a time-periodic problem . . . . .	52
7.3	Example: the periodically forced oscillator . . . . .	53
1.	The damped forced oscillator . . . . .	54
2.	The undamped forced oscillator . . . . .	55
<b>8</b>	<b>Hamiltonian systems</b>	<b>63</b>
8.1	Definition and basic properties . . . . .	63
8.2	Symplectic or canonical transformations . . . . .	67
8.3	Completely integrable Hamiltonian systems . . . . .	72
<b>9</b>	<b>Symbolic dynamics</b>	<b>75</b>
9.1	The Bernoulli shift map . . . . .	75
9.2	Smale's horseshoe . . . . .	77
9.3	More complicated horseshoes . . . . .	84
9.4	Horseshoes in dynamical systems . . . . .	85
9.5	Example: the Hénon map . . . . .	86
<b>10</b>	<b>Indicators of chaos</b>	<b>91</b>
10.1	Lyapunov exponents for one-dimensional maps . . . . .	91
10.2	Lyapunov exponents for higher-dimensional maps . . . . .	92
10.3	Fractal dimension . . . . .	94
<b>11</b>	<b>Normal forms</b>	<b>99</b>
11.1	Preparation steps . . . . .	99
11.2	Quadratic terms . . . . .	100
11.3	Example: the Takens-Bogdanov normal form . . . . .	103
11.4	Cubic terms . . . . .	104
11.5	The Normal Form Theorem . . . . .	105
<b>12</b>	<b>Bifurcations in vector fields</b>	<b>107</b>
12.1	Preliminaries . . . . .	107
12.2	The saddle-node bifurcation . . . . .	110
12.3	The transcritical bifurcation . . . . .	114
12.4	The pitchfork bifurcation . . . . .	116
12.5	The Hopf bifurcation . . . . .	118
1.	Preparation steps and complexification . . . . .	119
2.	Second-order terms . . . . .	120
3.	Third-order terms . . . . .	121
4.	General discussion of the normal form . . . . .	122
5.	Discussion of the Hopf bifurcation . . . . .	123

<b>13 Bifurcations in maps</b>	<b>129</b>
13.1 The period-doubling bifurcation . . . . .	129
13.2 The logistic map . . . . .	132
1. Fixed points . . . . .	132
2. Period-two orbits . . . . .	134
3. Beyond period-two orbits: superstable orbits . . . . .	136
13.3 Renormalization theory: an introduction . . . . .	139



# Chapter 1

## Useful resource materials

### 1.1 Internet

- **pplane:** A useful java tool for drawing phase portraits of two-dimensional systems. See <http://math.rice.edu/~dfield/dfpp.html>.
- **Caltech's Chaos course:** an entire on-line course with many cool applets and demonstrations. The link here is to a box-counting dimension applet. See [http://www.cmp.caltech.edu/~mcc/Chaos\\_Course/](http://www.cmp.caltech.edu/~mcc/Chaos_Course/).

### 1.2 Software

- **Dynamics Solver.** A software package for the simulation of dynamical systems. Tons of features. Not always intuitive, but pretty easy to start with. See <http://tp.lc.ehu.es/jma/ds/ds.html>. Freeware.
- **Phaser.** A software package for the simulation of dynamical systems. Looks great, but non-intuitive steep learning curve. See <http://www.phaser.com/>. A single license if \$90.

### 1.3 Books

- **Nonlinear Dynamics and Chaos**, by Steven H. Strogatz, Perseus Books Group, 2001. This book provides a very readable introduction to dynamical systems, with lots of applications from a large variety of areas sprinkled throughout.
- **Dynamics, the Geometry of Behavior** by Ralph H. Abraham and Christopher D. Shaw. See <http://www.aerialpress.com/aerial/DYN/>. There's some history here: this book is commonly referred to as the picture book of dynamical systems. Ralph Abraham is one of the masters of the subject. His exposition together with the

drawings of Chris Shaw makes a lot of sometimes difficult concepts very approachable and intuitive. A true classic. Unfortunately, the printed edition is unavailable. An ebook edition is available from the website listed.

- **Nonlinear Oscillations, Dynamical Systems, and Bifurcations of Vector Fields** (Applied Mathematical Sciences Vol. 42) by John Guckenheimer and Philip Holmes, Springer, 1983. In many ways a precursor to our current textbook. A great reference text.

## 1.4 Other

# Chapter 2

## Introduction and terminology about flows and maps

In this course, we will study two types of systems. Some of the systems will depend on a continuous time variable  $t \in \mathbb{R}$ , while others will depend on a discrete time variable  $n \in \mathbb{Z}$ . As much as possible our techniques will be developed for both types of systems, but occasionally we will encounter methods that only apply to one of these two descriptions.

### 2.1 Continuous time systems: flows

Consider the first-order differential system

$$x' = f(x, t), \tag{2.1}$$

where  $x \in \mathbb{R}^N$ , and  $f : D \times I \rightarrow \mathbb{R}^N$  is a real-valued vector function from some subset  $D$  of  $\mathbb{R}^N$  and some real time interval  $I$ . Here  $t$  is the independent variable,  $x$  is the vector of dependent variables, and the prime denotes differentiation with respect to time. Equation (2.1) is the most general form of a nonautonomous continuous-time system. If the vector function  $f$  does not explicitly depend on  $t$ , then the system is called autonomous.

The main result from the standard theory of differential equations about such systems is the Cauchy theorem on the existence and uniqueness of solutions satisfying the initial condition

$$x(t_0) = x_0, \quad t_0 \in I, \quad x_0 \in D. \tag{2.2}$$

**Theorem 1 (Cauchy)** *Let  $f(x, t) \in C^r(D \times I)$ . Then there exists a unique solution  $\phi(t_0, x_0, t)$  of the initial-value problem*

$$\begin{cases} x' = f(x, t) \\ x(t_0) = x_0 \end{cases}, \tag{2.3}$$

for  $|t - t_0|$  sufficiently small. This solution is a  $C^r$  function of  $x_0$ ,  $t_0$  and  $t$ .

We refer to the solution  $\phi(t_0, x_0, t)$  of the system (2.1) as the flow of the system. Note that we have

$$\phi(t_0, x_0, t_0) = x_0 \quad (2.4)$$

and

$$\frac{\partial \phi}{\partial t} = f(\phi(t_0, x_0, t), t), \quad (2.5)$$

so that, indeed,  $x = \phi(t_0, x_0, t)$  is the unique solution of the initial-value problem (2.3).

An important distinction between autonomous and nonautonomous systems is that the evolution of the state  $x$  satisfying an autonomous system depends only on  $x$ , not on  $t$ . In other words, the evolution of  $x$  depends on where we are, but not on when we are there. If someone else were to come to the same state  $x$  at a later time, they would undergo the same evolution. In terms of direction fields, this implies that an autonomous differential system has a unique direction field, whereas the direction field of a nonautonomous system is different at any time  $t$ . Similarly, the phase space of an autonomous system has a unique tangent vector at every point, whereas a nonautonomous system may have different tangent vectors at any time  $t$ . There are some important consequences of this:

- If the system is autonomous, every point of the phase space has only a single solution curve going through it. This solution follows the unique tangent vector at the point.
- If the system is nonautonomous, there can be several solution curves through a given point in the phase space. The solutions are still tangent to the tangent vector at the point, but depending on when the given solution gets to the point, the tangent vector may change.

Figure 2.1 shows the direction field for an autonomous system. The direction field does not change from time to time. The direction field for a nonautonomous system looks similar (bunch of vectors of different size), but it will change through time.

## 2.2 Discrete time systems: maps

Consider the first-order difference system

$$x_{n+1} = F(x_n, n), \quad (2.6)$$

where  $x_n \in \mathbb{R}^N$ , and  $F : D \times I \rightarrow \mathbb{R}^N$  is a real-valued vector function from some subset  $D$  of  $\mathbb{R}^N$  and some real, discrete time interval  $I \subset \mathbb{Z}$ . Here  $n$  is the discrete independent variable,  $x_n$  is the vector of dependent variables. Equation (2.6) is the most general form of a nonautonomous discrete-time system. If the vector function  $F$  does not explicitly depend on  $n$ , the system is called autonomous.

Next we introduce some notation. We have

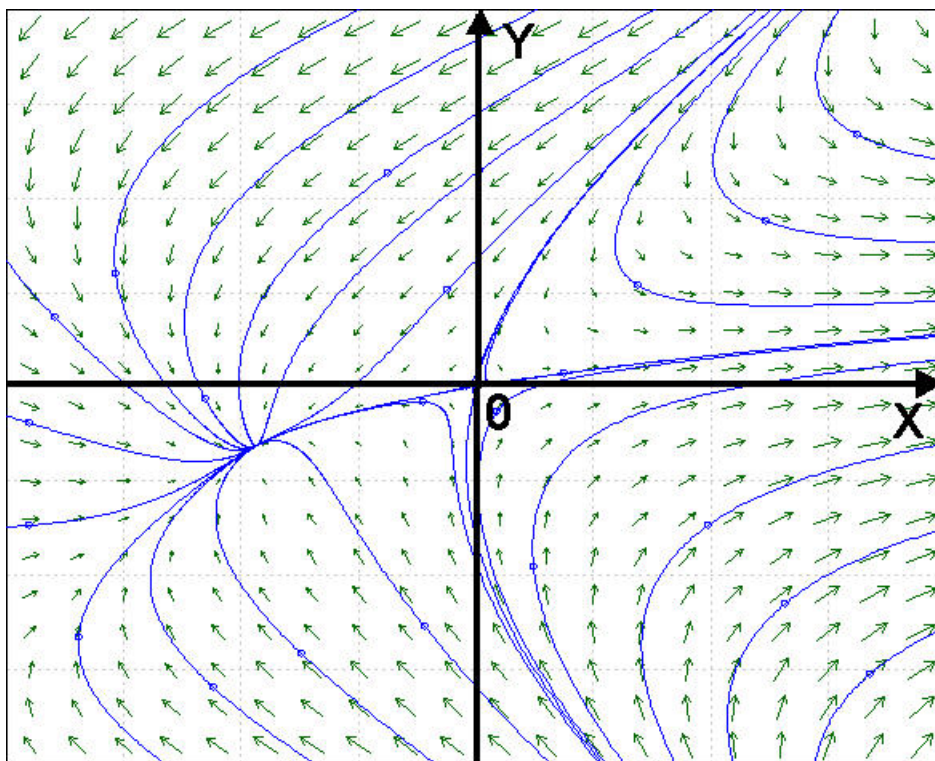


Figure 2.1: The direction field for the system  $x' = 2x - y + x^2 - y^2$ ,  $y' = x - 3y$ . Some solution curves are indicated as well. The figure was generated using `pplane`.

$$x_{n+2} = F(x_{n+1}) = F(F(x_n)), \quad (2.7)$$

$$x_{n+3} = F(x_{n+2}) = F(F(x_{n+1})) = F(F(F(x_n))), \quad (2.8)$$

etc.

To avoid writing such nested functions, we could write something like

$$x_{n+3} = F \circ F \circ F(x_n), \quad (2.9)$$

but even this is cumbersome. Further, it doesn't allow for a compact way to indicate how many iterations we are considering. Thus, we instead write (admittedly confusing)

$$x_{n+3} = F^3(x_n), \quad (2.10)$$

or, in general,

$$x_{n+k} = F^k(x_n), \quad (2.11)$$

where we define

$$F(F(x)) = F^2(x), \quad (2.12)$$

and so on.

**Example 1** Consider the logistic equation (it won't be the last time!)

$$x_{n+1} = \alpha x_n(1 - x_n), \quad (2.13)$$

where  $\alpha$  is a parameter. Then

$$\begin{aligned} F^2(x) &= F(F(x)) = F(\alpha x(1 - x)) \\ &= \alpha(\alpha x(1 - x))(1 - \alpha x(1 - x)), \end{aligned}$$

which is different (quite!) from

$$[F(x)]^2 = \alpha^2 x^2(1 - x)^2.$$

## 2.3 So, what's the theory of dynamical systems all about?

Let's first reiterate what the theory of differential equations is all about. Then we can see what the difference is. In the theory of differential equations, the object is to examine the behavior of individual solutions of differential equations as a function of the independent variable.

In contrast, the goal of the theory of dynamical systems is to understand the behavior of the whole ensemble of solutions of the given dynamical system, as a function of either initial conditions, or as a function of parameters arising in the system. Figure 2.2 illustrates this: let  $S$  be a "blob" (technical term) of initial conditions. As we turn on the dynamical variable ( $n$  or  $t$ ), this blob evolves and gets deformed. We wish to understand how it deforms. To this end, we need to consider an entire set of solutions, not just a single solution. It is also clear from the figure that geometrical techniques could be very useful for us, and indeed they are. The modern theory of dynamical systems uses a lot of geometry, especially differential geometry and topology. We will encounter this a little bit, but mostly we'll get by without.

It should be clear from the above that there is a lot of overlap between the theory of differential equations and the theory of dynamical systems. Just like the difference between pure and applied mathematics, the difference is mainly an issue of attitude: how does one approach the subject, and what questions does one ask.

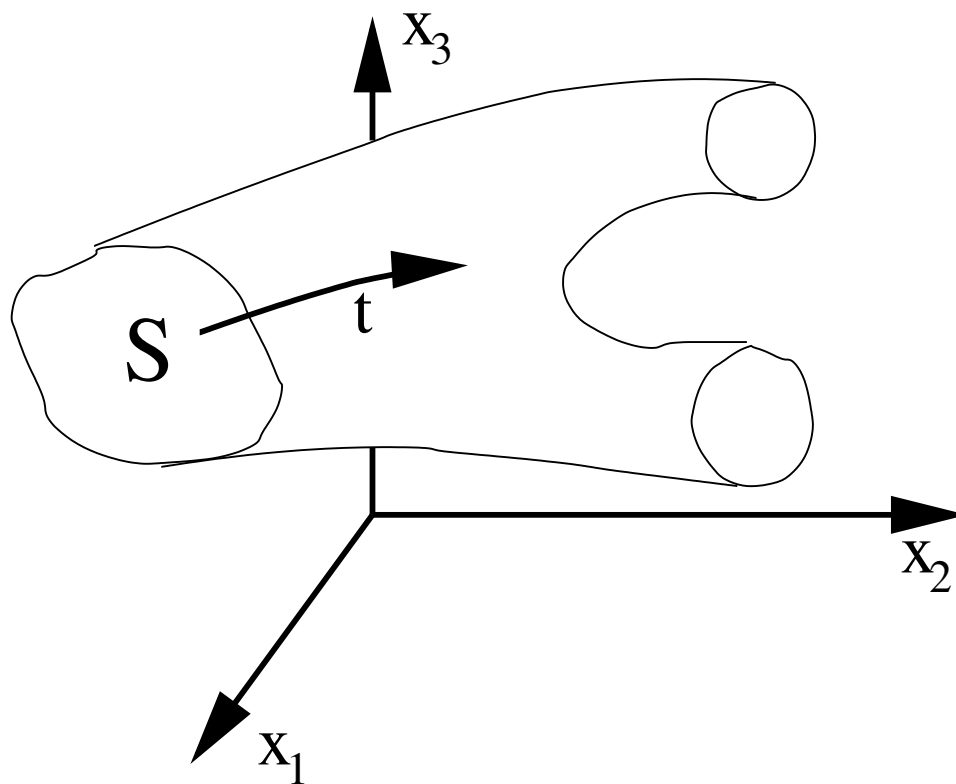


Figure 2.2: A cartoon of the evolution of a “blob” of initial conditions.



# Chapter 3

## Equilibrium solutions and their stability

In order to start to understand the phase space of a dynamical system, we start by considering the equilibrium solutions of such systems.

### 3.1 Equilibrium solutions of flows

Consider an autonomous system

$$x' = f(x). \tag{3.1}$$

An equilibrium solution  $\hat{x}$  of this system is a constant solution of this system of differential equations (why did we require that the system was autonomous?). By definition,  $\hat{x}' = 0$ , thus equilibrium solutions are determined by

$$f(\hat{x}) = 0. \tag{3.2}$$

This is an algebraic (as opposed to differential) system of equations. Unfortunately, it is typically nonlinear. Nevertheless, we usually prefer having to solve algebraic equations over differential equations. There are several reasons why equilibrium solutions receive the amount of attention they do:

- They are relatively easy to determine, as already stated above.
- They are singular points of the direction field of the system: at the singular point, no tangent vector is defined since  $\hat{x}' = 0$ . Thus, these solutions play a special role in the geometry of the phase space.
- As we'll discuss later, depending on their stability, they are candidates for the long-time asymptotics of nearby solutions.

For one-dimensional systems ( $N = 1$ ), the equilibrium solutions are easily read off. Equally easy to read off is the behavior of solutions near these equilibrium solutions. As we'll see in a little bit, this determines the stability of the equilibrium solutions. This is illustrated in Figure 3.1.

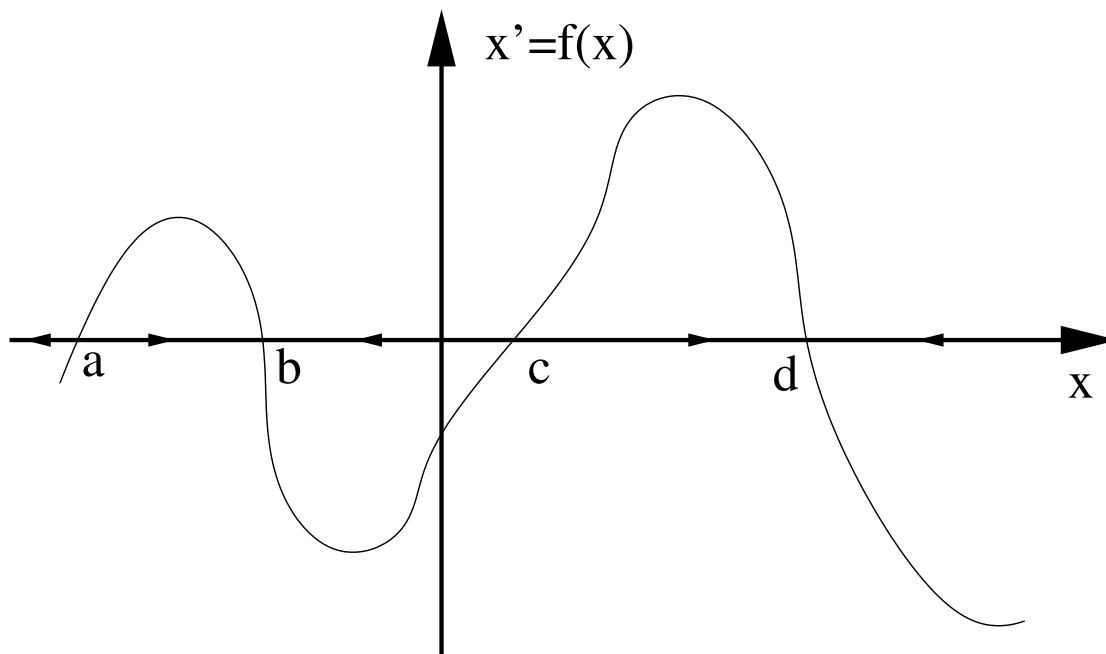


Figure 3.1: Equilibrium solutions for a one-dimensional flow. Here  $x_1 = a$ ,  $x_2 = b$ ,  $x_3 = c$  and  $x_4 = d$  are all equilibrium solutions. In this setting their stability is easily read off.

## 3.2 Equilibrium solutions of maps

Consider the difference system

$$x_{n+1} = F(x_n). \quad (3.3)$$

Also in this case can we define the notion of an equilibrium solution. As before, these are solutions that do not change under the dynamics. In the discrete setting this means

$$x_{n+1} = x_n \Leftrightarrow F(x_n) = x_n, \quad (3.4)$$

thus we have to solve the algebraic system of equations

$$\hat{x} = F(\hat{x}). \quad (3.5)$$

The solutions  $\hat{x}$  of these equations are the equilibrium solutions of (3.3). Just as for flows, the concept of equilibrium solutions does not make sense for nonautonomous maps (why?).

And, as for flows, there are several reasons why equilibrium solutions are important:

- They are relatively easy to determine, as already stated above.
- As we'll discuss later, depending on their stability, they are candidates for the long-time asymptotics of nearby solutions.

In the case of maps, it is less obvious to talk about the geometry of the phase space, as it would appear that we are losing the notion of continuity, since solutions consists of a countably discrete set of points. We'll see in a little bit how we salvage the continuity, to our advantage. At that point, the equilibrium solutions will have the same geometrical impact for maps that they do for flows.

For one-dimensional systems ( $N = 1$ ), the equilibrium solutions of maps are also easily read off. Not as easy to read off is the behavior of solutions near these equilibrium solutions. We'll discuss this in a little bit (perhaps in a homework problem ... Oh, the excitement!). This is illustrated in Figure 3.2.

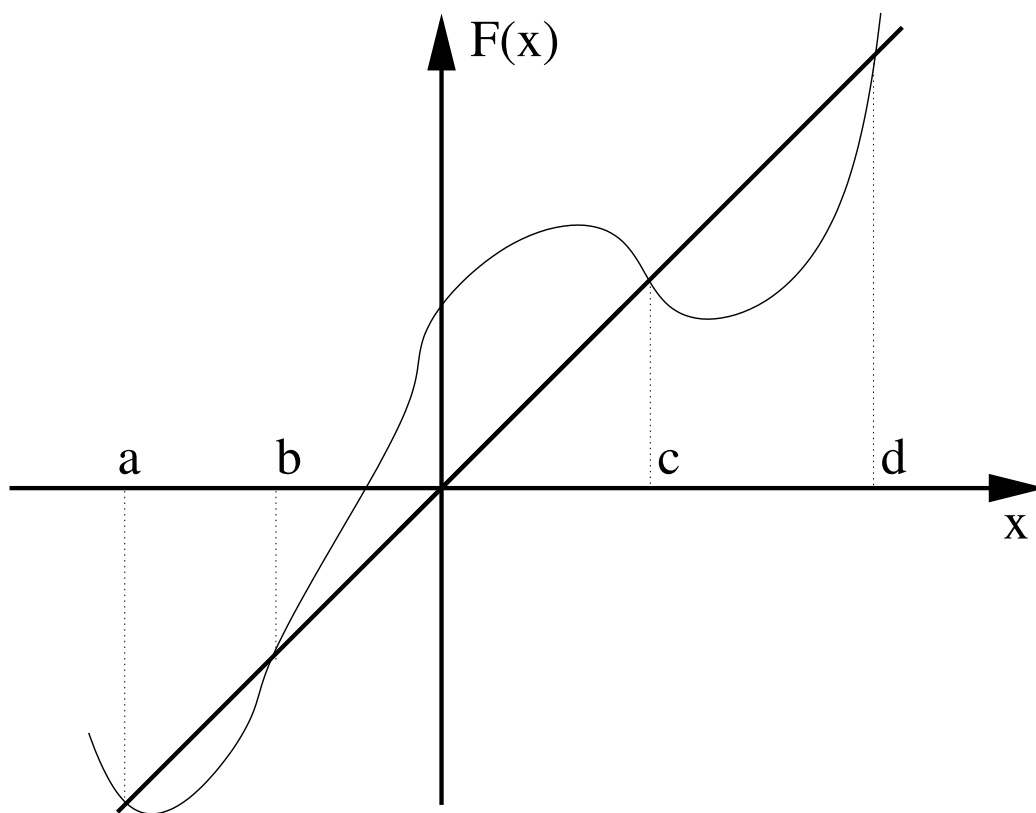


Figure 3.2: Equilibrium solutions for a one-dimensional map. Here  $x_1 = a$ ,  $x_2 = b$ ,  $x_3 = c$  and  $x_4 = d$  are all equilibrium solutions. Note that the indices here should not be confused with the index  $n$  in (3.3).

### 3.3 The stability of trajectories. Stability definitions

In Wiggins' book, you may find the definitions for this section for the case of flows. I'll give them for maps. You are expected to be familiar with both.

Consider the autonomous system

$$x_{n+1} = F(x_n), \quad x_n \in \mathbb{R}^n. \quad (3.6)$$

Let

$$\bar{x} = \{\bar{x}_0, \bar{x}_1, \dots, \bar{x}_k, \dots\} \quad (3.7)$$

be a solution of this system.

**Definition 1 (Lyapunov Stability)** *The solution  $\bar{x}$  is said to be stable in the sense of Lyapunov if  $\forall \epsilon > 0, \exists \delta(\epsilon) > 0 : |\bar{x}_{k_0} - y_{k_0}| < \delta \Rightarrow |\bar{x}_k - y_k| < \epsilon$  for  $k > k_0$ , and all solutions  $y$ .*

This definition is illustrated in Figure 3.3. Thus:

- Here's how the game is played: someone picks an  $\epsilon$ . We have to find a  $\delta$  (which will depend on  $\epsilon$ ) such that if we start within a distance of  $\delta$  of the given solution, we never wander more than  $\epsilon$  away. Clearly, the smaller  $\epsilon$  is chosen, the smaller we'll have to pick  $\delta$ , *etc.*
- According to this definition,  $y_k$  can wander, but not too far.

A stronger form of stability is *asymptotic stability*.

**Definition 2 (Asymptotic stability)** *The solution  $\bar{x}$  is said to be asymptotically stable if (i)  $\bar{x}$  is Lyapunov stable, and (ii)  $\exists \delta > 0 : |\bar{x}_{k_0} - y_{k_0}| < \delta \Rightarrow \lim_{n \rightarrow \infty} |\bar{x}_n - y_n| = 0$ .*

In other words, once the neighboring solution is close enough to the solution under investigation, it is trapped and it ultimately falls into our solution. It should be noted that the first condition is essential. It is not because all neighboring solutions approach the given solution that that solution is stable. An example of a phase portrait that satisfies the second condition but is not Lyapunov stable is given in Figure 3.4.

Sometimes, we're only worried about orbits approaching each other, without ever worrying about whether this happens in a synchronous sense. This is the concept of *orbital stability*. First we define the *forward orbit* of a solution.

**Definition 3 (Forward orbit)** *The forward orbit  $\theta^+(x^{(0)}, k_0)$  is the collection of all points on the trajectory of the solution through  $x^{(0)}$  that follow from  $x^{(0)}$ . In symbols:*

$$\begin{aligned} \theta^+(x^{(0)}, k_0) &= \{x \in \mathbb{R}^N \mid x = x_n, n \geq k_0, x_{k_0} = x^{(0)}\} \\ &= \{x^{(0)}, F(x^{(0)}), F^2(x^{(0)}), \dots\}. \end{aligned} \quad (3.8)$$

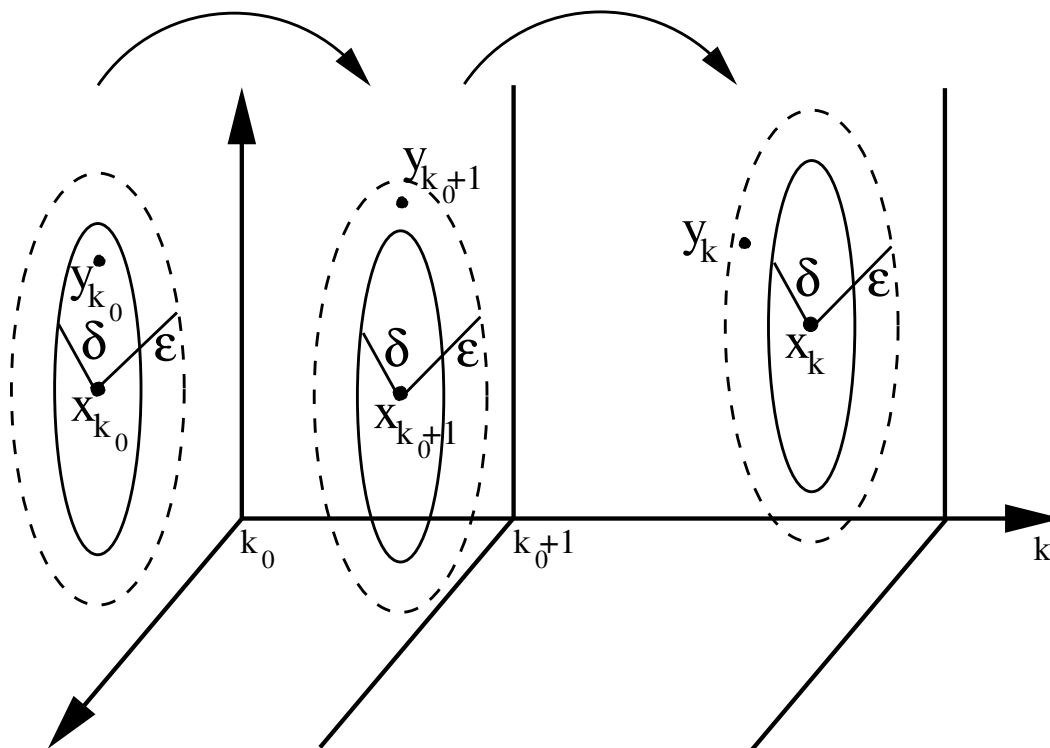


Figure 3.3: An illustration of Lyapunov's stability definition.

We use the forward orbit to define *orbital stability*:

**Definition 4 (Orbital stability)** *The solution  $\bar{x}$  is orbitally stable if  $\forall \epsilon > 0, \exists \delta(\epsilon) > 0 : |\bar{x}_{k_0} - y_{k_0}| < \delta \Rightarrow d(y_k, \theta^+(\bar{x}_{k_0}, k_0)) < \epsilon$  for  $k > k_0$ , and any solution  $y$ .*

Here we have used the concept of distance of a point to a set:  $d(x, S) = \inf_{s \in S} |x - s|$ . Thus, a solution is orbitally stable if the forward orbit of nearby solutions does not wander away from the forward orbit of the solution whose orbital stability we're investigating.

As before, there is the stronger concept of *asymptotic orbital stability*:

**Definition 5 (Asymptotic orbital stability)** *The solution  $\bar{x}$  is asymptotically orbitally stable if (i) it is orbitally stable, and (ii)  $\exists \delta > 0 : |\bar{x}_{k_0} - y_{k_0}| < \delta \Rightarrow \lim_{k \rightarrow \infty} d(y_k, \theta^+(\bar{x}_{k_0}, k_0)) = 0$ .*

### 3.4 Investigating stability: linearization

Let's look at some practical ways for establishing stability or instability. Let

$$x_n = \bar{x}_n + y_n, \tag{3.9}$$

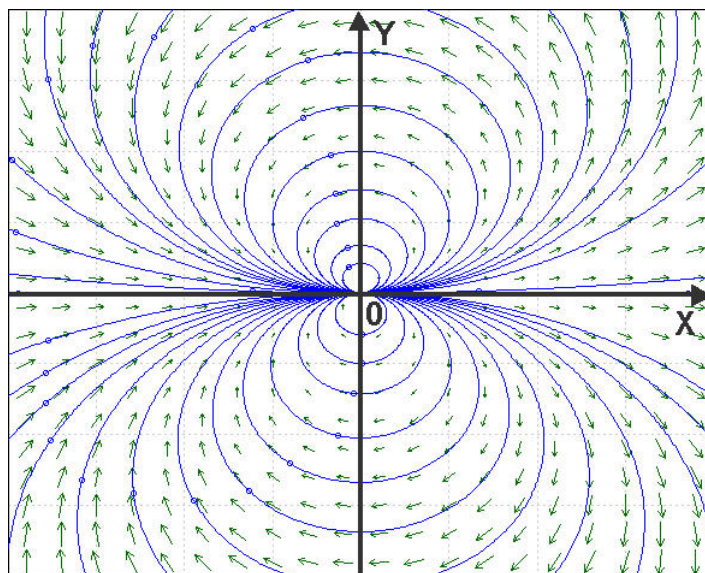


Figure 3.4: All solutions approaching the given solution does not imply stability. Here all trajectories ultimately approach the equilibrium solution, but not without wandering arbitrarily far away first. This is a phase portrait of the system  $x' = x^2 - y^2$ ,  $y' = 2xy$ . The plot was made using pplane.

where  $\bar{x}$  is the solution whose stability we want to examine. In essence, the above is nothing but a translation to examine what happens near  $\bar{x}$ . Thus, we may think of  $\bar{y}$  as small. Substitution in  $x_{n+1} = F(x_n)$  gives

$$\begin{aligned} \bar{x}_{n+1} + y_{n+1} &= F(\bar{x}_n + y_n) \\ &= F(\bar{x}_n) + DF(\bar{x}_n)y_n + \theta(|y_n|^2) \\ \Rightarrow y_{n+1} &= DF(\bar{x}_n)y_n + \theta(|y_n|^2). \end{aligned} \quad (3.10)$$

Here

$$DF(x_n) = \left( \frac{\partial F_j}{\partial x_k}(x_{k,n}) \right)_{j,k=1}^N, \quad (3.11)$$

the Jacobian of  $F(x)$ , evaluated at  $x = x_n$ . Here  $x_{k,n}$  denotes the  $k$ th component of the vector  $x_n$ . It might be reasonable to assume that the last term is significantly smaller than the previous term, so that it may suffice to consider

$$y_{n+1} = DF(\bar{x}_n)y_n. \quad (3.12)$$

This is the *linearization* of the dynamical system around the solution  $\bar{x} = (\bar{x}_0, \bar{x}_1, \dots)$ .

Usually, (3.12) is hard to solve. Admittedly, the problem is linear, which is easier than the original problem. On the other hand, it is usually nonautonomous, and no general methods

are known for its solution. Even if we could solve the linear problem, it remains to be seen what the effect of the neglected nonlinear terms will be.

### 3.5 Stability of equilibrium solutions

On the other hand, in the case where  $\bar{x}$  is an equilibrium solution, the problem (3.12) for  $y_n$  has constant coefficients, and it may be solved explicitly. With  $A = DF(\bar{x})$ , we have

$$y_{n+1} = Ay_n, \quad (3.13)$$

where  $A$  is a constant matrix. Let

$$y_n = \lambda^n v, \quad (3.14)$$

where  $\lambda$  is a constant, to be determined, and  $v$  is a constant vector, also to be determined. Substitution gives

$$Av = \lambda v. \quad (3.15)$$

Thus, the  $\lambda$ 's are the eigenvalues of  $A$ , while the  $v$ 's are their corresponding eigenvectors. Since the system is linear, the general solution may be obtained using superposition:

$$y_n = \sum_{k=1}^N \lambda_k^n v^{(k)}. \quad (3.16)$$

If the matrix  $A$  is not diagonalizable, some complications arise and we need to use generalized eigenvectors, but we've got the basic idea right.

Be that as it may, it is clear from the above that if all eigenvalues of  $A$  are inside the unit circle,  $|\lambda| < 1$ , then

$$\lim_{n \rightarrow \infty} y_n = 0. \quad (3.17)$$

In this case, the equilibrium solution  $\bar{x}$  is called *linearly asymptotically stable*. On the other hand, if there is even one  $\lambda$  for which  $|\lambda| > 1$ , then the corresponding fundamental solution grows exponentially, and the equilibrium solution  $\bar{x}$  is unstable. Indeed, one rotten apple spoils the bunch! If the largest eigenvalues (in modulus) are on the unit circle, then no conclusion about stability can be made and more information is required, as the higher-order terms are likely to have an influence.

**Definition 6 (Hyperbolic equilibrium point)** *An equilibrium point for which none of the eigenvalues of the linearization are on the unit circle is called hyperbolic.*

So, we can summarize our results as: **for a hyperbolic fixed point, the conclusions drawn from the linearization are accurate.** In the next chapter we'll start the investigation of what to do when no definite conclusions are possible from the linearization.



# Chapter 4

## Invariant manifolds

Let's start with a definition:

**Definition 7 (Invariant manifold)** *A manifold is invariant under a flow or map if solution trajectories starting from any point on the manifold are forever confined to the manifold, both when moving backward or forward in time.*

**Remarks:**

- For our purposes, we may think of a manifold as a surface embedded in  $\mathbb{R}^N$ , which is locally smooth.
- As stated, an invariant manifold only makes sense for invertible systems. For noninvertible systems, one can still consider positively (or forward) invariant sets.

### 4.1 Stable, unstable and center subspaces for linear, autonomous vector fields

Consider the linear autonomous system

$$y' = Ay, \tag{4.1}$$

where  $A$  is a constant  $N \times N$  matrix. We know that the behavior of solutions of this system is determined by the eigenvalues of  $A$ . Let's denote these by:

$$\Re\lambda < 0 \quad \lambda_1^{(S)}, \lambda_2^{(S)}, \dots, \lambda_s^{(S)}, \tag{4.2}$$

$$\Re\lambda > 0 \quad \lambda_1^{(U)}, \lambda_2^{(U)}, \dots, \lambda_u^{(U)}, \tag{4.3}$$

$$\Re\lambda = 0 \quad \lambda_1^{(C)}, \lambda_2^{(C)}, \dots, \lambda_c^{(C)}, \tag{4.4}$$

where, of course,  $s + u + c = N$ .

Corresponding to each eigenvalue there is a (possibly complex-valued) fundamental solution (or, alternatively, we may use the real and imaginary parts as fundamental solutions). The general solution is given by

$$\begin{aligned} y = & c_1^{(S)} y_1^{(S)}(t) + c_2^{(S)} y_2^{(S)}(t) + \dots + c_s^{(S)} y_s^{(S)}(t) + \\ & c_1^{(U)} y_1^{(U)}(t) + c_2^{(U)} y_2^{(U)}(t) + \dots + c_u^{(U)} y_u^{(U)}(t) + \\ & c_1^{(C)} y_1^{(C)}(t) + c_2^{(C)} y_2^{(C)}(t) + \dots + c_c^{(C)} y_c^{(C)}(t). \end{aligned} \quad (4.5)$$

The subspace of solutions

$$y^{(S)} = c_1^{(S)} y_1^{(S)}(t) + c_2^{(S)} y_2^{(S)}(t) + \dots + c_s^{(S)} y_s^{(S)}(t) \quad (4.6)$$

is the most general solution such that

$$\lim_{t \rightarrow \infty} y(t) = 0. \quad (4.7)$$

Here the 0 on the right-hand side is nothing but the equilibrium solution of the system we are considering. These fundamental solutions span a linear space in the phase space, referred to as the *stable subspace*  $E^S$ .

Similarly, the subspace of solutions

$$y^{(U)} = c_1^{(U)} y_1^{(U)}(t) + c_2^{(U)} y_2^{(U)}(t) + \dots + c_u^{(U)} y_u^{(U)}(t) \quad (4.8)$$

is the most general solution such that

$$\lim_{t \rightarrow -\infty} y(t) = 0. \quad (4.9)$$

These solutions also span a linear space (spanned by the respective eigenvectors), called the *unstable subspace*  $E^U$ .

Lastly, the *center subspace*  $E^C$  is spanned by the remaining fundamental solutions:

$$y^{(C)} = c_1^{(C)} y_1^{(C)}(t) + c_2^{(C)} y_2^{(C)}(t) + \dots + c_c^{(C)} y_c^{(C)}(t). \quad (4.10)$$

For these solutions, no definite limit statement as  $t \rightarrow \pm\infty$  can be made, without a more detailed investigation.

A similar classification is possible for maps, but with the role of the imaginary axis played by the unit circle. Let's look at an example instead.

**Example 2** Consider the two-dimensional map

$$\begin{cases} x_{n+1} = \lambda x_n + y_n \\ y_{n+1} = \mu y_n \end{cases}, \quad (4.11)$$

or, in matrix form:

$$\begin{pmatrix} x_{n+1} \\ y_{n+1} \end{pmatrix} = \begin{pmatrix} \lambda & 1 \\ 0 & \mu \end{pmatrix} \begin{pmatrix} x_n \\ y_n \end{pmatrix}. \quad (4.12)$$

The eigenvalues of this linear map are  $\lambda$  and  $\mu$ , with respective eigenvectors  $(1, 0)^T$  and  $(1, \mu - \lambda)^T$ , so that the general solution is

$$\begin{pmatrix} x_n \\ y_n \end{pmatrix} = c_1 \begin{pmatrix} 1 \\ 0 \end{pmatrix} \lambda^n + c_2 \begin{pmatrix} 1 \\ \mu - \lambda \end{pmatrix} \mu^n. \quad (4.13)$$

This is the form of the general solution for  $\lambda \neq \mu$ .

1. If  $|\lambda|, |\mu| > 1$ , then  $(0, 0)^T$  is an unstable node and

$$E^S = \emptyset, \quad E^U = \mathbb{R}^2, \quad E^C = \emptyset. \quad (4.14)$$

2. If  $|\lambda|, |\mu| < 1$ , then  $(0, 0)^T$  is a stable node and

$$E^S = \mathbb{R}^2, \quad E^U = \emptyset, \quad E^C = \emptyset. \quad (4.15)$$

3. If  $|\lambda| > 1, |\mu| < 1$ , then  $(0, 0)^T$  is a saddle (unstable), and

$$\begin{aligned} E^S &= \{(x, y) \in \mathbb{R}^2 : (\mu - \lambda)x = y\}, \\ E^U &= \{(x, y) \in \mathbb{R}^2 : y = 0\}, \\ E^C &= \emptyset. \end{aligned} \quad (4.16)$$

4. If  $|\lambda| = 1, |\mu| > 1$ , then  $(0, 0)^T$  is unstable, and

$$E^S = \emptyset, \quad E^C = \{(x, 0) \in \mathbb{R}^2\}, \quad E^U = \{(x, y) \in \mathbb{R}^2 : y = (\mu - \lambda)x\}. \quad (4.17)$$

Note that in this case,  $(0, 0)^T$  is not necessarily an isolated equilibrium point.

5. Let's look at the case  $\lambda = \mu$ . Now the solution is of the form (check this!)

$$\begin{pmatrix} x_n \\ y_n \end{pmatrix} = c_1 \begin{pmatrix} 1 \\ 0 \end{pmatrix} \lambda^n + c_2 \lambda^n \left( n \begin{pmatrix} 1 \\ 0 \end{pmatrix} + \begin{pmatrix} 0 \\ 1 \end{pmatrix} \right). \quad (4.18)$$

In terms of determining  $E^S$ ,  $E^U$  and  $E^C$ , the specific form of the general solution matters less than where the eigenvalues lie. Specifically, the form of the second fundamental solution with the generalized eigenvector has no impact on this. As an example, consider the case when  $\lambda = -1$ . This results in an eigenvalue of multiplicity two on the unit circle, thus

$$E^S = \emptyset, \quad E^C = \mathbb{R}^2, \quad E^U = \emptyset, \quad (4.19)$$

*despite the fact that one of the two fundamental solutions is algebraically diverging from the equilibrium set.*

Knowing all this linear stuff, the important question is: **“What can be said for nonlinear systems?”**

## 4.2 Nonlinear, autonomous systems

As before, the system

$$x' = f(x), \quad x \in \mathbb{R}^N \quad (4.20)$$

may be linearized around a fixed point  $\bar{x}$ : set

$$x = \bar{x} + y. \quad (4.21)$$

Then

$$\begin{aligned} x' &= \bar{x}' + y' \\ &= y' \\ &= f(\bar{x} + y) \\ &= f(\bar{x}) + Df(\bar{x})y + \theta(|y|^2) \\ &= Df(\bar{x})y + \theta(|y|^2) \\ &= Ay + R(y), \end{aligned} \quad (4.22)$$

where  $R(y)$  denotes the higher-order residual terms, and  $A = Df(\bar{x})$ , the Jacobian of  $f(x)$ , evaluated at the fixed point  $\bar{x}$ .

We now introduce a coordinate transformation:

$$y = T \begin{pmatrix} u \\ v \\ w \end{pmatrix}, \quad (4.23)$$

where  $T$  denotes a constant matrix, to be chosen for our convenience in a little while. Also,  $u$ ,  $v$ , and  $w$  are vectors of the same dimension as  $E^S$ ,  $E^U$  and  $E^C$  respectively. We get

$$\begin{aligned}
T \begin{pmatrix} u' \\ v' \\ w' \end{pmatrix} &= AT \begin{pmatrix} u \\ v \\ w \end{pmatrix} + R \left( T \begin{pmatrix} u \\ v \\ w \end{pmatrix} \right) \\
\Rightarrow \begin{pmatrix} u' \\ v' \\ w' \end{pmatrix} &= T^{-1}AT \begin{pmatrix} u \\ v \\ w \end{pmatrix} + T^{-1}R \left( T \begin{pmatrix} u \\ v \\ w \end{pmatrix} \right). \tag{4.24}
\end{aligned}$$

The linear transformation  $T$  is chosen so that

$$T^{-1}AT = \begin{pmatrix} A_S & 0 & 0 \\ 0 & A_U & 0 \\ 0 & 0 & A_C \end{pmatrix}, \tag{4.25}$$

where  $A_S$  is an  $s \times s$  matrix with eigenvalues with negative real part,  $A_U$  has eigenvalues with positive real part, and  $A_C$  has eigenvalues on the imaginary axis. These different block matrix parts have solutions spanning  $E^S$ ,  $E^U$  and  $E^C$  respectively. Our new equations become

$$\begin{cases} u' = A_S u + R_S(u, v, w) \\ v' = A_U v + R_U(u, v, w) \\ w' = A_C w + R_C(u, v, w). \end{cases}, \tag{4.26}$$

where  $R_S$ ,  $R_U$  and  $R_C$  are all nonlinear functions (no linear parts) of their arguments. Our question is: ‘‘How do  $E^S$ ,  $E^U$  and  $E^C$  extend (if they do) when the nonlinear terms are taken into account?’’. The answer is provided by the following theorem, which we state without proof.

**Theorem 2 (Local stable, unstable, and center manifold theorem)** *Suppose the system*

$$x' = f(x), \quad x \in \mathbb{R}^N$$

*is  $r$  times differentiable. Then the fixed point  $\bar{x}$  has an  $r$ -times differentiable  $s$ -dimensional stable manifold,  $u$ -dimensional unstable manifold, and  $c$ -dimensional center manifold, denoted  $W_{loc}^S(\bar{x})$ ,  $W_{loc}^U(\bar{x})$ , and  $W_{loc}^C(\bar{x})$ , respectively. These manifolds are all tangent to their respective linear counterparts. The trajectories in  $W_{loc}^S(\bar{x})$  and  $W_{loc}^U(\bar{x})$  have the same asymptotic behavior as those in  $E^S$  and  $E^U$ .*

**Remarks:**

- This theorem holds for flows and for maps.
- The global stable, unstable and center manifolds  $W^S(\bar{x})$ ,  $W^U(\bar{x})$ , and  $W^C(\bar{x})$  are obtained by extending all trajectories in the local manifolds  $W_{loc}^S(\bar{x})$ ,  $W_{loc}^U(\bar{x})$ , and  $W_{loc}^C(\bar{x})$  forward and backward in time.

- The global stable, unstable and center manifolds  $W^S(\bar{x})$ ,  $W^U(\bar{x})$  and  $W^C(\bar{x})$  are not necessarily manifolds, as we will see. In their case the name “manifold” is inherited from their local counterparts, and it has no further meaning.

In many practical cases, Taylor expansions for the local manifolds of a fixed point may be obtained as follows: Suppose we have an  $N$ -dimensional system. Further suppose that we have already determined from the linear analysis that the equilibrium point in question has an invariant subspace of codimension one, *i.e.*, a hypersurface. Such a surface can be represented as the solution set of a single equation in  $\mathbb{R}^N$ . Lastly, suppose that the linear analysis told us that this subspace was not orthogonal to the  $x_N$  axis. Using the implicit function theorem, this means we can write the equation for the hypersurface as

$$x_N = h(x_1, \dots, x_{N-1}). \quad (4.27)$$

This equation for the invariant manifold of the fixed point  $\bar{x} = (\bar{x}_1, \dots, \bar{x}_{N-1}, \bar{x}_N)$  is our starting point. If it was not possible to solve for the variable  $x_N$  it is possible to solve for one of the other variables instead. Since the manifold is invariant, we may take a derivative. We get

$$x'_N = \frac{\partial h}{\partial x_1} x'_1 + \dots + \frac{\partial h}{\partial x_{N-1}} x'_{N-1}. \quad (4.28)$$

Substituting the dynamical system in this equation gives

$$f_N(x) = \sum_{k=1}^{N-1} \frac{\partial h}{\partial x_k} f_k(x). \quad (4.29)$$

This is the master equation to work with: both sides are expanded in a Taylor series around  $\bar{x}$ . The Taylor expansions of  $f_k(x)$ ,  $k = 1, \dots, N$  are known, whereas that of  $h(x_1, \dots, x_{N-1})$  is not known. Thus, (4.29) gives a system of equations (by equating coefficients of different powers of  $x$ ) for the unknown coefficients.

The procedure is similar for maps. This is illustrated in the next example.

**Example 3** Consider the nonlinear system

$$\begin{cases} x_{n+1} = -\frac{5}{2}x_n + y_n \\ y_{n+1} = -\frac{3}{2}x_n + y_n + x_n^3 \end{cases}. \quad (4.30)$$

The fixed points of this system are given by

$$\begin{aligned} & \begin{cases} x_n = -\frac{5}{2}x_n + y_n \\ y_n = -\frac{3}{2}x_n + y_n + x_n^3 \end{cases} \\ \Rightarrow & \begin{cases} \frac{7}{2}x_n = y_n \\ 0 = -\frac{3}{2}x_n + x_n^3 \end{cases} \\ \Rightarrow & P_1 = (0, 0), \quad P_2 = \left( \sqrt{\frac{3}{2}}, \frac{7}{2}\sqrt{\frac{3}{2}} \right), \quad P_3 = \left( -\sqrt{\frac{3}{2}}, -\frac{7}{2}\sqrt{\frac{3}{2}} \right). \end{aligned} \quad (4.31)$$

- **The behavior in the neighborhood of  $P_1$ :** *the linearized system around  $P_1 = (0, 0)$  is*

$$\begin{cases} x_{n+1} = -\frac{5}{2}x_n + y_n \\ y_{n+1} = -\frac{3}{2}x_n + y_n \end{cases}, \quad (4.32)$$

with eigenvalues  $-2$  and  $1/2$ , and corresponding eigenvectors  $(2, 1)^T$  and  $(1, 3)^T$ . Thus, the general solution of this linear system is

$$\begin{pmatrix} x_n \\ y_n \end{pmatrix} = c_1(-2)^n \begin{pmatrix} 2 \\ 1 \end{pmatrix} + c_2(1/2)^n \begin{pmatrix} 1 \\ 3 \end{pmatrix}. \quad (4.33)$$

We might call  $P_1$  a saddle point. Since  $P_1$  is a hyperbolic fixed point, we may conclude that close to  $P_1$ , the behavior is as shown in Figure 4.1.

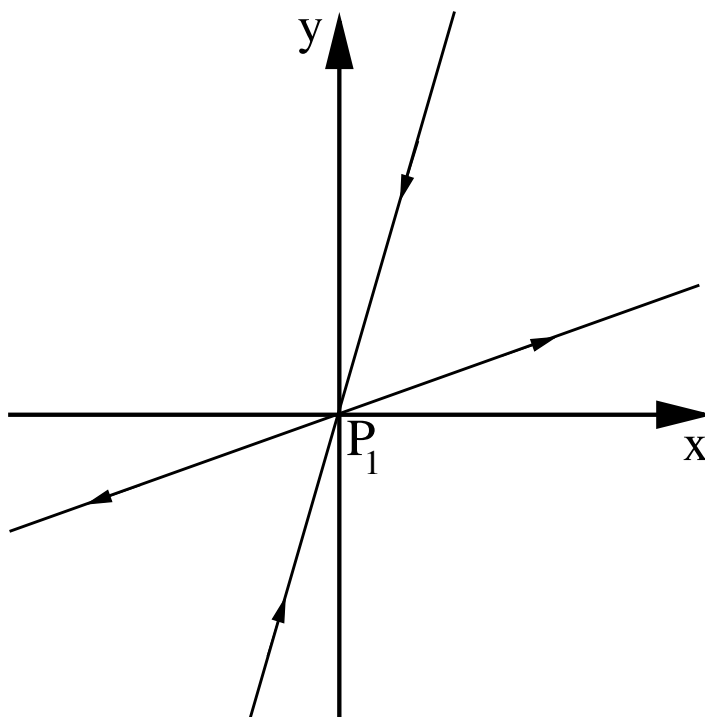


Figure 4.1: The behavior near the fixed point  $P_1$ , using the linear dynamics.

Let's find the one-dimensional stable and unstable manifold at  $P_1$ . We may assume this is of the form

$$y = ax + bx^2 + cx^3 + \dots, \quad (4.34)$$

since none of the linear manifolds are vertical at  $P_1$ . If a point  $(x_n, y_n)$  is on this manifold, then

$$y_n = ax_n + bx_n^2 + cx_n^3 + \dots \quad (4.35)$$

On the other hand, if this manifold is to be invariant, then the first iterate of  $(x_n, y_n)$  should be on it as well:

$$y_{n+1} = ax_{n+1} + bx_{n+1}^2 + cx_{n+1}^3 + \dots \quad (4.36)$$

Now we substitute the dynamical system (4.30) in for  $(x_{n+1}, y_{n+1})$ . This gives

$$-\frac{3}{2}x_n + y_n + x_n^3 = a \left( -\frac{5}{2}x_n + y_n \right) + b \left( -\frac{5}{2}x_n + y_n \right)^2 + c \left( -\frac{5}{2}x_n + y_n \right)^3 + \dots \quad (4.37)$$

In this equation, we get to replace  $y_n$  by the equation of the manifold:  $y_n = ax_n + bx_n^2 + cx_n^3 + \dots$ . This results in an equation that only involves  $x_n$ , which is supposed to be arbitrary. Thus we may equate coefficients of different powers of  $x_n$ . This results in equations for  $a, b, \dots$

From the linear terms we find  $a = 1/2$  or  $a = 3$ , which is consistent with the linear analysis done above, since these are just the slopes of the eigenvectors. If we continue the calculations with  $a = 1/2$ , we'll find the local unstable manifold. On the other hand, using  $a = 3$  will result in the local stable manifold.

Doing this, we find:

$$W_{loc}^U : \quad y = \frac{1}{2}x - \frac{2}{17}x^3 + \theta(x^5), \quad (4.38)$$

and

$$W_{loc}^S : \quad y = 3x + \frac{8}{17}x^3 + \theta(x^5). \quad (4.39)$$

This allows us to conclude that the behavior near  $P_1$  is as is indicated in Figure 4.2.

- **The behavior in the neighborhood of  $P_2$ :** Doing similar calculations around  $P_2$ , one finds that it is a saddle point as well. Furthermore,

$$W_{loc}^U : \quad y = \frac{7}{2}\sqrt{\frac{3}{2}} + \frac{7 - \sqrt{97}}{4} \left( x - \sqrt{\frac{3}{2}} \right) + \frac{12\sqrt{6}}{59 + \sqrt{97}} \left( x - \sqrt{\frac{3}{2}} \right)^2 + \theta(x^3), \quad (4.40)$$

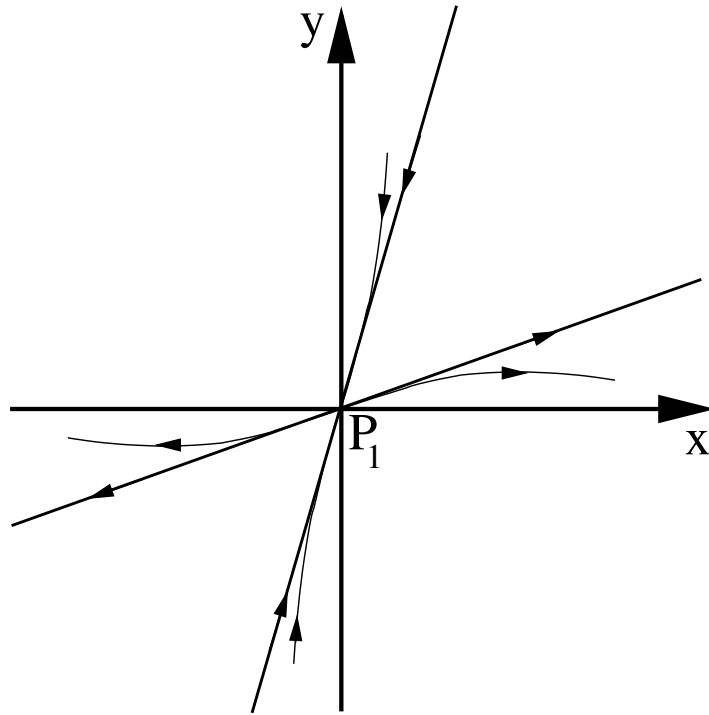


Figure 4.2: The behavior near the fixed point  $P_1$ , indicating the local invariant manifolds.

is a representation of the local unstable manifold. Similarly,

$$W_{loc}^S : y = \frac{7}{2}\sqrt{\frac{3}{2}} + \frac{7 + \sqrt{97}}{4} \left( x - \sqrt{\frac{3}{2}} \right) - \frac{12\sqrt{6}}{-59 + \sqrt{97}} \left( x - \sqrt{\frac{3}{2}} \right)^2 + \theta(x^3), \quad (4.41)$$

gives the local stable manifold.

- **The behavior in the neighborhood of  $P_3$ :** Repeating this around  $P_3$ , one finds that it too is a saddle point, with

$$W_{loc}^U : y = -\frac{7}{2}\sqrt{\frac{3}{2}} + \frac{7 - \sqrt{97}}{4} \left( x + \sqrt{\frac{3}{2}} \right) - \frac{12\sqrt{6}}{-59 + \sqrt{97}} \left( x + \sqrt{\frac{3}{2}} \right)^2 + \theta(x^3), \quad (4.42)$$

is a representation of the local unstable manifold. Lastly,

$$W_{loc}^S : y = -\frac{7}{2}\sqrt{\frac{3}{2}} + \frac{7 + \sqrt{97}}{4} \left( x + \sqrt{\frac{3}{2}} \right) + \frac{12\sqrt{6}}{-59 + \sqrt{97}} \left( x + \sqrt{\frac{3}{2}} \right)^2 + \theta(x^3), \quad (4.43)$$

*gives the local stable manifold.*

*We may summarize these results graphically in Figure 4.3. Note that we've used artistic freedom in assuming that the unstable manifolds for  $P_2$  and  $P_3$  merge into the stable manifold for  $P_1$ . This is, in fact, true. However, the analysis we have done to this point does not warrant this conclusion.*

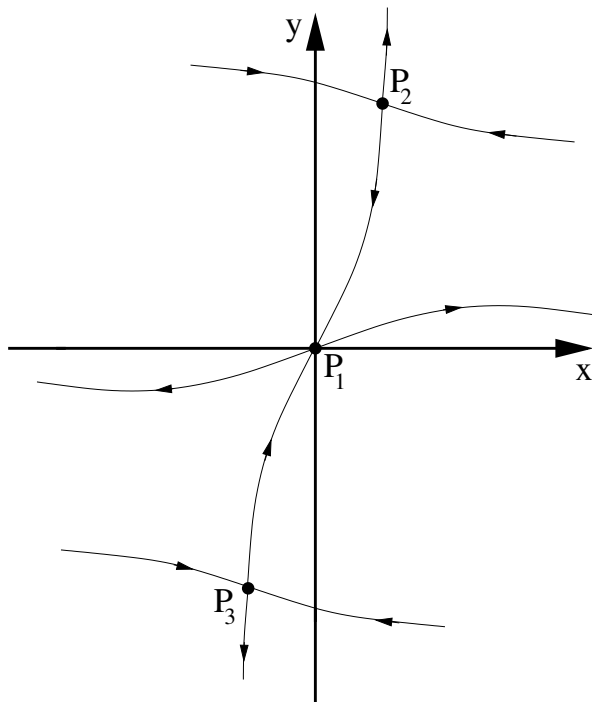


Figure 4.3: The behavior near the fixed points  $P_1$ ,  $P_2$ , and  $P_3$ . Indicated are the local invariant manifolds.

### Remarks.

- So far, we've only talked about invariant manifolds associated with fixed points. We could also consider invariant manifolds of other trajectories. Specifically, we might be interested in invariant manifolds of periodic orbits. We will touch on some aspects of this later.
- An important issue related to invariant manifolds is their possible persistence under perturbations. In other words, we want to know about the stability of invariant manifolds.
- The invariant manifolds divide the phase space in smaller parts. Is it possible to consider the dynamics restricted to one of these manifolds? If so, we have reduced the dimensionality of the system under consideration. We will return to this when we examine center manifold dynamics in more detail.

### 4.3 The transverse intersection of invariant manifolds of maps

To close of this chapter, we briefly consider the scenario of the one-dimensional stable and unstable manifold of a saddle point  $P$  of a two-dimensional map intersecting transversally, as shown in Figure 4.4c.

Consider the map

$$\begin{cases} x_{n+1} &= y_n \\ y_{n+1} &= (a + by_n^2)y_n - x_n \end{cases}, \quad (4.44)$$

where  $a = 2.693$  and  $b = -104.888$ . This example is due to Ricardo Carretero-González. The figures are generated by taking a numerically dense set of points on the stable and unstable linear subspaces  $E^S$  and  $E^U$  of the fixed point  $(0,0)$  (Figure 4.4a). These points are iterated forward (unstable manifold) and backward (stable manifold) in time. After some number of iterations, the nonlinear effects become apparent, and one observes the emergence of  $W_{loc}^S$  and  $W_{loc}^U$  (Figure 4.4b). Further iterations shows the transverse crossing of  $W^S$  and  $W^U$ , at the point  $P_0$ . Thus  $P_0$  is on both the stable and unstable manifold of  $P$ . It follows that  $P_1 = F(P_0)$  and  $P_{-1} = F^{-1}(P_0)$  are on both invariant manifolds as well, by invariance. The same is true for all their preimages and images under the map  $F$ . This leads to the picture of a homoclinic tangle, as shown in Figure 4.4c-d. We see that in this homoclinic tangle the motion is unpredictable: a slight change in the initial condition near  $P$  will result in entirely different motion. The presence of such a tangle will always lead to chaos. We'll investigate homoclinic tangles more extensively later.

### 4.4 The Center manifold reduction

Let's return briefly to our investigation of the center manifold. Suppose we have a dynamical system

$$x' = f(x), \quad (4.45)$$

with  $x \in \mathbb{R}^N$ , and  $f(x) \in C^r(a, b)$ . Assume this system has an equilibrium point  $x_0$ :  $f(x_0) = 0$ . Suppose this equilibrium point is not hyperbolic. Then there exists a center manifold of this fixed point,  $W^C$ . Further, suppose that  $W^U = \emptyset$ , as often happens in dissipative systems. In this case, the stability of  $x_0$  is governed by the dynamics on  $W^C$ . Typically,  $W^C$  is lower dimensional than the original system. We would expect that all contribution from  $W^S$  become exponentially small as  $t \rightarrow \infty$ . This is another good reason to consider the dynamics restricted to  $W^C$ : it is lower dimensional, and it dominates the dynamics near  $x_0$  for large  $t$ . In this section we explore how to make efficient use of this. It should be noted that the ideas presented here are perhaps even more important for infinite-dimensional systems, where a center manifold reduction may bring us down to a finite-dimensional setting.

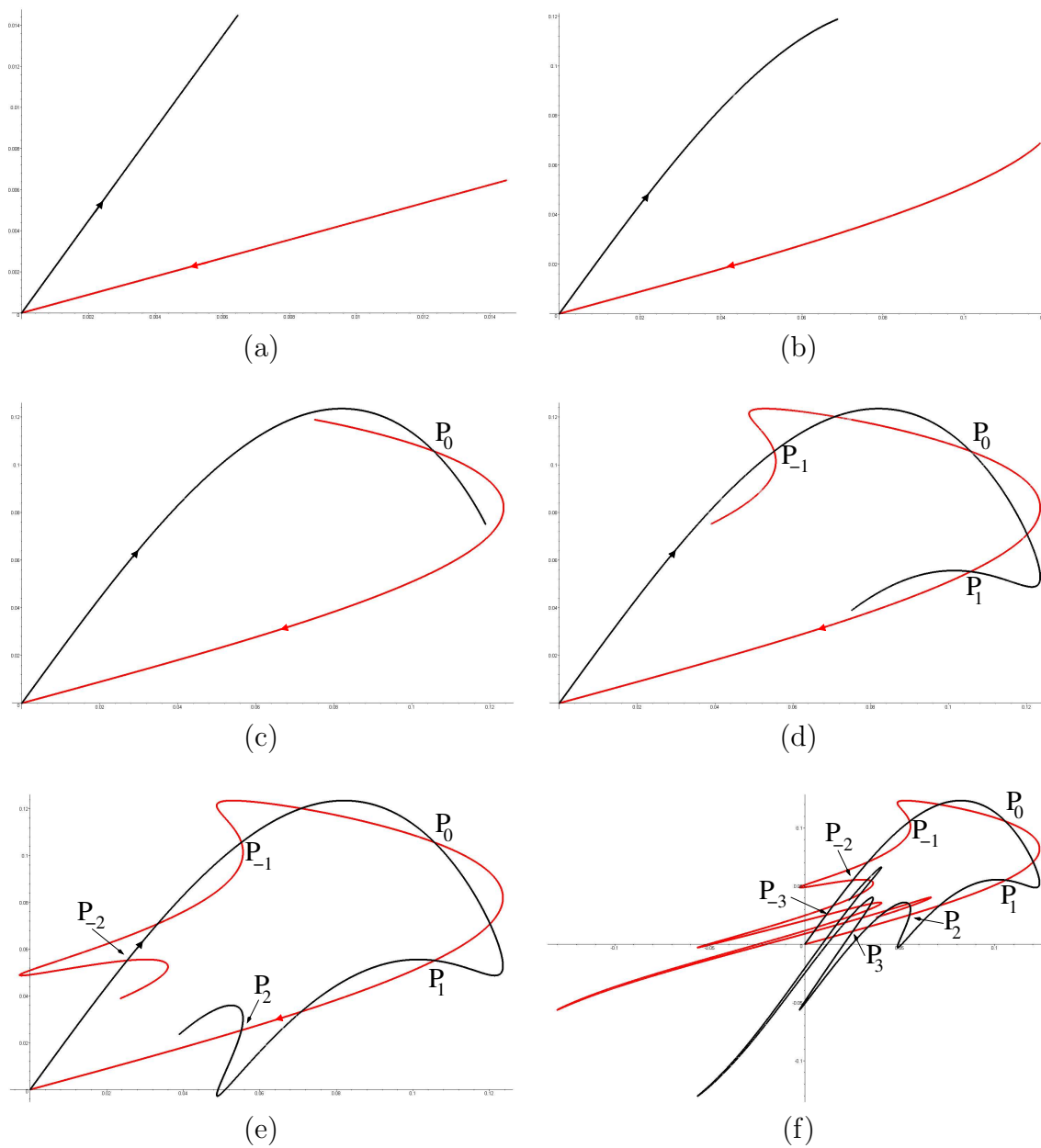


Figure 4.4: The homoclinic connection (actually, half of it) of the fixed point  $(0,0)$  of the map (4.44).

Let's make the general ideas stated above more concrete. Let's write the dynamical system so that the stable and central dynamics in the linear approximation are separated, as we've done before. Thus

$$\begin{cases} x' &= Ax + f(x, y) \\ y' &= By + g(x, y) \end{cases}, \quad (4.46)$$

with  $(x, y) \in \mathbb{R}^c \times \mathbb{R}^s$ . Here  $A$  has only purely imaginary eigenvalues (possibly including 0), and  $f(x, y)$  is of second order. Further, all eigenvalues of  $B$  are negative or have negative real part and  $g(x, y)$  is of second order too. We have already defined the center manifold before. The question we face now is: "how do we determine the dynamics on it?"

**Theorem 3** *There exists a  $C^r$  center manifold for our system, which may be represented as*

$$y = h(x), \quad (4.47)$$

*locally near the equilibrium point. Then the dynamics on this center manifold is obtained from*

$$x' = Ax + f(x, h(x)), \quad (4.48)$$

*with  $x \in \mathbb{R}^c$ .*

We won't prove this theorem here. Instead, we'll look at another theorem (Oh boy!):

**Theorem 4 (Stability of non-hyperbolic fixed points)** *Suppose the zero solution of our center manifold system is stable (asymptotically stable) (unstable), then the zero solution of our originating system is also stable (asymptotically stable) (unstable).*

*Further, if the zero solution of our center manifold system is stable, then if  $(x(t), y(t))$  is a solution of the originating system with  $x(0)$  and  $y(0)$  sufficiently small, there is a solution  $u(t)$  of the center manifold system such that as  $t \rightarrow \infty$  we have*

$$\begin{cases} x &= u(t) + \theta(e^{-\gamma t}) \\ y &= h(u(t)) + \theta(e^{-\gamma t}) \end{cases}, \quad (4.49)$$

*where  $\gamma > 0$  is a constant.*

Another theorem without proof. How terribly unsatisfying. Kind of like an algorithm without a computer. So, let's put all this to work: what is it good for?

**Example 4** *consider the system*

$$\begin{cases} x' &= x^2y - x^5 \\ y' &= -y + x^2 \end{cases}. \quad (4.50)$$

*Clearly,  $(0, 0)$  is a fixed point. Let's examine its stability. The matrix of the linearization is*

$$\begin{pmatrix} 0 & 0 \\ 0 & -1 \end{pmatrix}, \quad (4.51)$$

with  $\lambda_1 = 0$  and  $\lambda_2 = -1$ . As a first approach, we might contemplate neglecting  $y$  altogether, as this linear result seems to say that close to the equilibrium point  $y$  decays exponentially. This would result in the equation

$$x' = -x^5, \quad (4.52)$$

whose phase line dynamics is shown in Figure 4.5. So, we're led to conclude that the origin is a stable fixed point. As it turns out, this is incorrect.

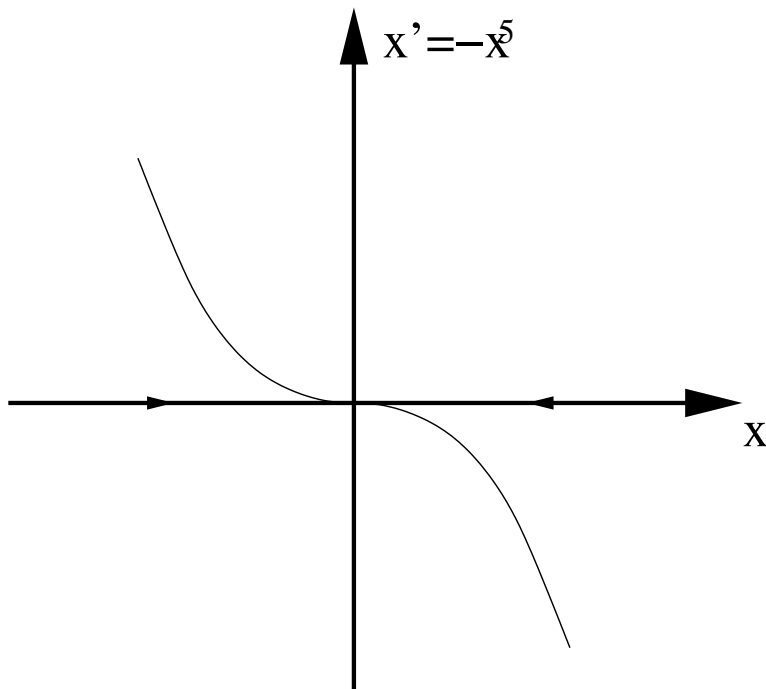


Figure 4.5: The phase-line dynamics of  $x' = -x^5$ .

Let us proceed to find the center manifold dynamics. First, we find the center manifold, as before. We find

$$y = h(x) = x^2 + \theta(x^4). \quad (4.53)$$

It follows that the dynamics on the center manifold is dictated by

$$x' = x^4 - x^5 + \theta(x^8), \quad (4.54)$$

which gives the phase line picture of Figure 4.6. It follows that the origin is an unstable fixed point. Note that this figure suggests the presence of a fixed point along the center manifold away from the origin. This is only suggestive: our center manifold reduction is only valid near the original fixed point and it is not justified to conclude the existence of this fixed point from this calculation. The two-dimensional phase plane for the original system is

shown in Figure 4.7. As it turns out, a second (asymptotically stable) fixed point does exist at  $(1, 1)$ .

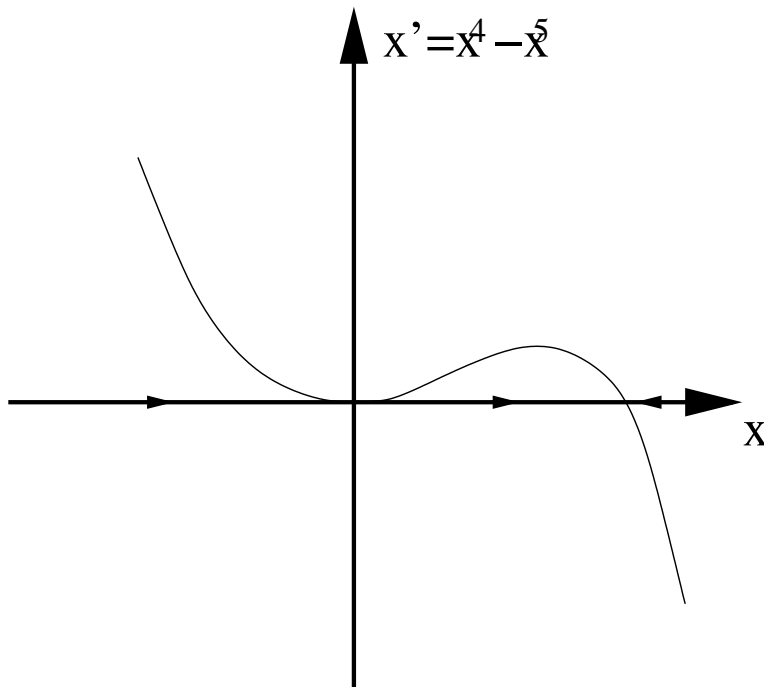


Figure 4.6: The phase-line dynamics of  $x' = x^4 - x^5$ .

It should be noted there are examples where the tangent approximation (*i.e.*, neglecting the elements along  $W^S$ ) predicts instability, but the center manifold approach shows the solution is actually stable.

## 4.5 Center manifolds depending on parameters: a first foray into bifurcation theory

Suppose we are investigating

$$\begin{cases} x' = Ax + f(x, y, \epsilon) \\ y' = By + g(x, y, \epsilon) \end{cases}, \quad (4.55)$$

where  $A$  and  $B$  are as in the previous section. Further, we assume they do not depend on  $\epsilon$ . In other words, the effects of the small parameter only arise at the level of the nonlinear terms, or we include the effect of  $\epsilon$  on any of the linear terms with  $f(x, y, \epsilon)$  and  $g(x, y, \epsilon)$ . This is often treated by introducing a new dynamical equation, namely

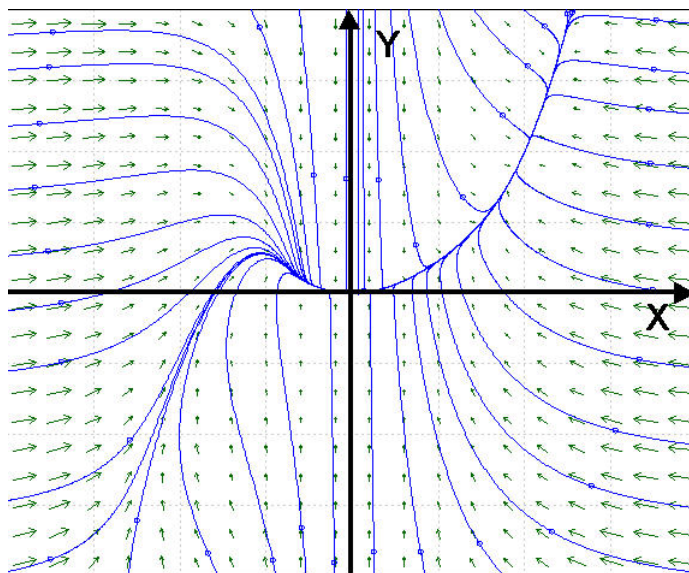


Figure 4.7: The full phase portrait of the system 4.50. The figure was produced using pplane.

$$\begin{cases} x' = Ax + f(x, y, \epsilon) \\ y' = By + g(x, y, \epsilon) \\ \epsilon' = 0 \end{cases}, \quad (4.56)$$

where we proceed as before, but terms like  $\epsilon x$  are now considered nonlinear! Let's illustrate this using an example.

**Example 5** Consider the Lorenz equations:

$$\begin{cases} x' = \sigma(y - x) \\ y' = \epsilon x + x - y - xz \\ z' = -\beta z + xy \end{cases}, \quad (4.57)$$

where  $\sigma$  and  $\beta$  are regarded as positive constants and  $\epsilon$  is a scalar parameter. Linearizing around the fixed point  $(0, 0, 0)$  gives the matrix

$$\begin{pmatrix} -\sigma & \sigma & 0 \\ 1 & -1 & 0 \\ 0 & 0 & -\beta \end{pmatrix}, \quad (4.58)$$

for  $\epsilon = 0$ , with eigenvalues  $0$ ,  $-\beta$  and  $-\sigma - 1$ , and respective eigenvectors

$$\begin{pmatrix} 1 \\ 1 \\ 0 \end{pmatrix}, \begin{pmatrix} 0 \\ 0 \\ 1 \end{pmatrix}, \begin{pmatrix} \sigma \\ -1 \\ 0 \end{pmatrix}. \quad (4.59)$$

Using these eigenvectors, we construct the transformation

$$\begin{pmatrix} x \\ y \\ z \end{pmatrix} = \begin{pmatrix} 1 & \sigma & 0 \\ 1 & -1 & 0 \\ 0 & 0 & 1 \end{pmatrix} \begin{pmatrix} u \\ v \\ w \end{pmatrix}, \quad (4.60)$$

which results in the new system (check!)

$$u' = \frac{\sigma(u + \sigma v)(\epsilon - w)}{1 + \sigma}, \quad (4.61)$$

$$v' = -(1 + \sigma)v + \frac{(u + \sigma v)(-\epsilon + w)}{1 + \sigma}, \quad (4.62)$$

$$w' = -\beta w + (u + \sigma v)(u - v), \quad (4.63)$$

$$\epsilon' = 0. \quad (4.64)$$

Note that we are treating  $\epsilon$  as a new variable. This system implies that we can choose the equations of the local center manifold as

$$v = h_1(u, \epsilon), \quad (4.65)$$

$$w = h_2(u, \epsilon). \quad (4.66)$$

Now we're in for some really tedious algebra. Using a Taylor expansion for  $h_1(u, \epsilon)$  and  $h_2(u, \epsilon)$ , we find (more checking!)

$$v = h_1(u, \epsilon) = -\frac{1}{(1 + \sigma)^2} u \epsilon + \dots, \quad (4.67)$$

$$w = h_2(u, \epsilon) = \frac{1}{\beta} u^2 + \dots \quad (4.68)$$

Substitution of this in the transformed system results in (and another check!)

$$u' = \frac{\sigma u}{1 + \sigma} \left( 1 - \frac{\epsilon \sigma}{(1 + \sigma)^2} + \dots \right) \left( \epsilon - \frac{1}{\beta} u^2 + \dots \right). \quad (4.69)$$

Of course, there's still the equation  $\epsilon' = 0$ . The above equation allows us to conclude that for  $\epsilon < 0$  (small),  $u = 0$  is a stable fixed point, whereas for  $\epsilon > 0$  (small),  $u = 0$  is an unstable fixed point.

We will return to questions like this when we treat bifurcations.



# Chapter 5

## Periodic solutions

For flows, we have the following definition:

**Definition 8 (Periodic solution of a continuous time system)** *A solution of  $x' = f(x)$  through  $x_0$  is said to be periodic of period  $T$  if there exists a  $T > 0$  such that  $x(t, x_0) = x(t + T, x_0)$ , for all  $t \in \mathbb{R}$ .*

A similar definition holds for maps:

**Definition 9 (Periodic solution of a discrete time system)** *A solution of  $x_{n+1} = F(x_n)$  through  $x_0$  is said to be periodic of period  $k$  if  $F^k(x_0) = x_0$ .*

In this chapter we start our study of periodic solutions of dynamical systems.

### 5.1 The nonexistence of periodic orbits for two-dimensional autonomous vector fields

Consider the two-dimensional (planar) system

$$\begin{cases} x' = f(x, y) \\ y' = g(x, y) \end{cases}, \quad (5.1)$$

from which it follows immediately that

$$\frac{dy}{dx} = \frac{g(x, y)}{f(x, y)}. \quad (5.2)$$

The following theorem holds.

**Theorem 5 (Bendixson)** *If  $\partial f/\partial x + \partial g/\partial y$  is not identically 0 and does not change sign on a simply connected region  $D$  of the phase space, then (5.1) has no closed orbits in this region.*

**Proof.** We prove this by contradiction. Assume there is a closed orbit  $\Gamma$  in  $D$ . Then we have

$$\oint_{\Gamma} f(x, y)dy - g(x, y)dx = 0. \quad (5.3)$$

By Greene's theorem,

$$\int_S \left( \frac{\partial f}{\partial x} + \frac{\partial g}{\partial y} \right) dx dx = 0, \quad (5.4)$$

where  $S$  denotes the inside of  $\Gamma$ . If  $\partial f/\partial x + \partial g/\partial y \neq 0$  and does not change sign, this last equality cannot hold. Hence, there cannot be any closed orbits in  $D$ . ■

**Example 6** Consider the system

$$\begin{cases} x' = y \\ y' = x - x^3 - \delta y + x^2 y, \end{cases} \quad (5.5)$$

where  $\delta > 0$  is a parameter. The fixed points of this system are given by (for  $\delta > 1$  and  $\delta < 1 + 2\sqrt{2}$ )

$$P_1 = (0, 0), \quad P_2 = (1, 0), \quad P_3 = (-1, 0). \quad (5.6)$$

The phase portrait of this system is given in Figure 5.1. You should check that  $P_1$  is indeed a saddle point, and  $P_2$  and  $P_3$  are stable spiral points.

Next, we compute

$$\frac{\partial f}{\partial x} + \frac{\partial g}{\partial y} = -\delta + x^2. \quad (5.7)$$

The zeros of this occur when  $x^2 = \delta$ , which implies  $x = \pm\sqrt{\delta}$ . These two vertical lines are also indicated in Figure 5.1. By Bendixson's theorem, there are no closed orbits to the right of, to the left of, and in between these two lines. Thus, if there are any closed orbits for this problem, they have to cross at least one of these two lines. From Figure 5.1, we see that a closed orbit does appear to exist, but it does in fact cross both vertical lines.

## 5.2 Vector fields possessing an integral

A flow

$$x' = f(x) \quad (5.8)$$

has the integral (conserved quantity)  $I(x)$  if  $I(x)$  is constant along trajectories of the flow:

$$I'(x) = \nabla I \cdot x' = \nabla I \cdot f(x) = 0. \quad (5.9)$$

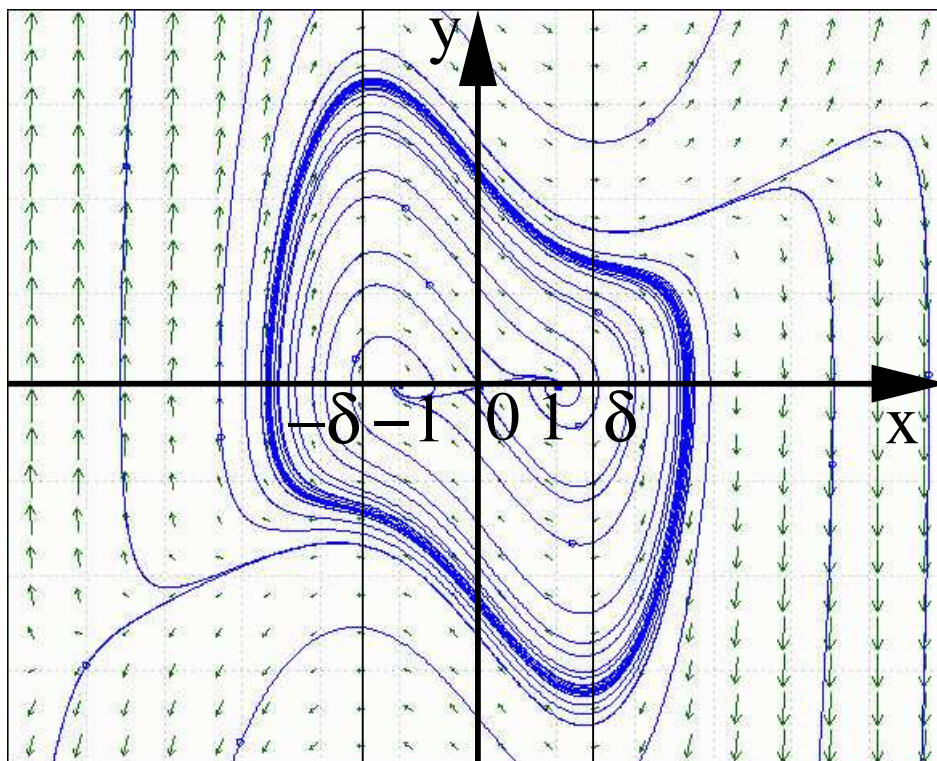


Figure 5.1: The phase portrait for the system (5.5). The plot was made using pplane.

In such a case, the dynamics takes place on the level sets of the integral, which foliates the phase space. Clearly, the more integrals, the more constrained the motion is, as it has to exist on the intersection of the different level sets.

**Example 7** Consider the first-order system of differential equations describing the pendulum:

$$\begin{cases} q' = p \\ p' = -\frac{g}{l} \sin q \end{cases} \quad (5.10)$$

We claim that

$$E = \frac{1}{2}p^2 - \frac{g}{l} \cos q \quad (5.11)$$

is an integral of this system. We easily verify this:

$$E' = pp' + q' \frac{g}{l} \sin q = p \left( -\frac{g}{l} \sin q \right) + p \frac{g}{l} \sin q = 0. \quad (5.12)$$

It follows that the dynamics takes place on the level sets of  $E$ . Since the pendulum system is two-dimensional, this almost completely determines the motion in the phase plane (up to

the direction of time). This is of great benefit to us: fully integrating the equations of motion of the pendulum requires elliptic functions, which we may now avoid. The phase portrait for the pendulum is shown in Figure 5.2. Some level sets of  $E$  are indicated as well.

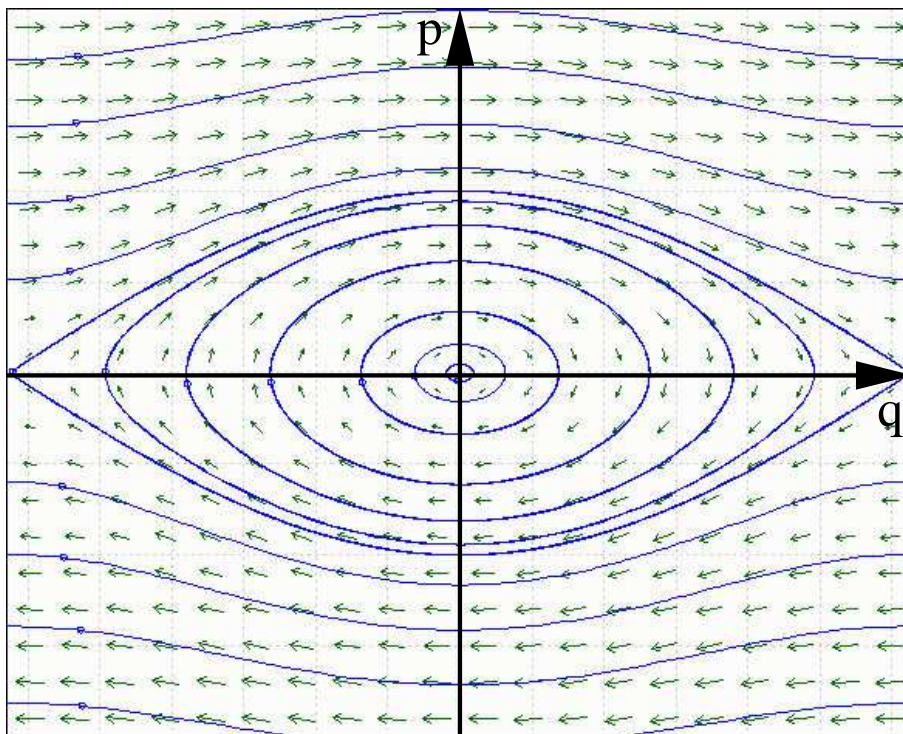


Figure 5.2: The phase portrait for the pendulum. The plot was made using pplane.

# Chapter 6

## Properties of autonomous vector fields and maps

### 6.1 General properties of autonomous vector fields

Consider

$$x' = f(x), \quad x \in \mathbb{R}^n. \quad (6.1)$$

For an autonomous system like this, if  $x(t)$  is a solution, then so is  $x(t + \tau)$ , for any real  $\tau$ . Indeed:

$$x'(t + \tau) = x'(t)|_{t \rightarrow t + \tau} = f(x(t))|_{t \rightarrow t + \tau} = f(x(t + \tau)). \quad (6.2)$$

We group the remaining properties in the following theorem.

**Theorem 6** *For an autonomous system  $x' = f(x)$ ,  $x \in \mathbb{R}^N$ , with  $f$   $r$  times differentiable, the following properties hold: (i)  $x(t, x_0)$  is  $r$  times differentiable; (ii)  $x(0, x_0) = x_0$ ; and (iii)  $x(t + s, x_0) = x(t, x(s, x_0))$ .*

**Proof.** The first property was already stated when we stated the existence/uniqueness theorem. The second property is true by definition. Thus only (iii) requires any additional effort to prove. It is referred to as the *group property* of the solutions of the dynamical system. It does *not* hold for solutions of non-autonomous systems. To prove this property, consider both  $x(t + s, x_0)$  and  $x(t, x(s, x_0))$  at  $t = 0$ :

$$x(t + s, x_0)|_{t=0} = x(s, x_0), \quad (6.3)$$

and

$$x(t, x(s, x_0))|_{t=0} = x(0, x(s, x_0)) = x(s, x_0), \quad (6.4)$$

where the second equality follows from (ii). Thus, both are equal at  $t = 0$ . Next we show that they satisfy the same differential equation. If we manage to do this, the desired result follows from the existence/uniqueness theorem. Let  $y_1(t) = x(t + s, x_0)$ . Then

$$y_1' = x'(t + s, x_0) = f(x(t + s, x_0)) = f(y_1). \quad (6.5)$$

Next, let  $y_2 = x(t, x(s, x_0))$ . Then

$$y_2' = x'(t, x(s, x_0)) = f(x(t, x(s, x_0))) = f(y_2), \quad (6.6)$$

which is what we had to prove. ■

## 6.2 Liouville's theorem

Again we consider the autonomous system

$$x' = f(x), \quad (6.7)$$

with flow  $\phi_t(x_0) = \phi(x_0, t)$ . Let  $D_0$  be a compact set of initial data in our phase space. Let  $D_t = \phi_t(D_0)$  be the image of  $D_0$  under the flow of the vector field. Lastly, let  $V(0)$  and  $V(t)$  respectively denote the volume of  $D_0$  and  $D_t$ .

**Theorem 7 (Liouville)** *Under the above conditions, we have*

$$\left. \frac{dV}{dt} \right|_{t=0} = \int_{D_0} \nabla \cdot f dx. \quad (6.8)$$

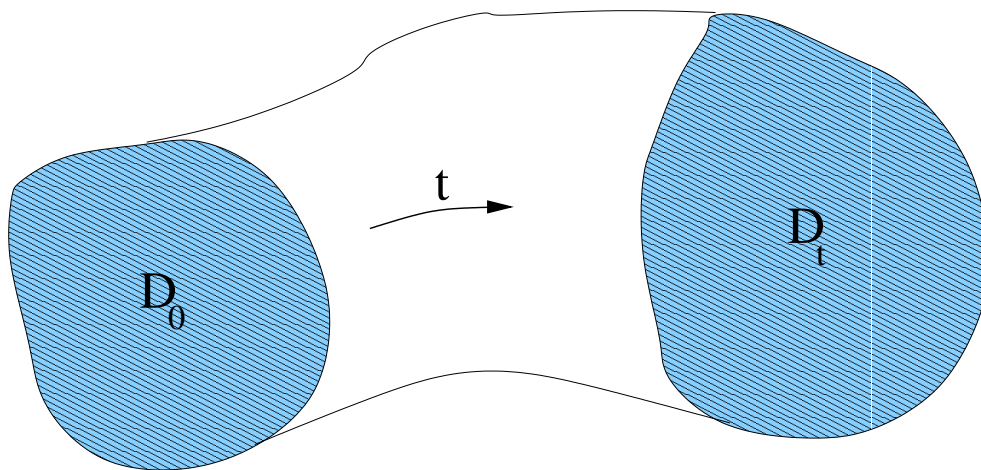


Figure 6.1: The dynamics of a blob of phase space.

**Proof.** Regarding the flow of the dynamical system as a transformation on the initial region  $D_0$ , we get

$$V(t) = \int_{D_0} \det \left( \frac{\partial \phi_t}{\partial x} \right) dx, \quad (6.9)$$

where the integrand is the Jacobian of the transformation. On the other hand,

$$\phi_t(x) = x + f(x)t + \theta(t^2), \quad (6.10)$$

which is essentially Euler's method. Then

$$\begin{aligned} & \frac{\partial \phi_t}{\partial x} = I + \frac{\partial f}{\partial x} t + \theta(t^2) \\ \Rightarrow & \det \left( \frac{\partial \phi_t}{\partial x} \right) = \det \left( I + \frac{\partial f}{\partial x} t + \theta(t^2) \right) \\ \Rightarrow & = 1 + t \operatorname{tr} \left( \frac{\partial f}{\partial x} \right) + \theta(t^2) \\ \Rightarrow & V(t) = \int_{D_0} \left[ 1 + t \operatorname{tr} \left( \frac{\partial f}{\partial x} \right) + \theta(t^2) \right] dx \\ \Rightarrow & \frac{V(t) - V(0)}{t - 0} = \frac{1}{t} \int_{D_0} \left[ 1 + t \operatorname{tr} \left( \frac{\partial f}{\partial x} \right) + \theta(t^2) - 1 \right] dx \\ & = \int_{D_0} \left[ \operatorname{tr} \left( \frac{\partial f}{\partial x} \right) + \theta(t) \right] dx \\ & = \int_{D_0} \left[ \operatorname{tr} \left( \frac{\partial f}{\partial x} \right) \right] dx + \theta(t) \\ \Rightarrow & V'(0) = \int_{D_0} \nabla \cdot f dx, \end{aligned} \quad (6.11)$$

which is what we had to show. ■

Since the initial time  $t_0$  was arbitrary, we have the more general result

$$V'(t_0) = \int_{D_{t_0}} \nabla \cdot f dx, \quad (6.12)$$

for any  $t_0$ .

Liouville's theorem is extremely useful in a variety of circumstances: suppose that

$$\nabla \cdot f = c, \quad (6.13)$$

where  $c$  is some constant. Then Liouville's theorem becomes

$$V' = cV \quad \Rightarrow \quad V = V_0 e^{ct}. \quad (6.14)$$

Specifically, if  $c = 0$ , then  $V(t) = V(0)$ , and the phase space volume is conserved. Sometimes this last result (for  $c = 0$ ) is called Liouville's theorem as well.

### 6.3 The Poincaré recurrence theorem

Let's turn our attention to maps. The following is an important theorem for volume-preserving maps.

**Theorem 8 (Poincaré recurrence)** *Let  $F$  be a volume-preserving, continuous, one-to-one map, with an invariant set  $D$ , i.e.  $F(D) = D$ , which is compact. In any neighborhood  $U$  of any point of  $D$  there is a point  $x \in U$  such that  $F^n(x) \in U$ , for some  $n > 0$ .*

**Proof.** Consider the sequence

$$U, F(U), F^2(U), \dots, F^n(U), \dots \quad (6.15)$$

since  $F$  is volume preserving, the volume of each of these is identical. Since  $D$  has finite volume, the elements of the sequence cannot be all distinct. Thus they intersect. This implies the existence of integers  $k, l \geq 0$ ,  $k > l$  such that

$$F^k(U) \cap F^l(U) \neq \emptyset. \quad (6.16)$$

Thus

$$F^{k-l}(U) \cap U \neq \emptyset. \quad (6.17)$$

Let  $x$  be an element of this intersection. Then  $x \in U$  and  $F^n(x) \in U$ , where  $n = k - l$ . The theorem is proven. ■

Some remarks are in order:

- By regarding the flow of a vector field as a map on the phase space, this theorem also applies to volume-preserving flows.
- Since  $U$  may be chosen arbitrarily small, one way to phrase the theorem is to say that a volume preserving map on a compact set will return arbitrarily close to any point it starts from.
- The time it takes the map to return is called the *Poincaré recurrence time*. Note that it depends on the map, on the point, and on the size of the neighborhood  $U$ . In general, the Poincaré recurrence time may be extremely large, so large that it may not be observable in even the best numerical simulations, especially for higher-dimensional systems.

- The Poincaré recurrence theorem may be the single-most violated theorem in the theory of dynamical systems. Note that the theorem implies that a volume preserving map has no attractors. I have seen numerous presentations and read many papers where researchers proudly proclaim to have numerically computed attractors in complicated systems which are volume preserving! For instance, one may start with initial conditions that appear random. A complicated numerical scheme may be used to involve initial data for a long time, and one may observe it settling down to something much simpler. Hurray! At this point, one would be wise to check the numerical scheme for the presence of artificial dissipation, for instance.

## 6.4 The Poincaré-Bendixson theorem

Now we turn our attention to the asymptotic behavior of solutions of vector fields. The results of this section will set us up for the Poincaré-Bendixson theorem, one of the most fundamental results for flows in two dimensions.

**Definition 10 ( $\omega$ -limit point)** A point  $x_0 \in \mathbb{R}^N$  is called an  $\omega$ -limit point of  $x \in \mathbb{R}^N$  if there exists a sequence  $t_k$  with

$$\lim_{k \rightarrow \infty} t_k = \infty, \quad (6.18)$$

such that

$$\lim_{k \rightarrow \infty} \phi(t_k, x) = x_0. \quad (6.19)$$

An  $\alpha$ -limit point is defined similarly, but for points moving backward in time. The set of all  $\omega$ - ( $\alpha$ -) limit points of  $x$  is denoted  $\omega(x)$  ( $\alpha(x)$ ).

**Example 8** (See Figure 6.2) Consider the example of a fixed point  $x_0$  and its stable ( $W^S(x_0)$ ) and unstable ( $W^U(x_0)$ ) manifold. First, let  $x \in W^S(x_0)$ . Then

$$\omega(x) = \{x_0\}. \quad (6.20)$$

On the other hand, if  $x \in W^U(x_0)$ , then

$$\alpha(x) = \{x_0\}. \quad (6.21)$$

**Example 9** Consider a trajectory that is approaching a periodic orbit, as in Figure 6.3. We have

$$x_1 = \phi(t_1, x), \quad x_2 = \phi(t_2, x), \quad \dots, \quad (6.22)$$

This sequence converges to a certain  $x$ , contained on the periodic orbit. It is clear that by taking a different sequence  $t_1, t_2, \dots$ , any point on the periodic orbit may be obtained. Thus

$$\omega(x) = \{\text{periodic orbit}\}. \quad (6.23)$$

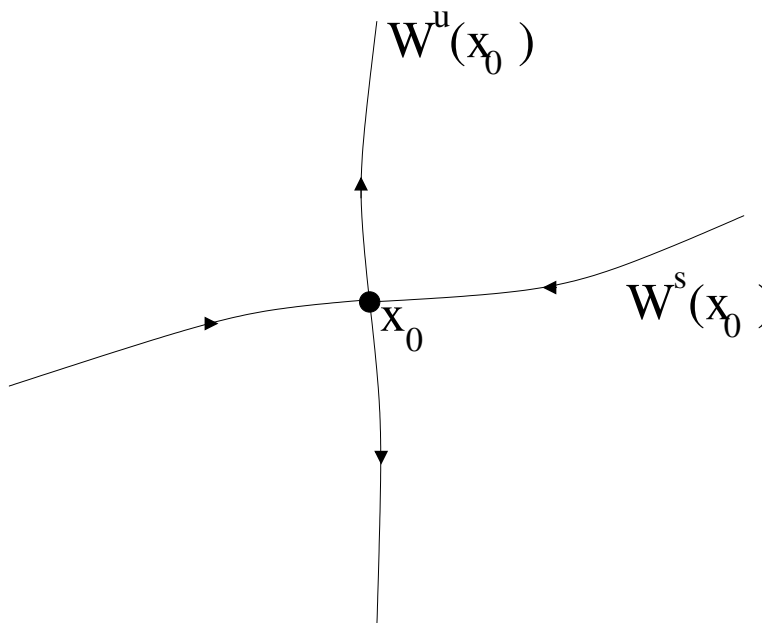


Figure 6.2: A fixed point and its stable and unstable manifolds.

We have the following definition:

**Definition 11 ( $\omega$ -limit set,  $\alpha$ -limit set)** *The set of  $\omega$ - ( $\alpha$ -) limit points of a flow is its  $\omega$ - ( $\alpha$ -) limit set.*

The following theorem summarizes many results about  $\omega$ -limit points.

**Theorem 9 (Properties of  $\omega$ -limit points)** *Let  $M$  be a positively invariant compact set of the flow  $\phi_t$ . Then, for  $p \in M$  we have (i)  $\omega(p) \neq \emptyset$ , (ii)  $\omega(p)$  is closed, (iii)  $\omega(p)$  is invariant under  $\phi_t$ , and (iv)  $\omega(p)$  is connected.*

**Proof.**

(i) Let  $\{t_k\}$  be a sequence of times, with  $\{p_k = \phi_{t_k}(p)\}$ . Since  $M$  is compact, the sequence  $\{p_k\}$  has a convergent subsequence. By restricting to this subsequence, we have constructed an element of  $\omega(p)$ .

(ii) We show instead that the complement of  $\omega(p)$  is open. Choose  $q \notin \omega(p)$ . Then  $q$  has a neighborhood  $U(q)$  which has no points in common with  $\{\phi_t(p), t > T\}$ , for  $T$  sufficiently large. Otherwise  $q$  would be a limit point, by construction. Since  $q$  is arbitrary, we are done.

(iii) The evolution of a limit point stays a limit point, which is obvious from its definition.

(iv) We prove this by contradiction. Suppose  $\omega(p)$  is not connected. Then this leads to the conclusion that  $\phi_t(p)$  is not connected, which violates the existence/uniqueness theorem.

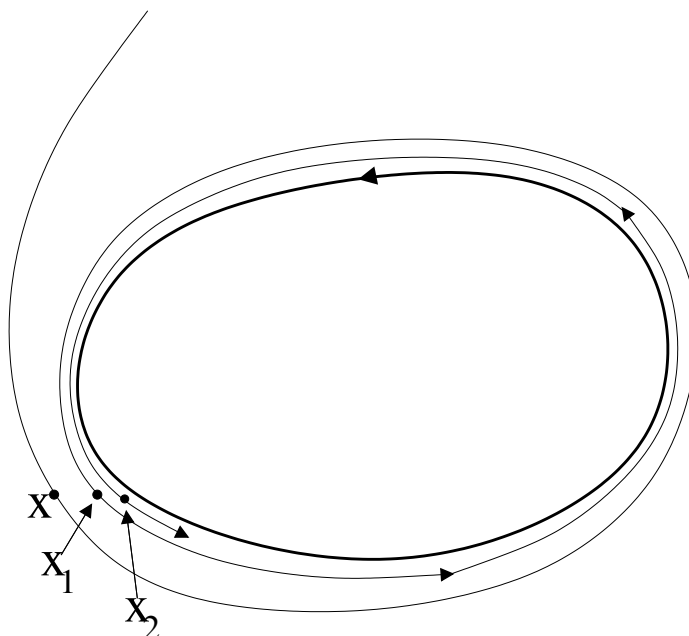


Figure 6.3: A limit cycle and an orbit approaching it.

This concludes the proof of the theorem. ■

We're inching closer to the proof of the Poincaré-Bendixson theorem. Consider the two-dimensional system

$$\begin{cases} x' = f(x, y) \\ y' = g(x, y) \end{cases}, \quad (6.24)$$

where

$$(x, y) \in P, \quad (6.25)$$

where  $P$  is either a plane, a cylinder or a sphere. The remaining results in this chapter all apply to one of these two-dimensional settings.

**Definition 12 (Transverse arc)** *An arc  $\Sigma$  (continuous and connected) is transverse to the vector field if  $\Sigma$  is never tangent to the vector field and contains no equilibrium points of it.*

Before we prove the main theorem, we need a few lemmas.

**Lemma 1** *Let  $\Sigma \subset M$  be transverse arc, where  $M$  is a positively invariant region. Then, for any  $p \in M$ ,  $\theta^+(p)$  intersects  $\Sigma$  in a monotone sequence: if  $p_i$  is the  $i$ -th intersection point, then  $p_i \in [p_{i-1}, p_{i+1}]$ , where this interval contains the set of points between  $p_{i-1}$  and  $p_{i+1}$ .*

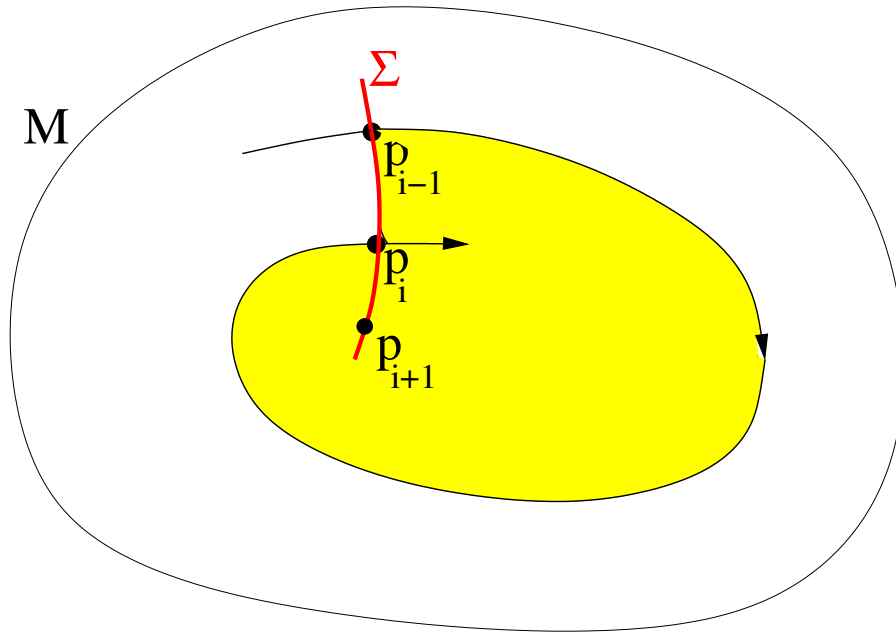


Figure 6.4: The graphical set-up for the monotonicity lemma.

**Proof.** First, if there's only one intersection, or none, we're done. Next, if there are multiple intersections, it follows that the yellow region in Figure 6.4 is positively invariant. Therefore  $\phi_t(p_i) = p_{i+1}$  is in the yellow region. Since, by definition,  $p_{i+1}$  is also on  $\Sigma$ , we have proven the lemma. ■

We have an immediate corollary.

**Corollary 1** *The number of elements of the set  $\omega(p) \cap \Sigma$  is 1 or 0.*

**Proof.** We prove this by contradiction. Suppose  $\omega(p)$  intersects  $\Sigma$  in two points  $q_1$  and  $q_2$ . Take a sequence  $\{p_k \in \theta(p)^+ \cap \Sigma\}$  which limits to  $q_1$ , and a sequence  $\{\hat{p}_k \in \theta(p)^+ \cap \Sigma\}$ , which limits to  $q_2$ . But  $\theta(p)^+$  intersects  $\Sigma$  in a monotone sequence by the monotonicity lemma. A monotone bounded sequence has a unique limit. The existence of two different limit points is a contradiction, which proves the corollary. ■

We need one more lemma.

**Lemma 2** *If  $\omega(p)$  does not contain any fixed points, then  $\omega(p)$  is a closed orbit.*

**Proof.** Choose  $q \in \omega(p)$ . Let  $x \in \omega(q) \subset \omega(p)$ . Thus  $x$  is not a fixed point. Next, we construct  $\Sigma$ , a transverse arc at  $x$ . We know that  $\theta^+(q)$  intersects  $\Sigma$  in a monotone sequence,  $\{q_n\} \rightarrow x$  as  $n \rightarrow \infty$ . Due to the invariance of  $\omega(p)$ ,  $q_n \in \omega(p)$ . But  $\omega(p)$  has at most one intersection point with  $\Sigma$ , thus  $q_n = x$ , for all  $n$ . It follows that the orbit of  $q$  is closed.

Now construct a transverse arc  $\Sigma'$  at  $q$ . We know that  $\omega(p)$  intersects  $\Sigma'$  only at  $q$ . Since  $\omega(q)$  is a union of orbits without fixed points and  $\omega(p)$  is connected,  $\omega(p) = \theta^+(q)$ . In other words,  $\omega(p)$  contains only the closed orbit of  $q$ . This finished the proof of the lemma. ■

We are now fully armed to prove the Poincaré-Bendixson theorem.

**Theorem 10 (Poincaré-Bendixson)** *Let  $M$  be a positively invariant region of a vector field, containing only a finite number of fixed points. Let  $p \in M$ . Then one of the following three possibilities holds: (i)  $\omega(p)$  is a fixed point; (ii)  $\omega(p)$  is a closed orbit; or (iii)  $\omega(p)$  consists of a finite number of fixed points  $p_1, \dots, p_n$  and orbits  $\gamma$  such that  $\alpha(\gamma) = p_i$  and  $\omega(\gamma) = p_j$ , where  $p_i$  and  $p_j$  are among the fixed points.*

**Proof.** If  $\omega(p)$  contains only fixed points, it must be a unique fixed point, since  $\omega(p)$  is connected. Next, if  $\omega(p)$  contains no fixed points, it is a closed orbit, by the previous lemma.

Now suppose  $\omega(p)$  contains both fixed points, and points that are not fixed. Let  $\gamma$  be a trajectory consisting of such nonfixed points. Then  $\omega(\gamma)$  and  $\alpha(\gamma)$  must be fixed points contained in  $\omega(p)$ . Indeed, if this were not the case, they would be periodic orbits, by the previous lemma. They can't be periodic orbits, as  $\omega(p)$  contains fixed points and is connected.

This finishes the proof of the Poincaré-Bendixson theorem. ■

Several remarks and questions are in order:

- In particular, the Poincaré-Bendixson theorem tells us that for two-dimensional, autonomous vector fields (in  $\mathbb{R}^2$ , on the cylinder or on the sphere) chaos is not possible: there cannot be any strange attractors, nor can there be any covering orbits. It should be noted that on  $\mathbb{T}^2$  (The two-dimensional torus), it is possible to have a dense orbit, which is a hallmark of chaos, as we will see.
- Do you see where we used that we were on  $\mathbb{R}^2$ , on the cylinder or on the sphere?
- Can you think of a phase portrait were situation (iii) would occur?



# Chapter 7

## Poincaré maps

We have now established, using the Poincaré-Bendixson theorem that two-dimensional autonomous flows exhibit only limited types of behavior. Thus, to witness the full range of possible behavior in flows, we have to either consider nonautonomous flows, or higher-dimensional flows. Either way, we end up with at least three effective dimensions. Even in the three-dimensional case, visualizing what is happening is a lot harder than in a two-dimensional setting.

In many cases, we may effectively decrease the dimension of the system under consideration by taking a Poincaré section of a flow, ending up with a Poincaré map.

### Remarks.

- Big caveat: there is no algorithmic way to determine how to construct a Poincaré map. There are a few pointers that help in specific cases. We'll discuss a few of these.
- Nowadays, essentially any map that is associated with a higher-dimensional flow is referred to as a Poincaré map, even if it strictly speaking isn't one.
- Although maps are often valid in their own right, to some extent the application of Poincaré maps to higher-dimensional flows justifies the attention we have devoted to maps.

### 7.1 Poincaré maps near periodic orbits

Consider the equation

$$x' = f(x), \quad x \in \mathbb{R}^N. \quad (7.1)$$

Let  $\phi(t, x_0)$  denote the flow generated from this equation. Suppose that  $\phi(t, \hat{x}_0)$  is a periodic solution of period  $T$ :

$$\phi(t + T, \hat{x}_0) = \phi(t, \hat{x}_0). \quad (7.2)$$

Now, let  $\Sigma$  denote an  $(n - 1)$ -dimensional surface, transverse to the flow, as illustrated in Figure 7.1.

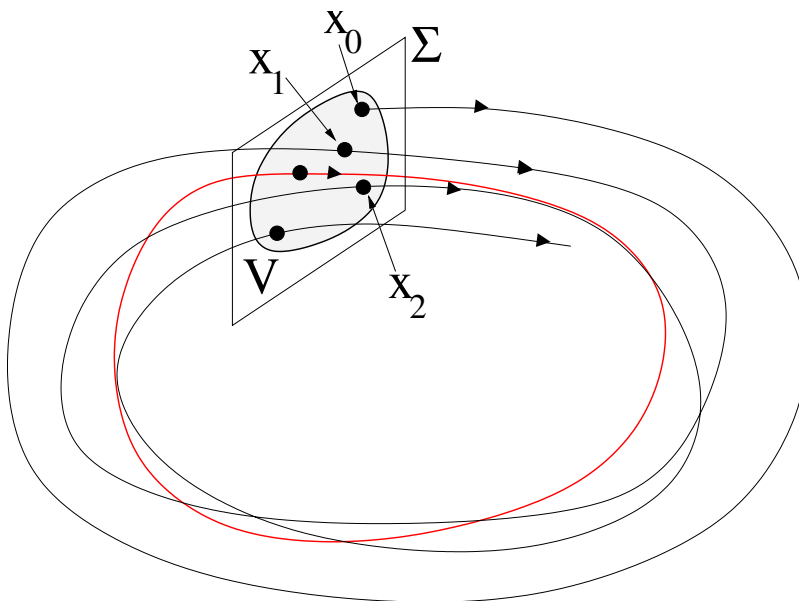


Figure 7.1: The Poincaré map near a periodic orbit.

Due to the continuity of the flow near the periodic orbit, there exists a region  $V \subset \Sigma$  which contains a set of initial conditions  $x_0$  we can use for our map: for every  $x \in V$ ,  $\phi(t, x)$  returns to  $\Sigma$ . This defines a map

$$P : V \rightarrow \Sigma : x \in V \rightarrow \phi(\tau(x), x) \in \Sigma, \quad (7.3)$$

where  $\tau(x)$  is the first return time of  $x$  to  $\Sigma$ . For instance,

$$\tau(\hat{x}_0) = T. \quad (7.4)$$

Note that it follows immediately that

$$P(x_0) = x_0, \quad (7.5)$$

and a periodic orbit of the flow is characterized as a fixed point of the map, which we call the Poincaré map. A periodic point of the Poincaré map  $P$  is a consequence of a periodic orbit of the flow of higher period than  $T$ , which pierces the transverse section  $\Sigma$  a multiple number of times.

**Example 10** Consider the system

$$\begin{cases} x' = \mu x - y - x(x^2 + y^2) \\ y' = x + \mu y - y(x^2 + y^2) \end{cases}, \quad (7.6)$$

where  $\mu > 0$ .

The phase portrait of this system is given in Figure 7.2.

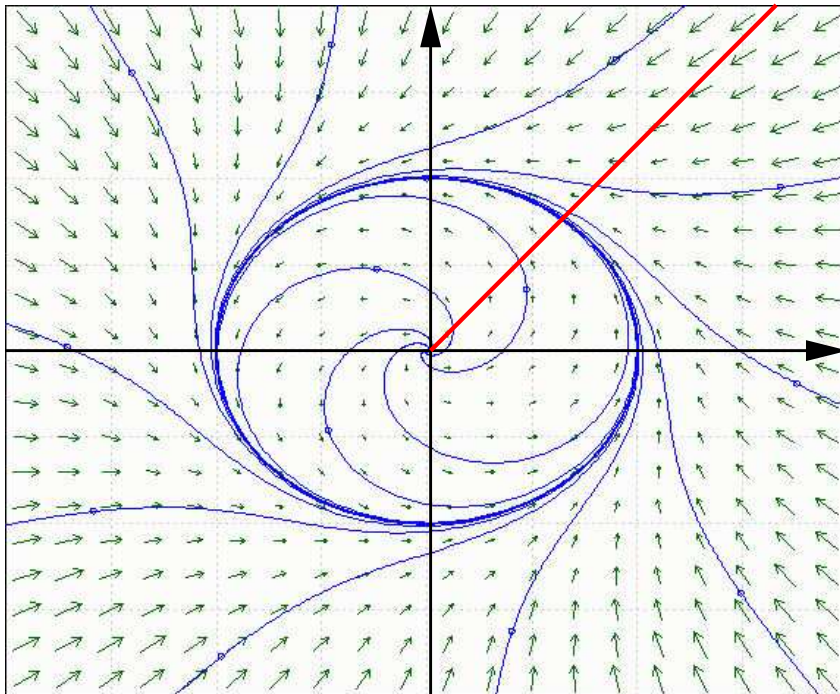


Figure 7.2: The phase portrait the system 7.6 with  $\mu = 1$ . The plot was made using pplane.

If we consider the system in polar coordinates

$$r^2 = x^2 + y^2, \quad \tan\theta = y/x, \quad (7.7)$$

then we obtain (check this!)

$$\begin{cases} r' = r(\mu - r^2) \\ \theta' = 1 \end{cases}. \quad (7.8)$$

We see immediately that the system has a periodic orbit given by  $r = \sqrt{\mu}$ . In order to explicitly construct the Poincaré map near this periodic orbit, we completely determine the flow of this system. In the polar coordinates  $(r, \theta)$ , we have

$$\phi_t(r_0, \theta_0) = \left( \left[ \frac{1}{\mu} + \left( \frac{1}{r_0^2} - \frac{1}{\mu} \right) e^{-2\mu t} \right]^{-1/2}, t + \theta_0 \right). \quad (7.9)$$

Now we are in a position to define our Poincaré section  $\Sigma$ :

$$\sigma = \{(r, \theta) \in \mathbb{R} \times S^1 \mid r > 0, \theta = \theta_0\}. \quad (7.10)$$

Note that we have omitted  $r = 0$ , to avoid the fixed point at the origin. This Poincaré section is indicated in Figure 7.2 as a red line. For this example, the resulting map on the cross section  $\Sigma$  may be constructed explicitly. We have (again, check this):

$$P : \Sigma \rightarrow \Sigma : r \rightarrow \left( \frac{1}{\mu} + \left( \frac{1}{r^2} - \frac{1}{\mu} \right) e^{-4\pi\mu} \right)^{-1/2}, \quad (7.11)$$

since the return time is  $2\pi$  for all orbits. We can check explicitly that the periodic orbit corresponds to a fixed point:

$$P(\sqrt{\mu}) = \left( \frac{1}{\mu} + \left( \frac{1}{\mu} - \frac{1}{\mu} \right) e^{-4\pi\mu} \right)^{-1/2} = \sqrt{\mu}, \quad (7.12)$$

as desired. The Poincaré map  $P$  is illustrated in Figure 7.3.

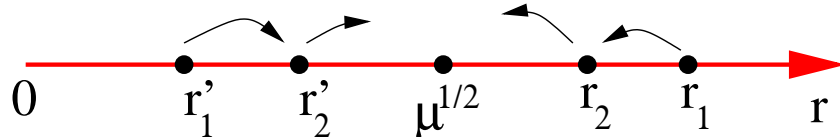


Figure 7.3: The Poincaré map  $P$  in action...

Using the Poincaré map, we can explicitly calculate the eigenvalue (there's only one, as it's a one-dimensional map) around the fixed point  $r = \sqrt{\mu}$ . We find (you know it's coming: check this)

$$\lambda = e^{-4\pi\mu} < 1, \quad (7.13)$$

from which the stability of the periodic orbit follows.

Clearly, Poincaré sections are especially useful for higher-dimensional settings, where they allow the reduction of the number of dimensions by one. The handouts I've provided from Abraham and Shaw on homoclinic tangles provide many examples of the usefulness of Poincaré sections. The dynamics of the higher-dimensional setting is significantly more complicated in these cases. For one, it is a lot easier to consider the stability of a fixed point, than that of a periodic orbit.

## 7.2 Poincaré maps of a time-periodic problem

Consider the following non-autonomous system

$$x' = f(x, t), \quad x \in \mathbb{R}^N, \quad (7.14)$$

where

$$f(x, t) = f(x, t + T), \quad (7.15)$$

and  $T$  is referred to as the (external) period. This system is rewritten as an autonomous system:

$$\begin{cases} x' &= f(x, (\theta - \theta_0)/\omega) \\ \theta' &= \omega, \end{cases}, \quad (7.16)$$

where

$$T = \frac{2\pi}{\omega}. \quad (7.17)$$

It follows immediately that

$$\theta = \omega t + \theta_0 \quad \text{mod } 2\pi. \quad (7.18)$$

We define the Poincaré section as

$$\Sigma = \{(x, \theta) \in \mathbb{R}^N \times S^1 \mid \theta = \bar{\theta}_0 \in (0, 2\pi]\}, \quad (7.19)$$

which is always transverse to the flow. The Poincaré map is

$$P : \Sigma \rightarrow \Sigma : x \left( \frac{\bar{\theta}_0 - \theta_0}{\omega} \right) \rightarrow x \left( \frac{\bar{\theta}_0 + 2\pi - \theta_0}{\omega} \right). \quad (7.20)$$

In the next section, an extended example of this is considered.

### 7.3 Example: the periodically forced oscillator

As an example of the Poincaré map for nonautonomous systems, consider the periodically forced oscillator:

$$x'' + \delta x' + \omega_0^2 x = \gamma \cos \omega t. \quad (7.21)$$

For all our considerations, we assume that  $\delta$  is small, so that we're in the case of subcritical damping:  $\delta^2 - 4\omega_0^2 < 0$ . In that case the solution of the unforced problem is

$$x_H = c_1 e^{-\delta t/2} \cos \bar{\omega} t + c_2 e^{-\delta t/2} \sin \bar{\omega} t, \quad (7.22)$$

where

$$\bar{\omega} = \frac{1}{2} \sqrt{4\omega_0^2 - \delta^2}. \quad (7.23)$$

It should be noted that  $\lim_{t \rightarrow \infty} x_H = 0$ . In other words, the long-time behavior of solutions of (7.21) is governed by the particular solution

$$x_P = A \cos \omega t + B \sin \omega t, \quad (7.24)$$

with

$$A = \frac{\gamma(\omega_0^2 - \omega^2)}{(\omega_0^2 - \omega^2)^2 + (\delta\omega)^2}, \quad B = \frac{\gamma\delta\omega}{(\omega_0^2 - \omega^2)^2 + (\delta\omega)^2}. \quad (7.25)$$

Writing down these formulas (which you should check; might be some \$'s in it!) we have assumed we are in the nonresonant case:  $(\delta, \omega) \neq (0, \omega_0)$ .

## 1. The damped forced oscillator

In order to construct the Poincaré map, we rewrite the equation (7.21) as a system:

$$\begin{cases} x' = y \\ y' = -\omega_0^2 x - \delta y + \gamma \cos \omega t \end{cases}, \quad (7.26)$$

or,

$$\begin{cases} x' = y \\ y' = -\omega_0^2 x - \delta y + \gamma \cos \theta \\ \theta' = \omega \end{cases}, \quad (7.27)$$

in autonomous form. Using the explicit form of the homogeneous and particular solutions, we may construct the Poincaré map explicitly. However, at this point we merely examine what the phase portrait of the map looks like, especially near the fixed point of the map corresponding to the periodic solution obtained from the particular solution:

$$\begin{aligned} x_P &= A \cos \omega t + B \sin \omega t \\ &= A \cos \theta + B \sin \theta \end{aligned} \quad (7.28)$$

$$\Rightarrow y_P = x'_P = -\omega A \sin \theta + \omega B \cos \theta. \quad (7.29)$$

We may choose  $\bar{\theta}_0 = 0 = \theta_0$ , resulting in

$$x_P \left( \frac{\bar{\theta}_0 - \theta_0}{\omega} \right) = x_P(0) = A, \quad (7.30)$$

and

$$x_P \left( \frac{\bar{\theta}_0 + 2\pi - \theta_0}{\omega} \right) = x_P(2\pi/\omega) = A. \quad (7.31)$$

Similarly,

$$y_P(0) = \omega B \quad (7.32)$$

is fixed, thus

$$P \begin{pmatrix} A \\ \omega B \end{pmatrix} = \begin{pmatrix} A \\ \omega B \end{pmatrix} \quad (7.33)$$

is a fixed point of the Poincaré map. Furthermore, all other solutions approach the periodic orbit (since  $x_H \rightarrow 0$ , as  $t \rightarrow \infty$ ), thus the fixed point is an asymptotically stable spiral (due to the subcritical damping) point of the Poincaré map  $P$ . The phase portrait of the map near the fixed point is displayed in Figure 7.4. The orbits of the map approach the fixed point along spirals.

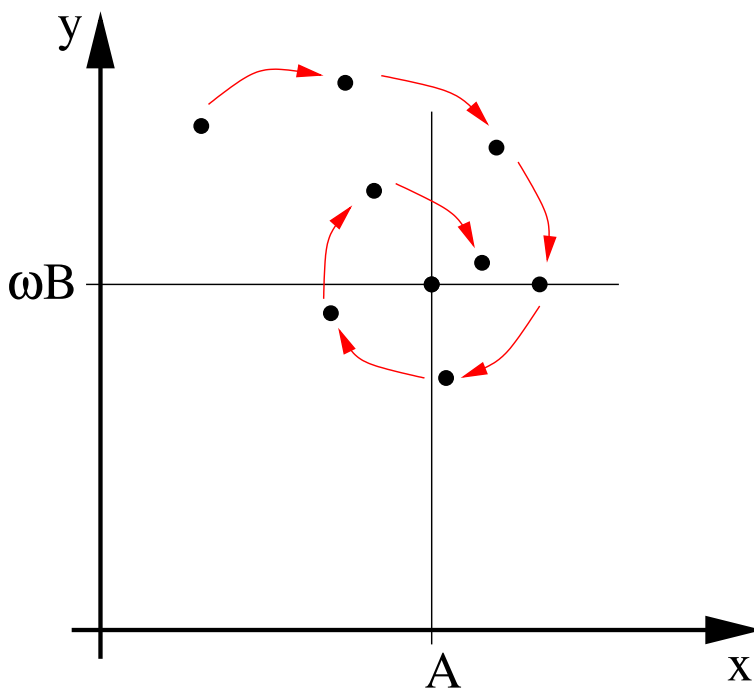


Figure 7.4: The Poincaré map  $P$  near the asymptotically stable spiral point corresponding to the particular solution of the forced oscillator.

## 2. The undamped forced oscillator

Next, we consider the case

$$\delta = 0. \quad (7.34)$$

We have

$$\begin{cases} x' = y \\ y' = -\omega_0^2 x + \gamma \cos \theta \\ \theta' = \omega. \end{cases} \quad (7.35)$$

Note that for the undamped case  $\omega_0$  is the natural frequency of the system. The solution is written as (remember we're assuming we don't have resonance!)

$$x = c_1 \cos \omega_0 t + c_2 \sin \omega_0 t + A \cos \omega t, \quad (7.36)$$

$$y = x' = -\omega c_1 \sin \omega_0 t + \omega c_2 \cos \omega_0 t - A\omega \sin \omega t. \quad (7.37)$$

From these equations,

$$x(0) = c_1 + A, \quad y(0) = \omega_0 c_2. \quad (7.38)$$

In order to construct the Poincaré map, we just need to find out what  $x(2\pi/\omega)$  and  $y(2\pi/\omega)$  are, and relate them to  $x(0)$  and  $y(0)$ . This is easily done:

$$\begin{aligned} x\left(\frac{2\pi}{\omega}\right) &= c_1 \cos\left(2\pi\frac{\omega_0}{\omega}\right) + c_2 \sin\left(2\pi\frac{\omega_0}{\omega}\right) + A \\ &= (x(0) - A) \cos\left(2\pi\frac{\omega_0}{\omega}\right) + \frac{y(0)}{\omega_0} \sin\left(2\pi\frac{\omega_0}{\omega}\right) + A, \end{aligned} \quad (7.39)$$

and

$$\begin{aligned} y\left(\frac{2\pi}{\omega}\right) &= -\omega_0 c_1 \sin\left(2\pi\frac{\omega_0}{\omega}\right) + \omega_0 c_2 \cos\left(2\pi\frac{\omega_0}{\omega}\right) \\ &= -\omega_0(x(0) - A) \sin\left(2\pi\frac{\omega_0}{\omega}\right) + y(0) \cos\left(2\pi\frac{\omega_0}{\omega}\right). \end{aligned} \quad (7.40)$$

Now it's easy to read off the Poincaré map  $P$ :

$$P : \begin{pmatrix} x \\ y \end{pmatrix} \rightarrow \begin{pmatrix} \cos 2\pi\frac{\omega_0}{\omega} & \frac{1}{\omega_0} \sin 2\pi\frac{\omega_0}{\omega} \\ -\omega_0 \sin 2\pi\frac{\omega_0}{\omega} & \cos 2\pi\frac{\omega_0}{\omega} \end{pmatrix} \begin{pmatrix} x \\ y \end{pmatrix} + \begin{pmatrix} A(1 - \cos 2\pi\frac{\omega_0}{\omega}) \\ A\omega_0 \sin 2\pi\frac{\omega_0}{\omega} \end{pmatrix}. \quad (7.41)$$

Even though this is a linear map, it's a bit complicated. Because of this, we let

$$z = x + i\frac{y}{\omega_0}. \quad (7.42)$$

You should verify that in this complex variable, the Poincaré map can be written as

$$P : z \rightarrow (z - A)e^{-i2\pi\omega_0/\omega} + A, \quad (7.43)$$

or, even more convenient,

$$P : z - A \rightarrow (z - A)e^{-i2\pi\omega_0/\omega}. \quad (7.44)$$

Using this coordinate representation, it is easy to see what's going on: The map  $P$  merely multiplies (scales, rotates)  $z - A$  by the factor  $e^{-i2\pi\omega_0/\omega}$ . Furthermore, we see immediately that

$$z = A \tag{7.45}$$

is a fixed point, which corresponds to the periodic orbit, since

$$x + i\frac{y}{\omega_0} = A \Rightarrow (x, y) = (A, 0). \tag{7.46}$$

In the original  $(x, y, \theta)$  coordinates, this fixed point corresponds to

$$\begin{cases} x = A \cos \omega t \\ y = -A\omega \sin \omega t \\ \theta = \omega t \pmod{2\pi}. \end{cases} \tag{7.47}$$

This represents a helix in three-dimensional space: it's a solution spiraling around a cylinder. Since  $\theta$  is defined modulo  $2\pi$ , this cylinder closes on itself, resulting in a torus. The Poincaré section then consists of cutting this torus at  $\theta = 0$ , and plotting where the solution is at all stages where it crosses this section. Our periodic solution (continuous time) goes around the torus once during a revolution, resulting in a single point in the Poincaré section. This motion is illustrated in Figure 7.5. For convenience we have flattened the torus into a square where the edges are to be identified.

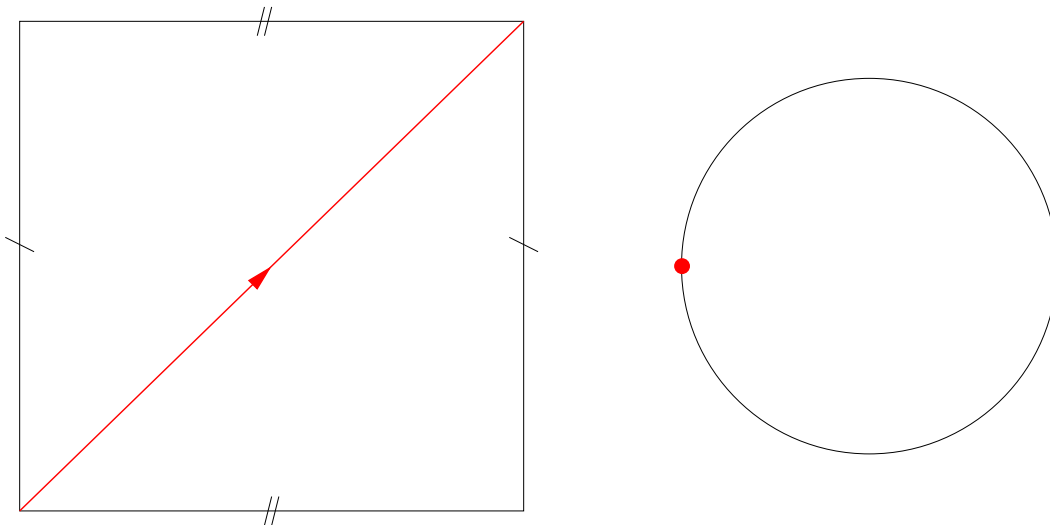


Figure 7.5: The motion of the periodic orbit on the torus (left; continuous time), and its corresponding picture using the Poincaré section (right).

In the remainder of this section we examine the other types of motion that take place on the Poincaré section. Clearly, all is determined by the ratio  $\omega_0/\omega$ .

## Superharmonic response

Suppose that

$$\omega_0 = n\omega, \quad (7.48)$$

where  $n > 1$  is an integer. Since the system responds to the forcing with a frequency that is greater than the forcing frequency, this case is called *ultra- or superharmonic response*. The Poincaré map becomes

$$P : \begin{pmatrix} x \\ y \end{pmatrix} \rightarrow \begin{pmatrix} 1 & 0 \\ 0 & 1 \end{pmatrix} \begin{pmatrix} x \\ y \end{pmatrix} + \begin{pmatrix} 0 \\ 0 \end{pmatrix} = \begin{pmatrix} x \\ y \end{pmatrix}, \quad (7.49)$$

or, using the complex notation,

$$P : z \rightarrow z. \quad (7.50)$$

Thus every point is a fixed point. In this case every orbit encircles the cylinder exactly  $n$  times between Poincaré sections. This motion is illustrated in Figure 7.6.

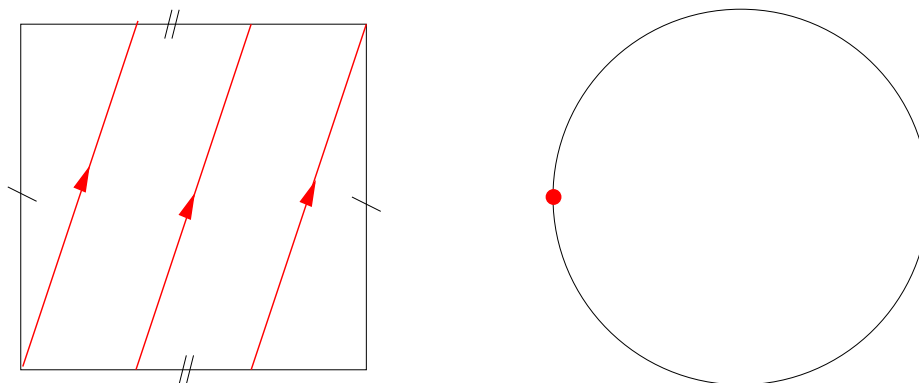


Figure 7.6: Superharmonic response:  $n = 3$ . The motion of the periodic orbit on the torus (left; continuous time), and its corresponding picture using the Poincaré section (right).

## Subharmonic response

Suppose that

$$\omega_0 = \omega/m, \quad (7.51)$$

where  $m > 1$  is an integer. Since the system responds to the forcing with a frequency that is less than the forcing frequency, this case is called *subharmonic response*. The Poincaré map is given by

$$P : \begin{pmatrix} x \\ y \end{pmatrix} \rightarrow \begin{pmatrix} \cos \frac{2\pi}{m} & \frac{1}{\omega_0} \sin \frac{2\pi}{m} \\ -\omega_0 \sin \frac{2\pi}{m} & \cos \frac{2\pi}{m} \end{pmatrix} \begin{pmatrix} x \\ y \end{pmatrix} + \begin{pmatrix} A(1 - \cos \frac{2\pi}{m}) \\ A\omega_0 \sin \frac{2\pi}{m} \end{pmatrix}, \quad (7.52)$$

or, using the complex notation,

$$P : z - A \rightarrow (z - A)e^{-i2\pi/m}. \quad (7.53)$$

Thus

$$P^m : z - A \rightarrow (z - A)(e^{-i2\pi/m})^m = z - A. \quad (7.54)$$

Thus, every point is a fixed point of  $P^m$ . This implies that every orbit goes through  $m$  Poincaré sections before it encircles the cylinder once. Thus, every orbit is periodic of period  $m$ . This motion is illustrated in Figure 7.7.

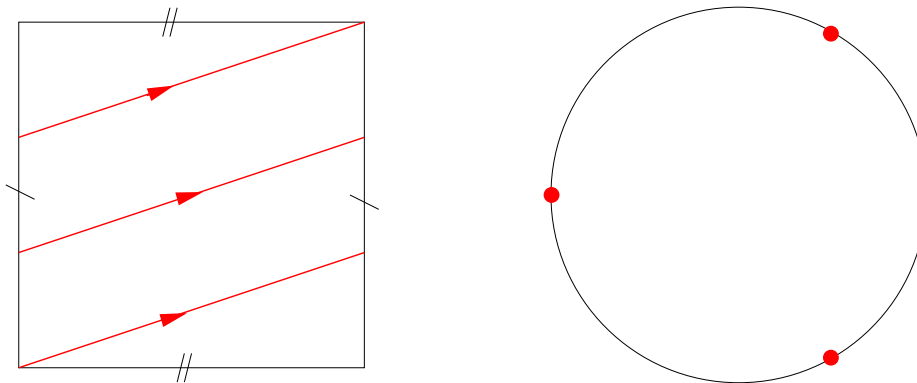


Figure 7.7: Subharmonic response:  $m = 3$ . The motion of the periodic orbit on the torus (left; continuous time), and its corresponding picture using the Poincaré section (right).

### Response of order $(m, n)$

Suppose that

$$\omega_0 = n\omega/m, \quad (7.55)$$

where  $m, n > 1$  are integers. The complex form of the Poincaré map is given by

$$P : z - A \rightarrow (z - A)e^{-i2\pi n/m}. \quad (7.56)$$

As in the previous case,

$$P^m : z - A \rightarrow (z - A)e^{-i2\pi n/m^m} = z - A. \quad (7.57)$$

Thus, every point is a fixed point of  $P^m$ . Every orbit goes through  $m$  Poincaré sections before it encircles the cylinder exactly  $n$  times. Thus, every orbit is periodic of period  $m$ . This motion is illustrated in Figure 7.8.

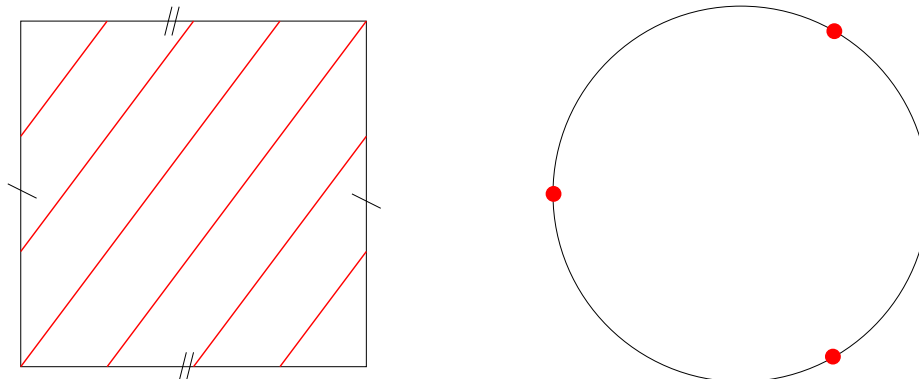


Figure 7.8: Response of order  $(m, n)$ :  $m = 3$ ,  $n = 4$ . The motion of the periodic orbit on the torus (left; continuous time), and its corresponding picture using the Poincaré section (right).

### Quasiperiodic response

Lastly, we have the case of quasi-periodic response. Suppose that

$$\frac{\omega}{\omega_0} \notin \mathbb{Q}, \quad (7.58)$$

then we get that no power of  $P$  is the identity. As a consequence, there is no periodic orbit, and we get a graphical representation as in Figure 7.9: the different intersection points densely fill in the circle. In terms of the continuous time variable, the entire torus is densely covered by the straight-line orbit with nonrational slope.

To obtain this result, we have used the following theorem.

**Theorem 11** *Suppose the circle  $S^1$  is rotated through an angle  $\alpha$  and  $\alpha$  is incommensurate with  $2\pi$ . Then the sequence*

$$S = \{\theta, \theta + \alpha, \theta + 2\alpha, \dots, (\text{mod } 2\pi)\}$$

*is everywhere dense on the circle.*

**Proof.** It is clear that no two elements in the sequence  $S$  are identical. Therefore  $S$  is truly infinite and never repeats.

Now, let  $k > 0$  be an arbitrary integer. Divide the circle in  $k$  equal-length half-open intervals of length  $2\pi/k$ . Among the first  $k + 1$  points of  $S$ , two must lie in the same interval, say

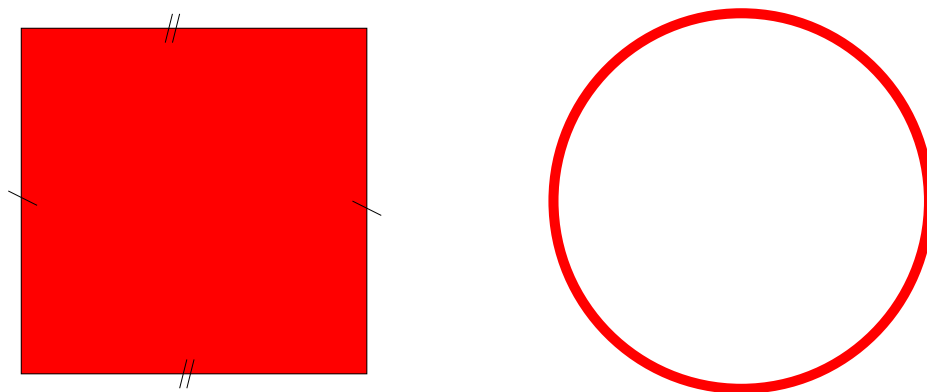


Figure 7.9: Quasiperiodic response: The motion of the periodic orbit on the torus (left; continuous time), and its corresponding picture using the Poincaré section (right).

$$\theta + p\alpha \text{ and } \theta + q\alpha \pmod{2\pi}, \quad (7.59)$$

where we have assumed that  $q > p$ . It follows that

$$(q - p)\alpha < \frac{2\pi}{k} \pmod{2\pi}. \quad (7.60)$$

Now we construct the sequence

$$\bar{S} = \{\theta, \theta + (q - p)\alpha, \theta + 2(q - p)\alpha, \dots, (\pmod{2\pi})\}. \quad (7.61)$$

Note that  $\bar{S} \subset S$ . All points in  $S$  are the same distance  $d$  apart, with  $d < 2\pi/k$ .

Now we are in a position to finish the proof: choose any point on  $S^1$ , and pick an  $\epsilon$  neighborhood around it. We choose  $k$  sufficiently large, so that  $2\pi/k < \epsilon$ . Thus, at least one of the elements of  $\bar{S}$  will lie in the  $\epsilon$  neighborhood. This concludes the proof. ■



# Chapter 8

## Hamiltonian systems

Thus far, we have talked about general systems, without using any of their specific properties. In this chapter, we look specifically at Hamiltonian systems and their properties. We will look also at the discrete equivalent of these systems, so-called symplectic maps. To finish off this chapter, we briefly discuss (without proof) the famous KAM theorem.

### 8.1 Definition and basic properties

**Definition 13 (Hamiltonian system)** *Given a function  $H(q, p)$ ,  $q \in \mathbb{R}^N$ ,  $p \in \mathbb{R}^N$ , a Hamiltonian system with canonical coordinates  $q$  and  $p$  is defined as*

$$\begin{cases} q' &= \frac{\partial H}{\partial p} \\ p' &= -\frac{\partial H}{\partial q} \end{cases}, \quad (8.1)$$

where the differentiation is componentwise. It should be noted that there are more general Hamiltonian systems that are expressed in coordinates that are not canonical. These will not be considered here.

**Example 11** *Consider a conservative mechanical system with coordinates  $q$ , momenta  $p$  and total energy*

$$H = \sum_{i=1}^N \frac{p_i^2}{2m_i} + V(q). \quad (8.2)$$

*Newton's equations for this system are equivalent to*

$$\begin{cases} q'_i &= \frac{\partial H}{\partial p_i} = \frac{p_i}{m_i} \\ p'_i &= -\frac{\partial H}{\partial q_i} = -\frac{\partial V}{\partial q_i} \end{cases}, \quad (8.3)$$

from which we obtain

$$m_i q_i'' = p_i' = -\frac{\partial V}{\partial q_i}, \quad (8.4)$$

which are Newton's equations indeed.

## Variational Formulation

Hamilton's equations may be derived from a variational principle: let

$$S = \int_{t=a}^{t=b} (pq' - H) dt. \quad (8.5)$$

Then

$$\delta S = 0 \Leftrightarrow \begin{cases} \frac{\delta S}{\delta q} = 0 = -\frac{\partial H}{\partial q} - p' \\ \frac{\delta S}{\delta p} = 0 = q' - \frac{\partial H}{\partial p}, \end{cases}, \quad (8.6)$$

from which Hamilton's equations follow.

## The symplectic matrix

Hamilton's equations may be written more concisely using the matrix

$$J = \begin{pmatrix} 0 & I \\ -I & 0 \end{pmatrix}, \quad (8.7)$$

where  $I$  denotes the  $N$ -dimensional identity matrix. Setting

$$x = \begin{pmatrix} q \\ p \end{pmatrix}, \quad (8.8)$$

we have

$$x' = J\nabla H. \quad (8.9)$$

The space of all  $x$ -vectors is referred to as the phase space of the Hamiltonian system. We denote a system with Hamiltonian  $H$  and phase space coordinates  $x$  as an  $(H, x)$  system.

## The Hamiltonian is conserved

**Theorem 12** *The Hamiltonian  $H$  of the Hamiltonian system  $(H, x)$  is a first integral of the system.*

**Proof.** The proof is an easy calculation:

$$\begin{aligned} H'(q, p) &= \frac{\partial H}{\partial q} q' + \frac{\partial H}{\partial p} p' \\ &= \frac{\partial H}{\partial q} \frac{\partial H}{\partial p} - \frac{\partial H}{\partial p} \frac{\partial H}{\partial q} \\ &= 0, \end{aligned}$$

which concludes the proof. ■

## Poisson brackets

**Definition 14 (Poisson bracket)** *The Poisson bracket of any two functions  $F$  and  $G$  defined on the phase space is given by*

$$\begin{aligned} \{F, G\} &= \frac{\partial F}{\partial q} \frac{\partial G}{\partial p} - \frac{\partial F}{\partial p} \frac{\partial G}{\partial q} \\ &= \sum_{j=1}^N \left( \frac{\partial F}{\partial q_j} \frac{\partial G}{\partial p_j} - \frac{\partial F}{\partial p_j} \frac{\partial G}{\partial q_j} \right). \end{aligned} \tag{8.10}$$

If  $\{F, G\} = 0$ , we say that  $F$  and  $G$  Poisson commute.

**Theorem 13** *The time derivative of any function defined on the phase space for the system  $(H, x)$  is given by*

$$F' = \{F, H\}. \tag{8.11}$$

**Proof.** This is another straightforward calculation:

$$\begin{aligned} F' &= \frac{\partial F}{\partial q} q' + \frac{\partial F}{\partial p} p' \\ &= \frac{\partial F}{\partial q} \frac{\partial H}{\partial p} - \frac{\partial F}{\partial p} \frac{\partial H}{\partial q} \\ &= \{F, H\}, \end{aligned}$$

by definition. This finishes the proof. ■

**Corollary 2**  *$F$  is an integral for the system  $(H, x)$  if and only if  $\{F, H\} = 0$ . In other words,  $F$  is conserved if and only if it Poisson commutes with the Hamiltonian.*

Hamilton's equations can be reformulated using the Poisson bracket. Indeed, the equations (8.1) are equivalent to

$$\begin{cases} q' &= \{q, H\} \\ p' &= \{p, H\} \end{cases}, \quad (8.12)$$

or

$$x'_i = \{x_i, H\}, \quad (8.13)$$

since

$$\{q_i, p_j\} = \delta_{ij}, \quad \{q_i, q_j\} = 0, \quad \{p_i, p_j\} = 0, \quad (8.14)$$

for  $i, j = 1 \dots N$ , and  $\delta_{ij}$  is the familiar Krönecker delta. Lastly, the Poisson bracket satisfies the following identities (check!):

$$\{F, aG_1 + bG_2\} = a\{F, G_1\} + b\{F, G_2\}, \quad (\text{Linearity}), \quad (8.15)$$

$$\{F, G\} = -\{G, F\} \quad (\text{Antisymmetry}), \quad (8.16)$$

$$\{F, \{G_1, G_2\}\} + \{G_1, \{G_2, F\}\} + \{G_2, \{F, G_1\}\} = 0 \quad (\text{The Jacobi identity}). \quad (8.17)$$

In the above,  $F, G, G_1$  and  $G_2$  are arbitrary functions defined on the phase space, and  $a, b$  are real constants.

## Commuting flows

For any  $F$  on the phase space, we may consider the vector field it generates:

$$\frac{dx}{dt_F} = J\nabla F = \{x, F\}, \quad (8.18)$$

where  $t_F$  denotes an evolution variable linked with the quantity  $F$ .

**Theorem 14 (Flows generated by first integrals mutually commute)** *If  $F$  is a first integral of the system  $(H, x)$ , then the vector fields generated by  $F$  and  $H$  commute.*

**Proof.** Again, a direct calculation, but a little more subtle now:

$$\begin{aligned} \frac{d}{dt_F} \frac{d}{dt_H} x &= \frac{d}{dt_F} \{x, H\} && (\text{By definition}) \\ &= \{\{x, H\}, F\} && (\text{By definition}) \\ &= -\{\{H, F\}, x\} - \{\{F, x\}, H\} && (\text{Jacobi identity}) \\ &= -\{\{F, x\}, H\} && (\text{since } \{H, F\} = 0) \\ &= \{\{x, F\}, H\} && (\text{Antisymmetry}) \\ &= \frac{d}{dt_H} \{x, F\} && (\text{By definition}) \\ &= \frac{d}{dt_H} \frac{d}{dt_F} x, && (\text{By definition}) \end{aligned}$$

which is what we had to prove. ■

## Hamiltonian flows are volume preserving

**Theorem 15** *Hamiltonian systems are volume preserving.*

**Proof.** We have to compute the divergence of the system equations:

$$\begin{aligned}\nabla \cdot (q', p') &= \left( \frac{\partial}{\partial q}, \frac{\partial}{\partial p} \right) \cdot \left( \frac{\partial H}{\partial q}, -\frac{\partial H}{\partial p} \right) \\ &= \frac{\partial^2 H}{\partial q \partial p} - \frac{\partial^2 H}{\partial p \partial q} \\ &= 0,\end{aligned}$$

which is what we had to show. ■

## 8.2 Symplectic or canonical transformations

**Definition 15 (Symplectic or canonical transformation)** *A symplectic or canonical transformation is a transformation*

$$(q, p) \rightarrow (Q, P) \tag{8.19}$$

*which leaves the Poisson bracket invariant.*

In other words,

$$\{F, G\}_{(Q, P)} = \{F, G\}_{(q, p)}, \tag{8.20}$$

where the notation  $\{F, G\}_{(Q, P)}$  is meant to signify that the Poisson bracket is expressed in terms of the variables  $Q$  and  $P$ . Imposing the above condition, we find that

$$A^T J A = J, \tag{8.21}$$

where  $A$  is the Jacobian of the transformation:

$$A = \begin{pmatrix} \frac{\partial Q}{\partial q} & \frac{\partial Q}{\partial p} \\ \frac{\partial P}{\partial q} & \frac{\partial P}{\partial p} \end{pmatrix}. \tag{8.22}$$

A matrix satisfying (8.21) is called a *symplectic matrix*. The following theorem characterizes the eigenvalues of a symplectic matrix.

**Theorem 16** *If  $\lambda \in \mathbb{C}$  is an eigenvalue of  $A$ , then so are  $\bar{\lambda}$ ,  $1/\lambda$ , and  $1/\bar{\lambda}$ . Further, the multiplicities of  $\lambda$  and  $1/\lambda$  are identical. Lastly, if  $\pm 1$  are eigenvalues, they have even multiplicity.*

**Proof.** Denote the characteristic equation of  $A$  by  $p(\lambda)$ . Then

$$\begin{aligned}
 p(\lambda) &= \det(A - \lambda I) \\
 &= \det(J(A - \lambda I)J^{-1}) \\
 &= \det[(JA - \lambda J)J^{-1}] \\
 &= \det[(A^{-T}J - \lambda J)J^{-1}] \\
 &= \det(A^{-T} - \lambda I) \\
 &= \det(A^{-1} - \lambda I) \\
 &= \det A^{-1} \det(I - \lambda A) \\
 &= \det(A^{-1}) \det\left(\frac{1}{\lambda}I - A\right) \lambda^{2N} \\
 &= \lambda^{2N} p(1/\lambda).
 \end{aligned}$$

From this it follows that if  $\lambda$  is a root of the characteristic equation, then so is  $1/\lambda$ . Further, since  $p(\lambda)$  has real coefficients,  $\bar{\lambda}$  is also a root. This proves that eigenvalues occur in quartets.

We have used the fact that  $A$  is symplectic, but also that the determinant of  $A$  is nonzero. Indeed, since  $A$  is symplectic, we have

$$\begin{aligned}
 &A^T J A = J \\
 \Rightarrow &\det(A^T J A) = \det J \\
 \Rightarrow &\det A^T \det J \det A = \det J \\
 \Rightarrow &(\det A)^2 = 1 \\
 \Rightarrow &\det A = \pm 1.
 \end{aligned}$$

In the homework, you'll show that  $\det A = 1$ .

Next, we'll talk about multiplicities. Suppose  $\lambda_0$  is an eigenvalue of  $A$  of multiplicity  $k$ . Then

$$p(\lambda) = (\lambda - \lambda_0)^k Q(\lambda), \quad (8.23)$$

where  $Q(\lambda)$  is of degree  $2N - k$ . Using the last line of the above, we have that

$$\begin{aligned}
 \lambda^{2N} p(1/\lambda) &= (\lambda - \lambda_0)^k Q(\lambda) \\
 &= (\lambda \lambda_0)^k \left(\frac{1}{\lambda_0} - \frac{1}{\lambda}\right)^k Q(\lambda),
 \end{aligned}$$

so that

$$p(1/\lambda) = \lambda_0^k \left(\frac{1}{\lambda_0} - \frac{1}{\lambda}\right)^k \frac{Q(\lambda)}{\lambda^{2N-k}}. \quad (8.24)$$

The left-hand side is a polynomial in  $1/\lambda$ , so the right-hand side must be as well. Specifically, the last fraction in the right-hand side must be polynomial in  $1/\lambda$  of degree  $2N - k$ . It follows that  $1/\lambda_0$  is an eigenvalue of multiplicity at least  $k$ . On the other hand, by reversing the roles of  $\lambda_0$  and  $1/\lambda_0$ , we obtain that the multiplicity of  $1/\lambda_0$  is at most  $k$ . It follows that  $1/\lambda_0$  is an eigenvalue of multiplicity exactly  $k$ .

Lastly, we look at the multiplicities of any eigenvalues located at  $\pm 1$ . For all other possible eigenvalues, there is either a quartet or pair of eigenvalues, meaning that after dividing  $p(\lambda)$  by all these factors, we are left with a polynomial of even degree that has roots at only 1 and/or  $-1$ . Thus it is of the form

$$(\lambda - 1)^m(\lambda + 1)^n, \quad (8.25)$$

where  $m$  ( $n$ ) is the multiplicity of 1 ( $-1$ ). We also know that  $m + n$  should be even. We also know that this remaining polynomial must have the symmetry on its coefficients so that the coefficients of  $\lambda^k$  equals the coefficient of  $\lambda^{d-k}$ , where  $d$  is the degree. It follows that the multiplicity of 1 is even, to preserve this symmetry. As a consequence, the multiplicity of  $-1$  is also even. This concludes the proof. ■

A picture of the location of an eigenvalue quartet is shown in Figure 8.1.

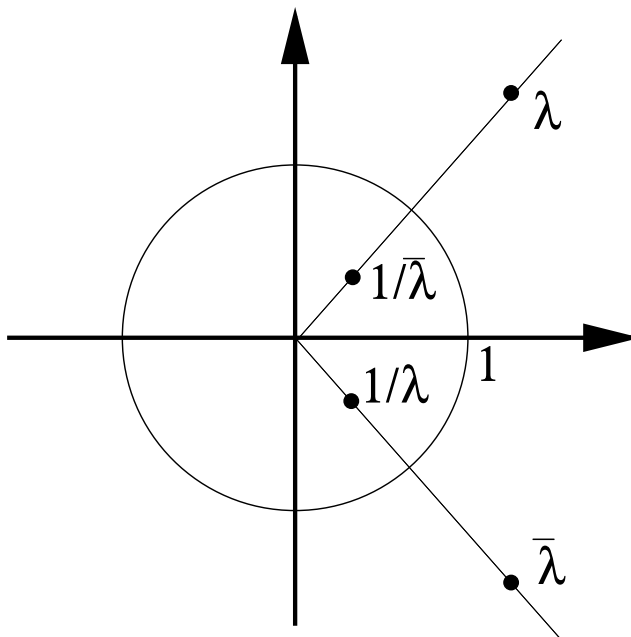


Figure 8.1: A quartet of eigenvalues of a symplectic matrix.

It follows from the definition of a symplectic matrix that the identity matrix is symplectic (in fact, the symplectic matrices form a group). Now suppose that we have a symplectic matrix that is an analytic perturbation of the identity matrix:

$$A(\epsilon) = I + \epsilon B + \theta(\epsilon^2), \quad (8.26)$$

with  $\epsilon$  small. In order for  $A(\epsilon)$  to be symplectic, we need

$$\begin{aligned} & (I + \epsilon B + \theta(\epsilon^2))^T J (I + \epsilon B + \theta(\epsilon^2)) = J \\ \Rightarrow & (I + \epsilon B^T + \theta(\epsilon^2))(J + \epsilon JB + \theta(\epsilon^2)) = J \\ \Rightarrow & J + \epsilon B^T J + \epsilon JB + \theta(\epsilon^2) = J \\ \Rightarrow & B^T J + JB = 0. \end{aligned} \quad (8.27)$$

A matrix  $B$  which satisfies this last equality is called an *infinitesimal symplectic matrix* or *infinitesimal symplectic transformation*. The following theorem explains the importance of infinitesimal symplectic matrices.

**Theorem 17** *The Jacobian of a Hamiltonian vector field is an infinitesimal symplectic transformation. Also, if the Jacobian of a vector field is an infinitesimal symplectic transformation, then that vector field is Hamiltonian.*

**Proof.** The first part is a straightforward calculation:

$$\begin{pmatrix} H_{pq} & H_{pp} \\ -H_{qq} & -H_{pq} \end{pmatrix} \begin{pmatrix} 0 & I \\ -I & 0 \end{pmatrix} + \begin{pmatrix} 0 & I \\ -I & 0 \end{pmatrix} \begin{pmatrix} H_{pq} & H_{pp} \\ -H_{qq} & -H_{pq} \end{pmatrix} = 0. \quad (8.28)$$

Here indices denote differentiation. This proves that the Jacobian of a Hamiltonian vector field is an infinitesimal symplectic transformation.

The second part is a bit more involved and requires the use of a *homotopy operator*: let

$$H = \int_0^1 (f(tx), Jx) dt, \quad (8.29)$$

where the parentheses denote a scalar product and  $f(x)$  is the given vector field. Then, for any  $v$  we have

$$\begin{aligned}
(\nabla H, v) &= \int_0^1 (t\nabla f(tx)v, Jx) dt + \int_0^1 (f(tx), Jv) dt \\
&= \int_0^1 t (J^T \nabla f(tx)v, x) dt + \int_0^1 (f(tx), Jv) dt \\
&= - \int_0^1 t (J \nabla f(tx)v, x) dt + \int_0^1 (f(tx), Jv) dt \\
&= \int_0^1 t ((\nabla f(tx))^T Jv, x) dt + \int_0^1 (f(tx), Jv) dt \\
&= \int_0^1 t (Jv, \nabla f(tx)x) dt + \int_0^1 (f(tx), Jv) dt \\
&= \int_0^1 t (\nabla f(tx)x, Jv) dt + \int_0^1 (f(tx), Jv) dt \\
&= \int_0^1 (t\nabla f(tx)x + f(tx), Jv) dt \\
&= \int_0^1 \left( Jv, \frac{d}{dt} t f(tx) \right) dt \\
&= (Jv, f(x)) \\
&= -(v, Jf(x)) \\
&= -(Jf(x), v).
\end{aligned}$$

Since  $v$  is arbitrary, we have that

$$\nabla H = -Jf(x) \quad \Rightarrow \quad f(x) = J\nabla H, \quad (8.30)$$

and thus  $f(x)$  is a Hamiltonian vector field, with Hamiltonian  $H$ . This concludes the proof.  $\blacksquare$

Just like symplectic matrices, infinitesimal symplectic matrices have a peculiar eigenvalue spectrum:

**Theorem 18** *Let  $B$  be an infinitesimal symplectic matrix, i.e.,  $JB + B^T J = 0$ . Then if  $\lambda$  is an eigenvalue of  $B$ , then so are  $-\lambda$ ,  $\bar{\lambda}$ , and  $-\bar{\lambda}$ . Further, if  $\lambda$  has multiplicity  $k$ , so does  $-\lambda$ . If  $\lambda = 0$  is an eigenvalue, it has even multiplicity.*

We do not prove this theorem here. You should try it, as it is very similar to the proof of the theorem on the spectrum of symplectic matrices.

We finish this section by two results linking back to canonical (symplectic) transformations: since the linearization of a Hamiltonian vector field is an infinitesimal symplectic transformation, it should come as no surprise that the flow generated by a Hamiltonian vector field is a canonical (or symplectic) transformation, with free parameter  $t$ . The converse

also holds: if the flow generated by a vector field is symplectic, then that vector field is Hamiltonian.

### 8.3 Completely integrable Hamiltonian systems

An  $N$ -degree of freedom Hamiltonian system

$$\begin{cases} q' &= \frac{\partial H}{\partial p} \\ p' &= -\frac{\partial H}{\partial q} \end{cases} \quad (8.31)$$

is *completely integrable* if there exist  $N$  functions

$$F_1 = H, F_2, \dots, F_N \quad (8.32)$$

such that (i) The  $F_i$  are functionally independent, and (ii) the  $F_i$  mutually Poisson commute. In other words, for all  $i, j = 1, \dots, N$  we have  $\{F_i, F_j\} = 0$ . In that case the  $F_i$  are said to be in involution.

It is obvious why the first requirement is there: otherwise some of the  $F_i$  can be written in terms of some of the others, and we cannot use them as new coordinates. On the other hand, if they are independent, we can transform to a new system of coordinates where the  $F_i$  play the role of the new momentum variables  $p_i$ , whence the involution requirement. We denote the joint levelset of all the  $F_i$ 's by  $M_f$ :

$$M_f = \{(q, p) \in \mathbb{R}^{2N} \mid F_i(q, p) = f_i, i = 1, \dots, N\}. \quad (8.33)$$

**Theorem 19 (Liouville-Arnol'd)** • *For almost all  $f$ ,  $M_f$  is a manifold, as differentiable as are the  $F_i$ 's. Of course,  $M_f$  is invariant and the motion is constrained to this levelset.*

- *If  $M_f$  is compact and connected, then it is diffeomorphic to the  $N$ -dimensional torus*

$$T^N = \{(\phi_1, \dots, \phi_N) \bmod 2\pi\}. \quad (8.34)$$

- *The flow generated by (8.31) gives rise to quasiperiodic linear motion on  $T^N$ . In angular coordinates on  $M_f$ , we have*

$$\frac{d\phi}{dt} = \omega(f). \quad (8.35)$$

We do not prove this theorem here. Rather, we proceed with our set-up to understand the celebrated (every May 12th) KAM theorem. It is possible to construct a canonical transformation

$$(q, p) \rightarrow (I, \theta), \quad (8.36)$$

where

$$I = I(F), \quad (8.37)$$

and

$$\theta \in T^N. \quad (8.38)$$

In these coordinates

$$H(q, p) = K(I), \quad (8.39)$$

and

$$\begin{cases} \theta' = \frac{\partial K}{\partial I} \\ I' = -\frac{\partial K}{\partial \theta} = 0 \Rightarrow I = \text{constant}. \end{cases} \quad (8.40)$$

Since  $K(I)$  does not depend on  $\theta$ , neither does  $\partial K / \partial I$ . Thus, if we define

$$\omega(I) = \frac{\partial K}{\partial I}, \quad (8.41)$$

then

$$\theta = \omega(I)t + \theta_0. \quad (8.42)$$

The coordinates  $(I, \theta)$  are referred to as *action-angle* variables.

### **KAM theory: perturbations of completely integrable systems**

Consider an integrable system, given in action-angle variables:

$$H_0(I), \quad \text{with coordinates } (I, \theta). \quad (8.43)$$

What can be said about perturbations of such a system? Quite a bit, it turns out, as long as the perturbation is Hamiltonian. In other words, the perturbed system remains Hamiltonian, say with Hamiltonian  $H(I, \theta)$ :

$$H(I, \theta) = H_0(I) + \epsilon H_1(I, \theta). \quad (8.44)$$

Further, we assume that  $H_0(I)$  is nondegenerate, *i.e.*

$$\det \left( \frac{\partial^2 H_0}{\partial I_i \partial I_j} \right) \neq 0. \quad (8.45)$$

Then the following theorem, due to **K**olmogorov, **A**rnol'd and **M**oser holds:

**Theorem 20 (KAM)** *If  $H_0(I)$  is real-analytic and nondegenerate, and if  $H(I, \theta)$  is in  $C^r(I, \theta)$ , with  $r > 2N$ , then for sufficiently small  $\epsilon$ , the perturbed system possesses smooth invariant  $N$ -tori, on which the flow is analytically conjugate to  $\phi' = \omega$ .*

As you might expect, we won't prove this theorem here. That would take an entire course in its own right. Note that two flows  $\phi, \psi$  are *topologically conjugate* if there exists a homeomorphism  $h$  such that

$$\phi = h^{-1} \circ \psi \circ h, \tag{8.46}$$

where  $\circ$  denotes composition. In other words, orbits of one flow are mapped continuously to orbits of the other flow. Geometrically speaking, the two flows are topologically indistinguishable. Two flows are *analytically conjugate* if  $h$  and its inverse are real-analytic.

In short, the KAM theorem ensures that small perturbations leave a lot of the structure of integrable systems unaffected.

# Chapter 9

## Symbolic dynamics and the Smale Horseshoe

Let's start by defining what we mean by a map being chaotic on a set  $\Omega$ .

**Definition 16** *The map  $\phi$  is chaotic on the set  $\Omega$  if (i)  $\phi$  is sensitively dependent on initial conditions, and (ii)  $\phi$  is topologically transitive on  $\Omega$ .*

We know what is meant by the first condition. The second condition means that there exists at least one orbit of  $\phi$  which is dense on  $\Omega$ .

### 9.1 The Bernoulli shift map

The phase space for this example is given by

$$\Sigma = \{\text{bi-infinite sequences of 0's and 1's}\}. \quad (9.1)$$

Thus, any element of  $\Sigma$  is of the form

$$\sigma = (\dots \sigma_{-n} \dots \sigma_{-1} \cdot \sigma_0 \sigma_1 \dots \sigma_n \dots), \quad (9.2)$$

such that

$$\sigma_i = 0 \text{ or } \sigma_i = 1, \quad (9.3)$$

for all  $i \in \mathbb{Z}$ . In this notation, the  $\cdot$  is used to denote where the central element in the sequence is. The phase space  $\Sigma$  becomes a normed space with the norm

$$\rho(\sigma, \bar{\sigma}) = \sum_{i=-\infty}^{\infty} \frac{|\sigma_i - \bar{\sigma}_i|}{2^{|i|}}. \quad (9.4)$$

You should check that, indeed, this does define a norm. Next, we define the Bernoulli shift map:

$$\alpha(\sigma) = (\dots\sigma_{-n}\dots\sigma_{-1}\sigma_0\cdot\sigma_1\dots\sigma_n\dots). \quad (9.5)$$

Thus the shift map moves all elements to the left, one position:

$$(\alpha(\sigma))_i = \sigma_{i+1}. \quad (9.6)$$

Clearly, the shift map is invertible. We now prove it has many other interesting properties.

**Theorem 21** *The Bernoulli shift map  $\alpha$  on  $\Sigma$  has*

- (i) *countably infinitely many periodic orbits,*
- (ii) *uncountably many nonperiodic orbits, and*
- (iii) *a dense orbit.*

**Proof.** (i) Consider any  $\sigma \in \Sigma$  which consists of a repeating sequence of digits. Suppose that

$$\sigma_{i+k} = \sigma_i, \quad i \in \mathbb{Z}, \quad (9.7)$$

for some positive integer  $k$ . Then

$$\alpha^k \sigma = \sigma, \quad (9.8)$$

which means that  $\sigma$  is a  $k$ -periodic point of  $\alpha$ . The collection of all such points is countable. Indeed, they may be enumerated as

$$\begin{aligned} &(\cdot\bar{0}), (\cdot\bar{1}), \\ &(\cdot\overline{01}), \\ &(\cdot\overline{001}), (\cdot\overline{011}), \\ &(\cdot\overline{0001}), (\cdot\overline{0011}), (\cdot\overline{0111}), \\ &\dots \end{aligned}$$

(ii) Any sequence  $\sigma$  that does not repeat gives rise to a nonperiodic orbit. Such sequences are uncountable: consider all real numbers between 0 and 1. These numbers may be represented in binary form. Those numbers whose binary form repeats are rational numbers. The others are irrational. We know that the irrational numbers are a full measure uncountable set. From this it follows that  $\alpha$  has an uncountable number of nonperiodic orbits.

(iii) Consider

$$\sigma = \text{concatenation of the root part of all periodic orbits}. \quad (9.9)$$

Then  $\sigma$  is dense in  $\Sigma$ , by construction: it will approach any sequence arbitrarily close, as all central parts occur somewhere down the line in  $\sigma$ . ■

One can show that a countable number of periodic orbits with arbitrarily large periods is sufficient to conclude sensitive dependence on initial conditions. Here, we prove this directly.

**Theorem 22** *The Bernoulli shift map  $\alpha$  is sensitively dependent on initial conditions, in  $\Sigma$ .*

**Proof.** Let  $\sigma, \bar{\sigma}$  be such that

$$\rho(\sigma, \bar{\sigma}) < \epsilon, \quad (9.10)$$

for  $\epsilon > 0$ . Otherwise,  $\sigma$  and  $\bar{\sigma}$  are arbitrary. This implies that the central digits of  $\sigma$  and  $\bar{\sigma}$  agree, but it puts no constraints on their digits sufficiently far from the center. It follows that a large enough number of shifts will make this difference arbitrarily large. This concludes the proof. ■

Having established that  $\alpha$  has a dense orbit on  $\Sigma$  and displays sensitive dependence on initial data, we have proven the following theorem:

**Theorem 23** *The Bernoulli shift map  $\alpha$  is chaotic on  $\Sigma$ .*

## 9.2 Smale's horseshoe

Before we get started, it should be pointed out that it is possible to give an analytical description of the Smale Horseshoe, just like we'll give a geometrical one. We'll stick to the geometrical picture, as is it more insightful, in my opinion.

Consider the map  $f$ , defined (at least picture-wise) in Figure 9.1. Thus

$$f : D \rightarrow D : [0, 1] \times [0, 1] \rightarrow [0, 1] \times [0, 1]. \quad (9.11)$$

It is possible to give an analytical description of this map, but for our purposes, the illustrations of Figure 9.1 may be more useful. The map  $f$  is referred to as the Baker's map. It is a composition of three elementary steps: (a) a stretching step, where the unit square is stretched to a long vertical strip; (b) a folding step, where this long vertical strip is bent in the shape of a horseshoe; and (c) an overlay step, where the map is restricted to its original domain.

The inverse map is remarkably similar: it also consists of a composition of three elementary steps, given by (a) a stretch, where the unit square is horizontally stretched; (b) a folding step, where a horseshoe is created, once again; and (c) an overlay step where the result is restricted to the unit square. All of this is illustrated in Figure 9.2.

Let's construct the invariant set of this map. A point is in the invariant set of a map if it remains in the set under all forward and backward iterates of the map.

### The forward iterates

The first few forward iterates of the map are shown in Figure 9.3. It follows from this figure that all points in the invariant set are confined to a middle-third cantor set collection

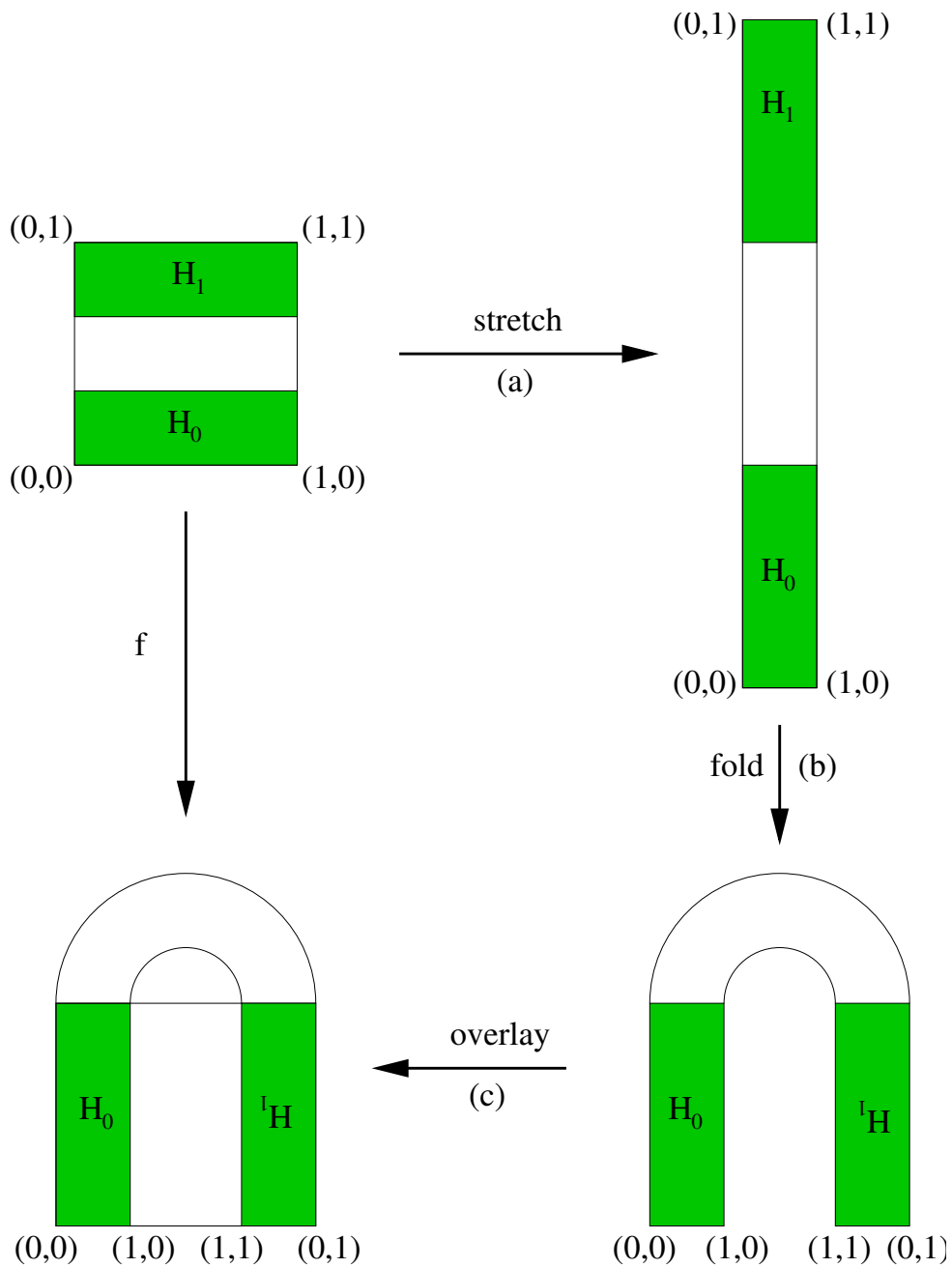


Figure 9.1: The action of the Baker's map.

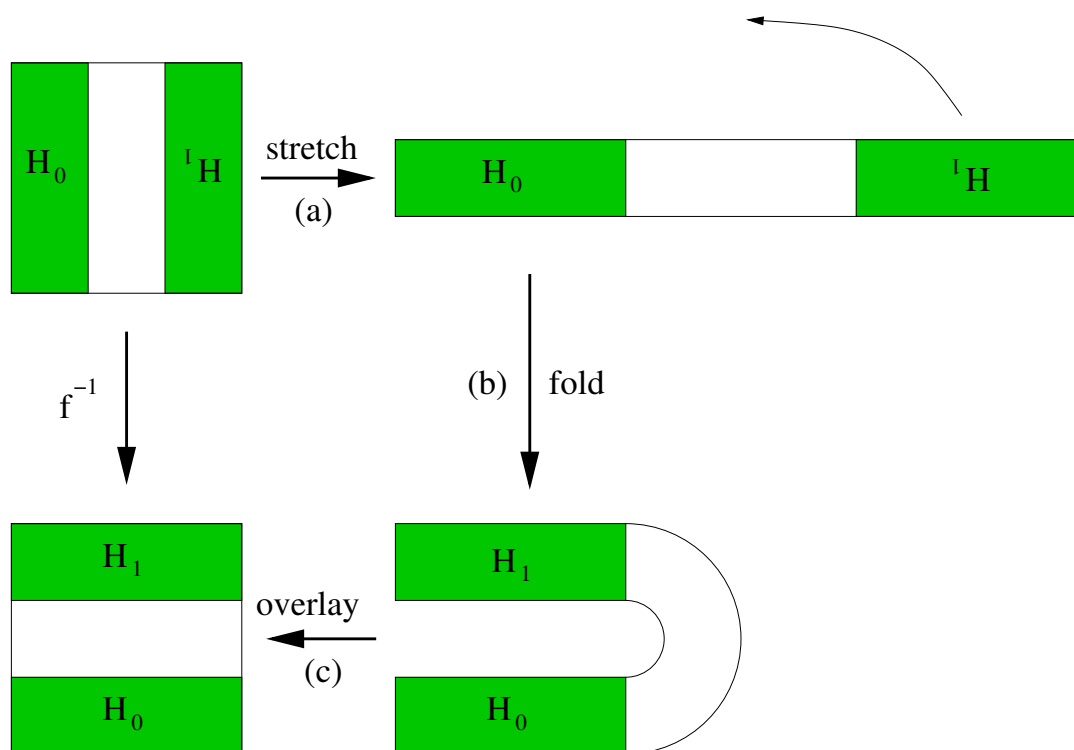


Figure 9.2: The action of the Baker's inverse map.

of vertical line segments. With each of the iterates, we associate an address, as shown in Figure 9.4.

Here's how the assigning of the address is done:

- **After one iteration:** the left strip is assigned a zero, the right strip a one.
- **After two iterations:** we transport addresses assigned at the previous iteration to their new location. In other words, the left-most strip inherits a zero, as does the right-most strip, since they both originate from the previous left strip. The other two strips inherit a one, as they originate from the previous right strip. Now we modify these inherited addresses: the two on the left get an extra zero (since they're at the left; the zero is added to the front). The two on the right get an extra one (since they're at the right; the one is added to the front).
- **After three iterations:** now we repeat this: after using the map again, all new strips inherit their old address, taking into account where they originate from. The strips left of center get an extra zero tagged to their front; the strips right of center get an extra one up front.
- *etc.* The number of digits in the address is equal to the number of iterates of  $f$ . It should also be clear that an address uniquely determines which vertical line we mean.

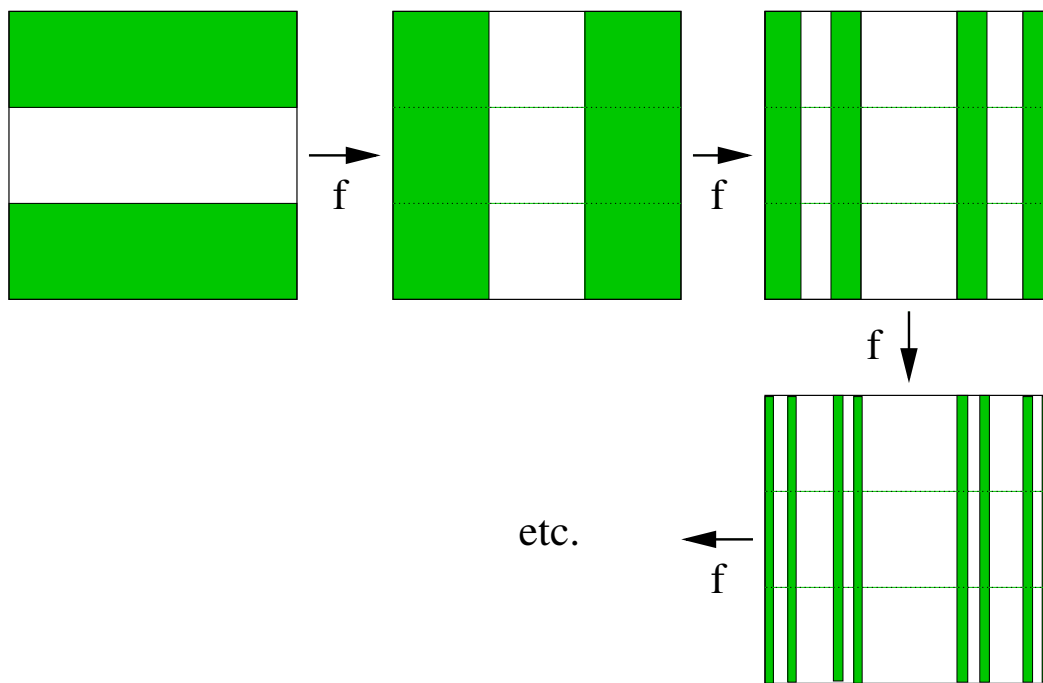


Figure 9.3: Several forward iterates of the Baker's map.

In the limit of an infinite number of forward iterates, every strip has associated with it an infinite sequence of zero's and one's.

## The backward iterates

This part is very similar to the previous part. See any copy and paste action? The first few backward iterates of the map are shown in Figure 9.5. It follows from this figure that all points in the invariant set are confined to a middle-third cantor set collection of horizontal line segments. With each of the iterates, we associate an address, as shown in Figure 9.5.

Here's how the assigning of the address is done:

- **After one iteration:** the bottom strip is assigned a zero, the top strip a one.
- **After two iterations:** we transport addresses assigned at the previous iteration to their new location. In other words, the bottom-most strip inherits a zero, as does the top-most strip, since they both originate from the previous bottom strip. The other two strips inherit a one, as they originate from the previous top strip. Now we modify these inherited addresses: the two on the bottom get an extra zero (since they're at the bottom; the zero is added to the front). The two on the top get an extra one (since they're at the top; the one is added to the front).

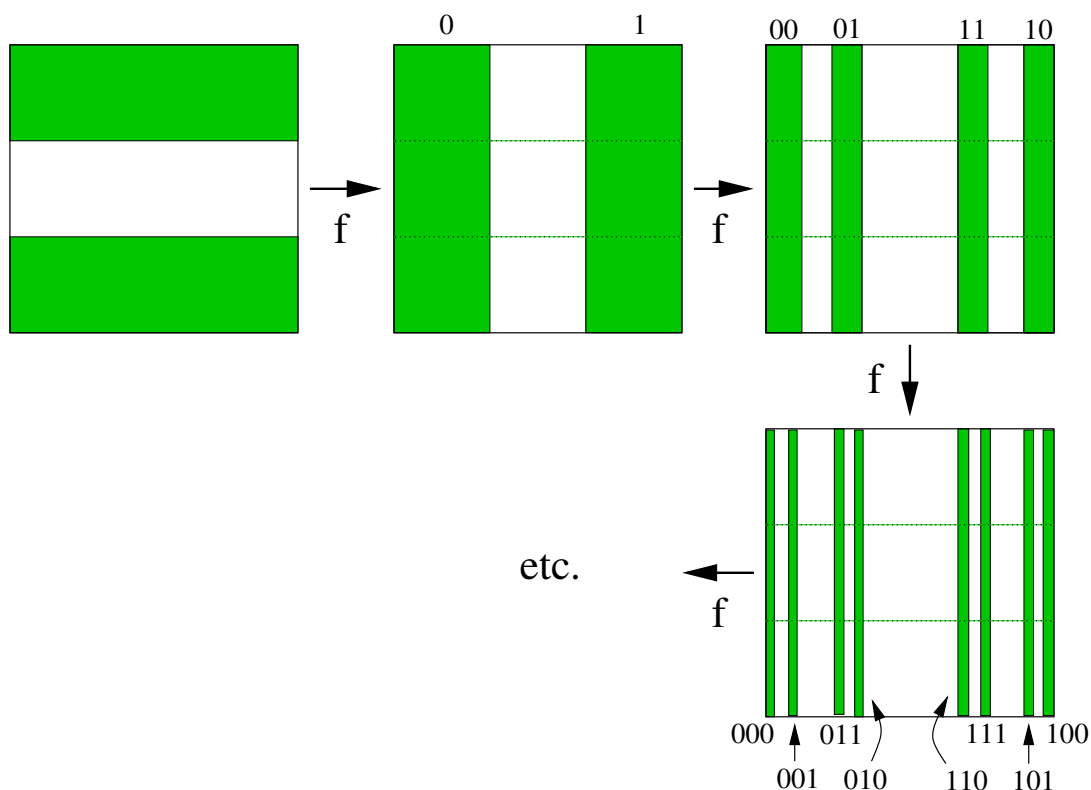


Figure 9.4: How to associate an address with different forward iterates of the Baker's map.

- **After three iterations:** now we repeat this: after using the map again, all new strips inherit their old address, taking into account where they originate from. The strips below center get an extra zero tagged to their front; the strips above center get an extra one up front.
- *etc.* The number of digits in the address is equal to the number of iterates of  $f^{-1}$ . It should also be clear that an address uniquely determines which horizontal line we mean. In the limit of an infinite number of backward iterates, every strip has associated with it an infinite sequence of zero's and one's.

## The invariant set

The invariant set is the intersection of the forward and backward invariant sets. It consists of the intersection of two Cantor line sets, one horizontal and one vertical. Thus, the invariant set is a point set, with an uncountable number of entries. You should remember that the points of the invariant set are not fixed points of the map  $f$ . Rather, they belong to a set of points which is invariant under the action of  $f$ , meaning that one point of the invariant set is mapped to another, under either a forward or backward iterate of  $f$ .

Taking the addresses we've constructed for the forward and backward iterates, we may

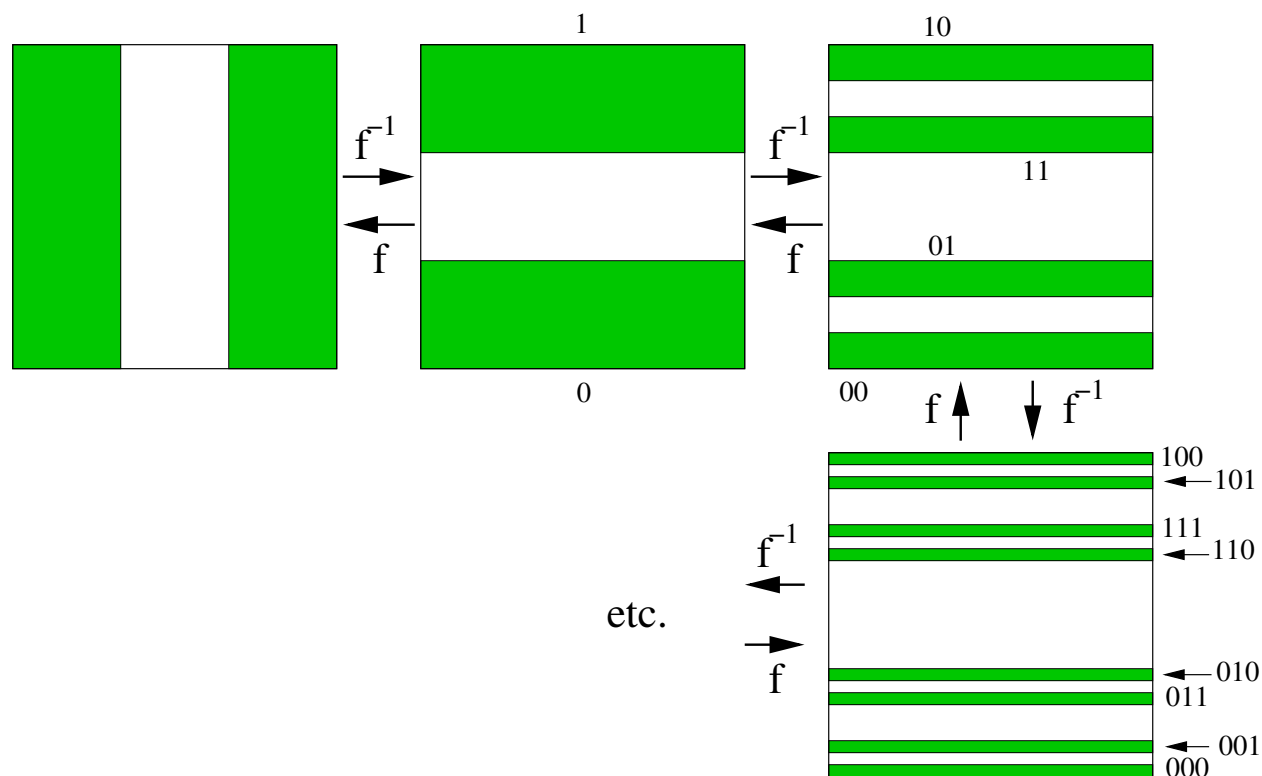


Figure 9.5: Several backward iterates of the Baker's map, with their associated addresses.

assign a unique bi-infinite address with every point  $P$  in the invariant set. We do this as follows: let

$$V_{\sigma_{-1}\sigma_{-2}\dots} \quad (9.12)$$

denote a unique vertical line. Similarly, let

$$H_{\sigma_0\sigma_1\sigma_2\dots} \quad (9.13)$$

denotes a unique horizontal line. Their unique intersection point  $P$  is assigned the address

$$\sigma(P) = (\dots \sigma_{-2}\sigma_{-1} \cdot \sigma_0\sigma_1\sigma_2\dots). \quad (9.14)$$

As before, we use the  $\cdot$  to denote the central element. Thus, with every address  $\sigma$  there corresponds a unique point  $P$  in the invariant set, and for every point in the invariant set, we have a unique address. In other words, through the assigning of addresses, we may identify the invariant set of the Baker's map with  $\Sigma$ , the phase space for the Bernoulli shift map. Sweet! Now, all this would be without merit if it didn't lead somewhere. But it does! It leads to a theorem (Nirvana!):

**Theorem 24** *The restriction of the Baker's map to its invariant set satisfies*

$$\alpha(\sigma(P)) = \sigma(f(P)), \quad (9.15)$$

where  $\alpha$  is the Bernoulli shift map,  $P$  is a point of the invariant set, and  $\sigma$  is an address, assigned as described above.

**Proof.** Since the Bernoulli shift map only shifts one digit, it suffices to consider the digits of  $\sigma(P)$  within 2 positions of the central marker. This means that in effect we have to consider a finite number of possibilities, which we now do<sup>1</sup>. Again, we proceed by doing this graphically. Since we only worry about the central part of the addresses, we can consider the first two layers of the invariant set, as shown in Figure 9.6.

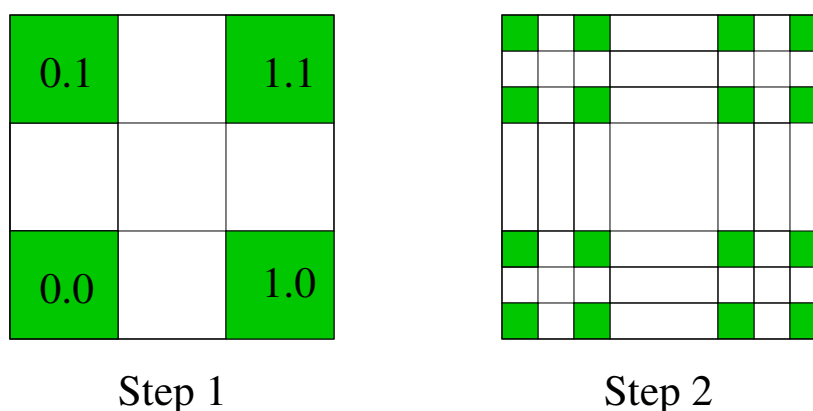


Figure 9.6: The first two layers, with some addressing, of the invariant set of  $f$ .

Let's check this for the red small square indicated in Figure 9.7. The central part of the address of any point in this square is  $\sigma(P) = (\dots 00 \cdot 01 \dots)$ . Thus

$$\alpha(\sigma(P)) = (\dots 000 \cdot 1 \dots). \quad (9.16)$$

On the other hand, the Baker's map  $f$  maps the small red square to the stretched blue rectangle. The addresses of all points on the invariant set in the blue rectangle are

$$\sigma(f(P)) = (\dots 0 \cdot 1 \dots), \quad (9.17)$$

which agrees with the action of the shift map.

One down, fifteen to go!

We now repeat this for the areas indicated in Figure 9.8. The reasoning is very similar to that for the first case. Consider the small red square. The central part of the address of any point in this square is  $\sigma(P) = (\dots 00 \cdot 10 \dots)$ . Thus

$$\alpha(\sigma(P)) = (\dots 001 \cdot 0 \dots). \quad (9.18)$$

---

<sup>1</sup>That means I'll do two of them. You should check a few more to ensure you're comfortable with this. Seriously.

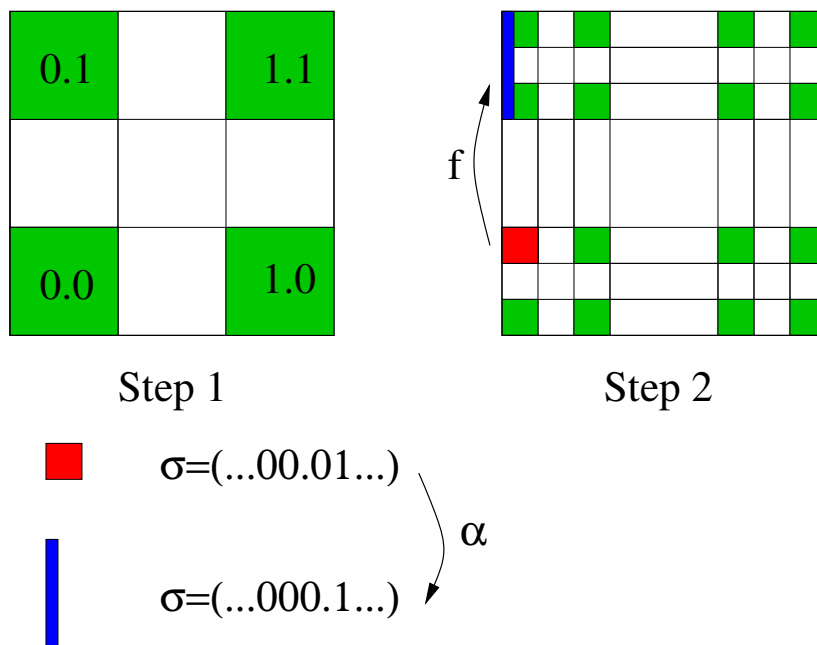


Figure 9.7: Checking the first of 16 cases...

On the other hand, the Baker's map  $f$  maps the small red square to the stretched blue rectangle. The addresses of all points on the invariant set in the blue rectangle are

$$\sigma(f(P)) = (\dots 1 \cdot 0 \dots), \quad (9.19)$$

which agrees with the action of the shift map.

As we said, there's 14 more cases to check, but you get the gist. We'll conclude the proof here, assuming the willingness and maturity of the reader to complete it. ■

We immediately conclude that **The Baker's map, restricted to its invariant set, is chaotic!** This is also a justification why we investigated the Bernoulli shift map in the first place. It was pretty easy to prove that it was chaotic. Now we've shown that the Baker's map restricted to its invariant set is chaotic. This has huge consequences for what follows: **in the sense of this construction, the presence of a horseshoe in a dynamical system is enough to consider the map to be chaotic, as least on some part of its phase space.**

### 9.3 More complicated horseshoes

More complicated horseshoes are possible. Consider the taffy map shown in Figure 9.9. This leads to a three-fold horseshoe, which requires the use of Bernoulli sequences with three symbols 0, 1 and 2. The map consists of a vertical stretch and a fold, followed by a

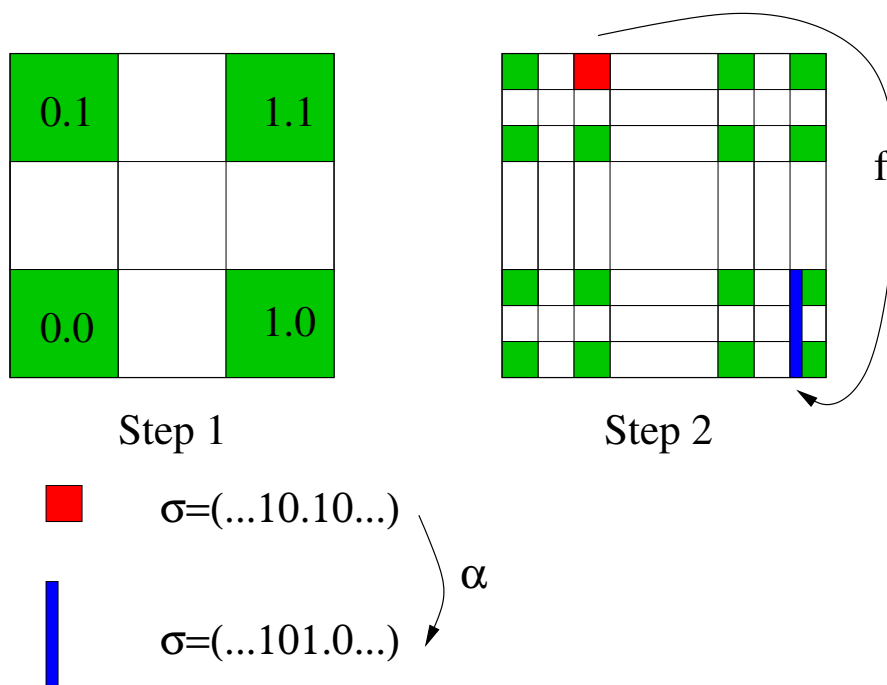


Figure 9.8: The second of 16 cases...

restriction back to the unit square. Further generalizations are obvious, although coming up with food-industry names for the maps involved is less obvious.

## 9.4 Horseshoes in dynamical systems

### Homoclinic tangles

Why do we spend all this time investigating horseshoe maps, even if they display chaotic behavior? The answer is predictable, but important: because these maps show up in dynamical systems all the time. Below is a first example. Remember the map

$$\begin{cases} x_{n+1} = y_n \\ y_{n+1} = (a + by_n^2)y_n - x_n \end{cases} \quad (9.20)$$

due to Ricardo Carretero-González? Here  $a = 2.693$  and  $b = -104.888$ . This example arose in the studies of Bose-Einstein condensates, trapped in a spatially period potential. We've already established numerically that this map with these parameters has a homoclinic tangle. In Figure 9.10, we choose an area (green) along the stable manifold, which we then evolve forward in time. After a few iterations (red), we see that the mapped area overlaps in a horseshoe-like fashion with the original area, allowing us to conclude the presence of a horseshoe whenever a homoclinic tangle is present. This implies the existence of a chaotic

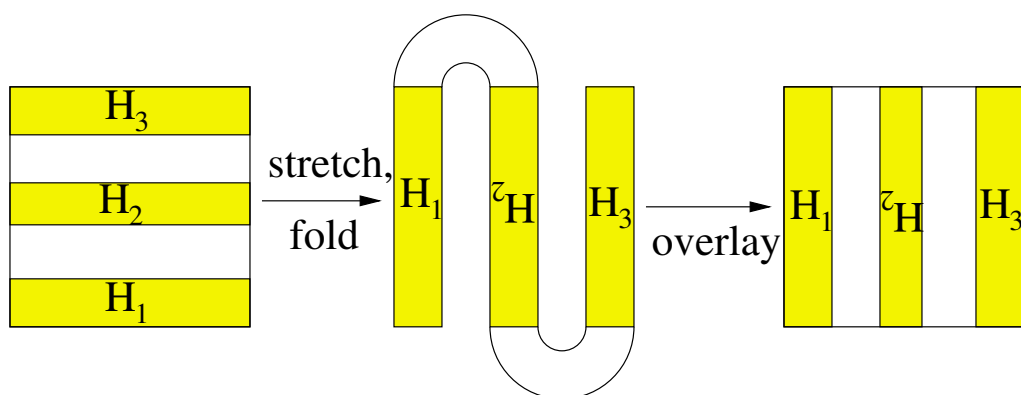


Figure 9.9: The taffy map, leading to a 3-symbol horseshoe...

map, restricted to the invariant set of the horseshoe. Thus, **homoclinic tangles imply chaotic behavior**, according to our earlier definition of chaos.

## Heteroclinic tangles

Heteroclinic tangles are obtained as perturbations of heteroclinic connections: these are connections between two different saddle point equilibria. Thus, the stable manifold of one fixed point transversely intersects the unstable manifold of the other fixed point. This is illustrated in Figure 9.11. One can show that heteroclinic tangles imply the existence of homoclinic tangles (of an iterate of the map, see Wiggins), from which again the presence of a set on which the map is chaotic follows.

## 9.5 Example: the Hénon map

Now that we have established that horseshoes imply chaos, we should remark how easily these may be observed in given systems. As an example, we look at the Hénon map:

$$T : \begin{cases} x & \rightarrow A - By - x^2 \\ y & \rightarrow x \end{cases}, \quad (9.21)$$

with inverse

$$T^{-1} : \begin{cases} x & \rightarrow y \\ y & \rightarrow \frac{1}{B}(A - x - y^2) \end{cases}. \quad (9.22)$$

In what follows, we choose  $A = 5$  and  $B = 0.3$ . In Figure 9.12, we plot the forward and backward iterate of the square with corners at  $(-3, -3)$  and  $(3, 3)$ . These images are easily computed analytically, using the prescriptions for the map  $T$  and its inverse  $T^{-1}$ . The image of the square gives rise to the horizontal horseshoe. Notice that the volume of the mapped image is significantly less than that of the original square. The image of the square under

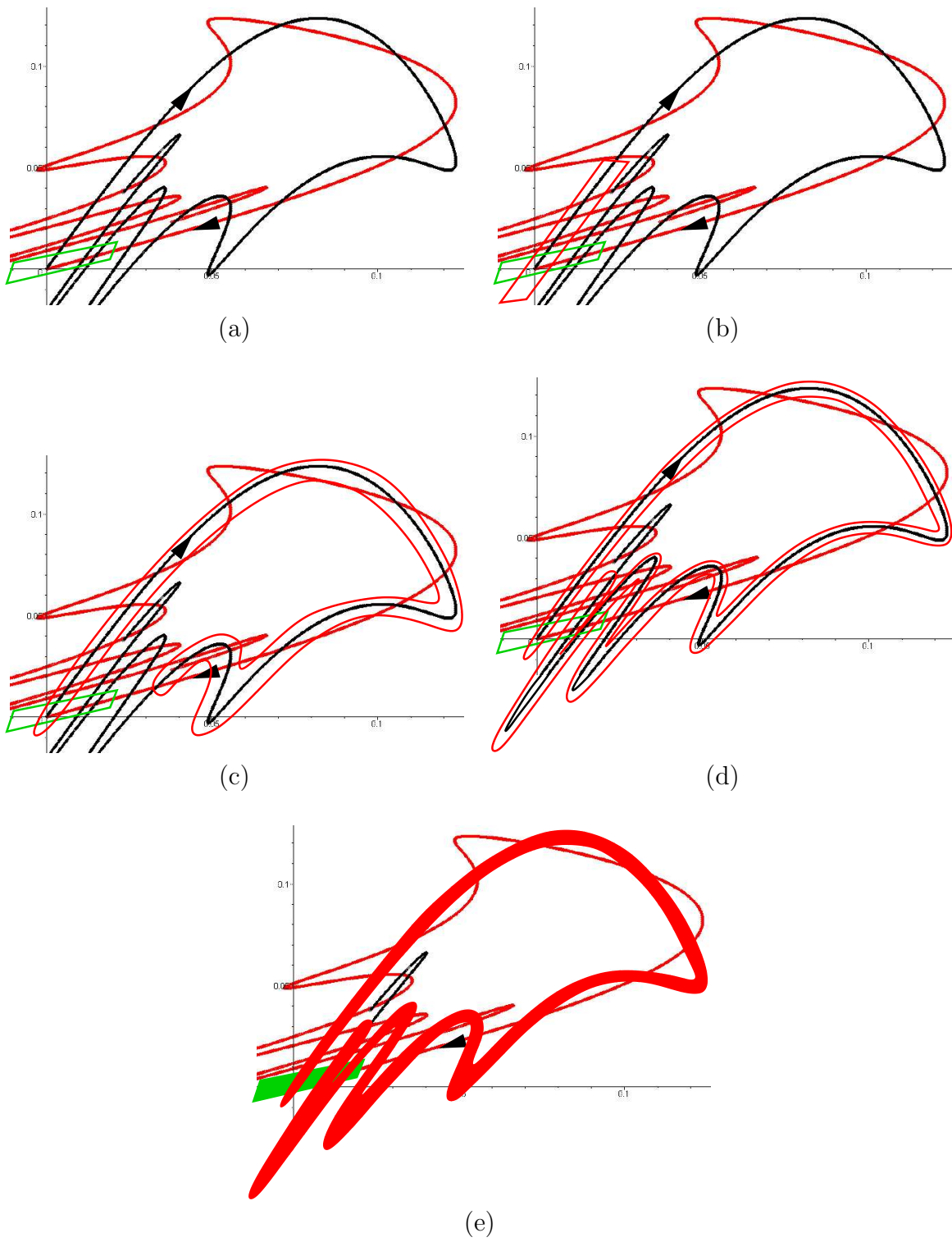


Figure 9.10: The presence of a horseshoe in a homoclinic tangle.

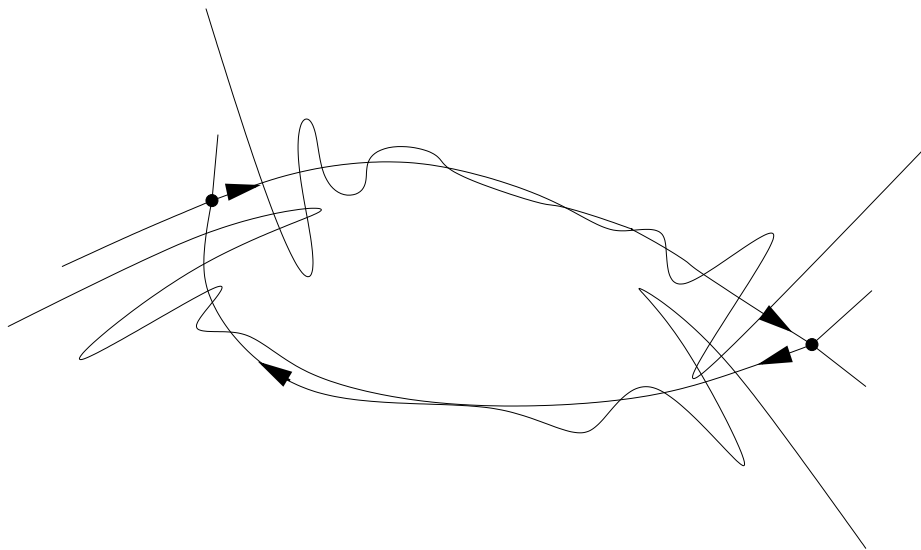


Figure 9.11: A cartoon of a heteroclinic tangle.

the inverse map is the larger vertical horseshoe. The two horseshoes overlap in 4 regions, all in the original square. From this, we see that one iteration of the Hénon map gives rise to a two-symbol horseshoe, from which we may conclude the presence of a set on which the dynamics is chaotic.

A similar construction may be done for the Standard Map, so as to establish the presence of a horseshoe on which the map is chaotic.

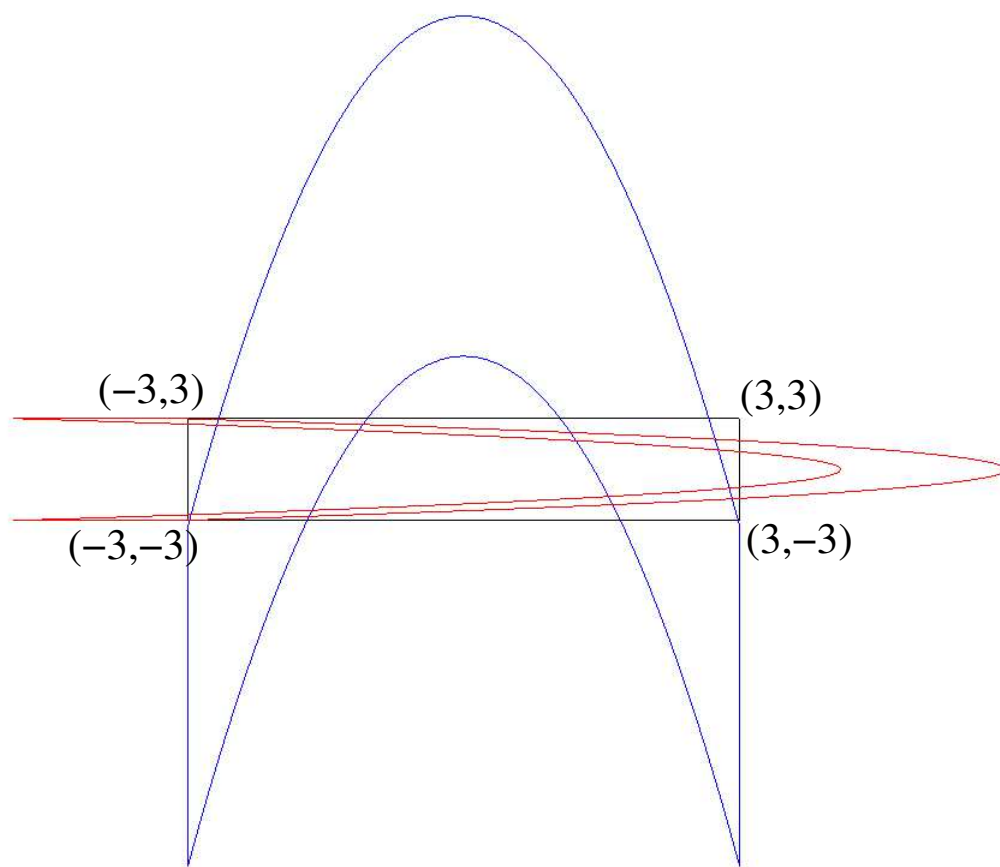


Figure 9.12: A horseshoe in the Hénon map.



# Chapter 10

## Indicators of chaos

In this chapter we consider two indicators of chaos that are especially useful for the numerical investigation of a given dynamical system.

### 10.1 Lyapunov exponents for one-dimensional maps

The Lyapunov exponent  $\lambda$  gives the average exponential rate of divergence of infinitesimal nearby initial conditions.

Consider a one-dimensional map

$$x_{n+1} = f(x_n). \quad (10.1)$$

The Lyapunov exponent is governed by

$$\Delta x_n = e^{\lambda n} \Delta x_0. \quad (10.2)$$

Here  $\Delta x_0$  is the difference between two initial conditions, and  $\Delta x_n$  is the difference between their  $n$ -th iterates. It follows that

$$e^{\lambda n} = \frac{\Delta x_n}{\Delta x_0} \sim \frac{dx_n}{dx_0}, \quad (10.3)$$

or

$$\lambda \sim \frac{1}{n} \ln \left| \frac{dx_n}{dx_0} \right|. \quad (10.4)$$

In order to obtain a result that is independent of  $n$ , we define

$$\lambda = \lim_{n \rightarrow \infty} \frac{1}{n} \ln \left| \frac{dx_n}{dx_0} \right|. \quad (10.5)$$

How is this computed? Note that

$$\begin{aligned}\frac{dx_n}{dx_0} &= \frac{dx_n}{dx_{n-1}} \frac{dx_{n-1}}{dx_{n-2}} \cdots \frac{dx_1}{dx_0} \\ &= f'(x_{n-1})f'(x_{n-2}) \cdots f'(x_0),\end{aligned}\tag{10.6}$$

so that

$$\lambda = \lim_{n \rightarrow \infty} \frac{1}{n} \ln |f'(x_{n-1})f'(x_{n-2}) \cdots f'(x_0)|.\tag{10.7}$$

The result on the right-hand side is typically independent of  $x_0$ , except for a set of measure zero, which might give rise to fixed points, periodic orbits *etc.*.

**Example 12** *Let's do a very simple example. Consider the map*

$$x_{n+1} = ax_n,\tag{10.8}$$

where  $a$  is constant. In other words,

$$f(x) = ax,\tag{10.9}$$

and thus

$$f'(x) = a,\tag{10.10}$$

independent of  $x$ . Then, using the above definition

$$\lambda = \lim_{n \rightarrow \infty} \frac{1}{n} \ln |a^n| = \ln |a|.\tag{10.11}$$

In almost all cases, this limit cannot be done analytically and numerical computations are used, with successively larger values of  $n$ .

## 10.2 Lyapunov exponents for higher-dimensional maps

How is the previous discussion extended for higher-dimensional systems? In the book you'll find the treatment for flows. I'll do it for maps here. As usual, familiarity with both is expected.

Consider the map

$$x_{n+1} = f(x_n),\tag{10.12}$$

where  $x_n \in \mathbb{R}^N$ , or some other  $N$ -dimensional set (like a sphere, a torus, *etc.*).

Let  $x_0$  be the initial condition with orbit denoted by  $x_n$ . Further, let  $y_0$  be an infinitesimal perturbation of  $x_0$ . Similarly,  $y_n$  denotes a similar infinitesimal perturbation that follows from  $y_0$  at step  $n$ . Simple linearization gives that  $y_0$  evolves according to

$$y_{n+1} = f'(x_n)y_n, \quad (10.13)$$

where  $f'(x_n)$  is the Jacobian of the map, evaluated at  $x_n$ . Hence

$$y_{n+1} = f'(x_n)f'(x_{n-1}) \cdots f'(x_0)y_0. \quad (10.14)$$

In analogy with the one-dimensional case, we let

$$\begin{aligned} \lambda(x_0, u_0) &= \lim_{n \rightarrow \infty} \frac{1}{n} \ln \frac{\|y_{n+1}\|}{\|y_0\|} \\ &= \lim_{n \rightarrow \infty} \frac{1}{n} \ln \|f'(x_n)f'(x_{n-1}) \cdots f'(x_0)u_0\|, \end{aligned} \quad (10.15)$$

where  $u_0$  is a unit vector. Thus,  $\lambda(x_0, u_0)$  may depend on the initial point, and on a direction  $u_0$ . For a given  $x_0$ , there may be  $N$  or fewer distinct Lyapunov exponents. For instance, if  $x_0$  is a fixed point of the map, then

$$x_n = x_{n-1} = \cdots = x_0. \quad (10.16)$$

It follows that

$$\lambda(x_0, u_0) = \lim_{n \rightarrow \infty} \frac{1}{n} \ln \|f'(x_0)^n u_0\|. \quad (10.17)$$

If  $u_0$  is an eigenvector of  $f'(x_0)$  with corresponding eigenvalue  $\lambda_0$ , then

$$\begin{aligned} \lambda(x_0, u_0) &= \lim_{n \rightarrow \infty} \frac{1}{n} \ln \|\lambda_0^n u_0\| \\ &= \lim_{n \rightarrow \infty} \frac{1}{n} \ln |\lambda_0^n| \|u_0\| \\ &= \ln |\lambda_0|, \end{aligned} \quad (10.18)$$

since  $\|u_0\| = 1$ . It follows that a different Lyapunov exponent is obtained for every eigenvector.

As for the one-dimensional case, the limit defining the Lyapunov exponent may hardly ever be evaluated analytically, if it even exists! The importance of Lyapunov exponents is that they indicate the sensitive dependence on initial conditions: a larger Lyapunov exponent indicates more sensitive dependence. This increases the likelihood of having a chaotic orbit. However, note that Lyapunov exponents do not have anything to say about whether or not the map is topologically transitive. Thus, they are only one useful indicator. And you get what you pay for.

### 10.3 Fractal dimension

We all know intuitively what is meant by the dimension of a set. On the other hand, when given a set, how would one actually *compute* its dimension? There are several ways of doing this, all resulting in slightly different definitions. Luckily these definitions agree on these case where we intuitively know the answer.

We will focus on the Box-counting dimension. In the book you can read up on the Hausdorff dimension, and on the similarity dimension.

Assume we have a set in an  $N$ -dimensional Cartesian space<sup>1</sup>. Now cover the set using  $N$ -dimensional cubes of length  $\epsilon$ , as shown in Figure 10.1. Let

$$\hat{N}(\epsilon) = \# \text{ of cubes required to cover the set.} \quad (10.19)$$

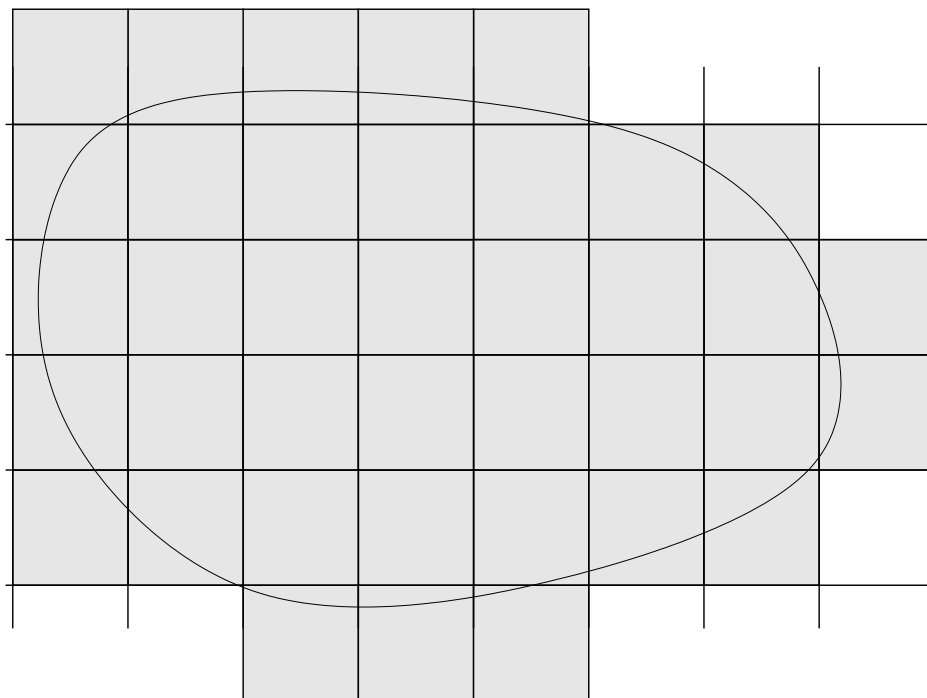


Figure 10.1: Covering a set using boxes of dimension  $N$  and of size  $\epsilon$ .

Then

$$D_0 = \lim_{\epsilon \rightarrow 0} \frac{\ln \hat{N}(\epsilon)}{\ln(1/\epsilon)} \quad (10.20)$$

is the *box-counting dimension* of the set. Let's do a few examples.

<sup>1</sup>So, we're assuming that we know what this means.

**Example 13 (A finite set of points in  $N$ -dimensional space)** *In this case, for sufficiently small  $\epsilon$ , we can always choose*

$$\hat{N}(\epsilon) = \#S, \quad (10.21)$$

where  $\#S$  is the number of points. Then

$$D_0 = \lim_{\epsilon \rightarrow 0} \frac{\ln \#S}{\ln(1/\epsilon)} = 0, \quad (10.22)$$

as expected.

**Example 14 (A curve in two-dimensional space)** *Using boxes length  $\epsilon$ , we need approximately*

$$\hat{N}(\epsilon) \approx \frac{L}{\epsilon} \quad (10.23)$$

boxes, for small  $\epsilon$ , where  $L$  is the arclength of the curve. Then

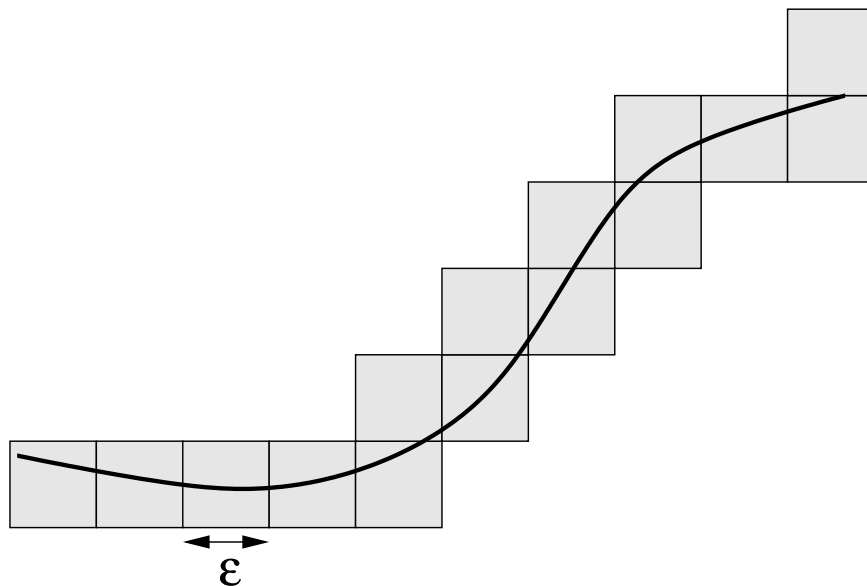


Figure 10.2: Covering a curve in dimension two, using boxes of dimension 2 and of size  $\epsilon$ .

$$\begin{aligned} D_0 &= \lim_{\epsilon \rightarrow 0} \frac{\ln L/\epsilon}{\ln 1/\epsilon} \\ &= \lim_{\epsilon \rightarrow 0} \frac{\ln L + \ln 1/\epsilon}{\ln 1/\epsilon} \\ &= 1, \end{aligned} \quad (10.24)$$

again, as expected.

A similar argument shows that the box-counting dimension for a two-dimensional area as shown in Figure 10.1 is indeed two. This is all good: for those sets where we intuitively know what their dimension should be, the box-counting dimension gives us the right answer.

Now, the way the box-counting dimension is defined it does not have to be an integer per se. Suppose we have a set which has non-integer dimension. This would be a strange set indeed! Often this points to trajectories that are nearly space filling, *etc.*. All of these are once again indicators of chaos.

**Definition 17 (Fractal)** *A fractal is an object with non-integer dimension.*

**Example 15 (The middle-1/3 Cantor set)** *Consider the middle-1/3 Cantor set, obtained by removing consecutive 1/3's from the unit interval, as indicated in Figure 10.3.*



Figure 10.3: Constructing the middle 1/3 Cantor set.

Since we're assuming that the limit exists, we may choose a sequence of  $\epsilon$ 's approaching zero:

$$\epsilon_n = (1/3)^n \rightarrow 0, \quad \text{as } n \rightarrow \infty. \quad (10.25)$$

Then

$$\hat{N}(\epsilon_n) = 2^n, \quad (10.26)$$

and

$$D_0 = \lim_{n \rightarrow \infty} \frac{\ln 2^n}{\ln 3^n} = \frac{\ln 2}{\ln 3} = 0.63 \dots \quad (10.27)$$

This is not an integer, and therefore the middle-1/3 is a fractal. The self-similar structure of this set (it's invariance under appropriate zooming) is typical of fractals.

**Example 16** *Another example is presented by the Koch curve. The first two steps of its construction are shown in Figure 10.4. At every step, we remove the middle one third of each line segment and we replace it with two line segments of the same length. The first one is rotated 60 degrees from the one that was removed, and the second one gets us back so that the whole set remains connected.*

We may use the same reasoning as above to let

$$\epsilon_n = (1/3)^n. \quad (10.28)$$

The number of two-dimensional boxes of this size we need is

$$\hat{N}(\epsilon_n) = 3 \cdot 4^{n-1}. \quad (10.29)$$

Thus

$$\begin{aligned} D_0 &= \lim_{n \rightarrow \infty} \frac{\ln 3 \cdot 4^{n-1}}{\ln 3^n} \\ &= \lim_{n \rightarrow \infty} \frac{\ln 4^n}{\ln 3^n} \\ &= \frac{\ln 4}{\ln 3} = 1.26 \dots \end{aligned} \quad (10.30)$$

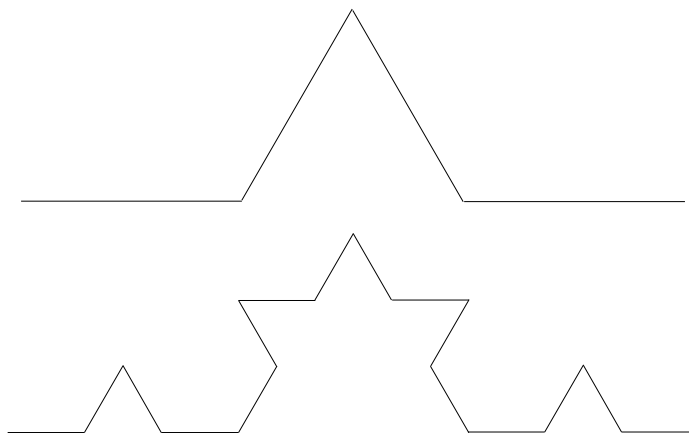


Figure 10.4: Constructing the Koch curve.

similarly, one may compute the box-counting dimension of strange attractors. Since we have not defined strange attractors yet, let's do so now.

**Definition 18 (Strange attractor)** *A strange attractor is an invariant set which is an attractor, and on which the dynamics is chaotic.*

One reason for the use of the adjective “strange” in this name is that strange attractors are often very strange indeed: very often they have non-integer dimension. Such might be the case for the Lorenz attractor. A numerically computed picture of the Lorenz attractor is shown in Figure 10.5. Using Lorenz's original parameters

$$D_0 = 2.001 \pm 0.017, \quad (10.31)$$

which is inconclusive: it could just be a two-dimensional object. Another way of computing the dimension, due to Kaplan and York results in

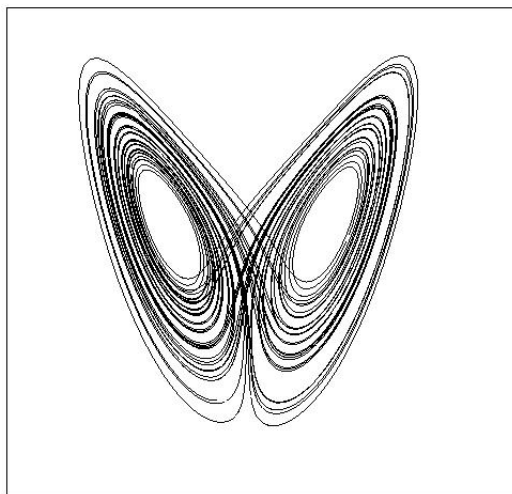


Figure 10.5: The Lorenz attractor.

$$D_{KY} = 2.062, \quad (10.32)$$

and the Lorenz attractor might be more than just a two-dimensional thing: it might have an urge to enter the third dimension.

For the Hénon attractor ( $A = 1.4$ ,  $B = 0.3$ ) (see Figure 10.6), one finds

$$D_0 = 1.12. \quad (10.33)$$

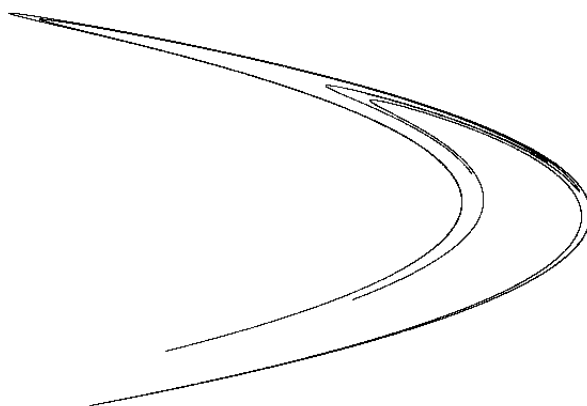


Figure 10.6: The Hénon attractor

# Chapter 11

## Normal form theory

The point of the method of normal forms is to find a way to express a given dynamical system in its simplest form, in order to explain certain phenomena. These “simplest” or “normal” forms are usually only valid locally, in a neighborhood of an orbit. Typically the orbit around which we construct the normal form is a fixed point or a periodic orbit. In general, the coordinate transformation which is used to express the system in its normal form is nonlinear. However, the amazing thing about normal form theory is that this transformation is found by solving a sequence of linear problems. We illustrate how to do this in this chapter.

The textbook covers both flows and maps. I’ll only deal with flows in these notes. The main points of the theory are similar.

### 11.1 Preparation steps

Consider the autonomous system

$$w' = G(w), \tag{11.1}$$

where  $w \in \mathbb{R}^N$ . We are interested in examining the system near a fixed point.

Before we start transforming the system for real, we take the following simple preparation steps. Suppose that  $w_0$  is a fixed point, *i.e.*,

$$G(w_0) = 0, \tag{11.2}$$

and  $G(w)$  is sufficiently differentiable, so that what follows is allowed.

1. **Translation to the origin:** let

$$v = w - w_0, \tag{11.3}$$

then  $v$  satisfies the system

$$v' = G(v + w_0) = H(v), \tag{11.4}$$

where the last equation defines  $H(v)$ . Note that now  $H(0) = 0$ . In effect, we have a new system with fixed point at the origin.

2. **Splitting off the linear part:** since  $H(0) = 0$ , the Taylor series in a neighborhood of the fixed point  $v = 0$  is given by

$$v' = DH(0)v + \hat{H}(v), \quad (11.5)$$

where  $\hat{H}(v)$  is at least quadratic in the components of  $v$ , and  $DH(0)$  is the Jacobian of  $H(v)$ , evaluated at  $v = 0$ .

3. **Transformation of the linear part:** let

$$v = Tx, \quad (11.6)$$

where  $T$  is the transformation matrix to bring  $DH(0)$  to its real Jordan form. We get

$$\begin{aligned} Tx' &= DH(0)Tx + \hat{H}(Tx) \\ x' &= T^{-1}DH(0)Tx + T^{-1}\hat{H}(Tx) \\ x' &= Jx + F(x). \end{aligned} \quad (11.7)$$

Here  $J$  is the real Jordan form of  $DH(0)$ , and  $F(x) = T^{-1}\hat{H}(Tx)$  is at least quadratic in the components of  $x$ .

## 11.2 Quadratic terms

We have finished the preparation steps. Let's get down to real business. Writing out the nonlinear part more explicitly, we have

$$x' = Jx + F_2(x) + F_3(x) + \dots + F_{r-1}(x) + \mathcal{O}(|x|^r), \quad (11.8)$$

if our vector field is  $r$  times differentiable. Here  $F_2(x)$  is quadratic in the components of  $x$ ,  $F_3(x)$  is of third order, and so on. Here's the big idea: close to our fixed point  $x = 0$ , the linear terms dominate, with the quadratic terms being the most important nonlinear terms. Let's do a transformation on  $x$ , to eliminate as many of the quadratic terms as possible. But we have to be careful: we don't want to mess up what we've accomplished thus far. We have managed to get to the simplest possible form for the linear terms. If we were to do a linear transformation, we'd mess this up. Thus we have to do something else.

Let

$$x = y + h_2(y), \quad (11.9)$$

where  $h_2(y)$  is a quadratic function of the components of  $y$ . Thus, for small  $|y|$ , this is a near-identity transformation, and we should retain the simple form of the linear terms. Let's see what we get:

$$y' + Dh_2(y)y' = Jy + Jh_2(y) + F_2(y + h_2(y)) + \dots + F_{r-1}(y + h_2(y)) + \mathcal{O}(|y|^r), \quad (11.10)$$

thus

$$(I + Dh_2(y))y' = Jy + Jh_2(y) + F_2(y) + \hat{F}_3(y) + \dots + \hat{F}_{r-1}(y + h_2(y)) + \mathcal{O}(|y|^r). \quad (11.11)$$

Here  $I$  denotes the identity matrix, and the hatted functions are obtained from the non-hatted ones by reordering terms. As before, the hatted functions are of the same degree in the components of  $y$  as indicated by their index. For  $y$  small, the matrix  $I + Dh_2(y)$  is invertible. Indeed,

$$(I + Dh_2(y))^{-1} = I - Dh_2(y) + \mathcal{O}(|y|^2). \quad (11.12)$$

Multiplying by this inverse matrix, we obtain

$$\begin{aligned} y' &= (I - Dh_2(y) + \mathcal{O}(|y|^2)) (Jy + Jh_2(y) + F_2(y) + \\ &\quad \hat{F}_3(y) + \dots + \hat{F}_{r-1}(y + h_2(y)) + \mathcal{O}(|y|^r)) \\ &= Jy + Jh_2(y) + F_2(y) - Dh_2(y)Jy + \hat{F}_3(y) + \dots + \hat{F}_{r-1}(y + h_2(y)) + \mathcal{O}(|y|^r). \end{aligned} \quad (11.13)$$

Thus the question becomes: “**Can we choose  $h_2(y)$  such that the quadratic terms in the above equation vanish?**” In other words, can we choose  $h_2(y)$  such that

$$Jh_2(y) - Dh_2(y)Jy + F_2(y) = 0? \quad (11.14)$$

If we can do this, we have managed to eliminate all quadratic terms! Quite a magic trick! The main part of the trick is that the above equation is a **linear** equation in  $h_2(y)$ . Wow!

Now, that being said, this equation is not trivial to solve. How do we proceed? We introduce a vectorspace structure on the polynomials of degree two and higher. We define the operator  $L_J^{(2)}$  by

$$L_J^{(2)}h = Jh_2 - Dh_2Jy, \quad (11.15)$$

or in general,

$$L_J^{(k)} h = Jh_k - Dh_k Jy. \quad (11.16)$$

With this definition, the equation we have to solve becomes

$$L_J^{(2)} h_2(y) = -F_2(y). \quad (11.17)$$

Next, denote by  $H_2$  the space of all quadratic polynomials in  $\mathbb{R}^N$ . Such a space has a finite-dimensional basis.

**Example 17** For  $N = 2$ , the space  $H_2$  is spanned by the following vectors:

$$x^2 \begin{pmatrix} 1 \\ 0 \end{pmatrix}, xy \begin{pmatrix} 1 \\ 0 \end{pmatrix}, y^2 \begin{pmatrix} 1 \\ 0 \end{pmatrix}, x^2 \begin{pmatrix} 0 \\ 1 \end{pmatrix}, xy \begin{pmatrix} 0 \\ 1 \end{pmatrix}, y^2 \begin{pmatrix} 0 \\ 1 \end{pmatrix}. \quad (11.18)$$

Clearly  $F_2(y) \in H_2$ . Also,  $h_2(y) \in H_2$ . We're trying to determine the linear combination  $h_2$  of the basis elements so that (11.17) is satisfied. To this end, let

$$h_2 = \sum_j \alpha_j \hat{e}_j, \quad (11.19)$$

where  $\{\hat{e}_j\}$  is a basis for  $H_2$ . Here the coefficients  $\alpha_j$  are to be determined. Similarly,  $F_2(y) = \sum_j f_j \hat{e}_j$ . We get

$$\sum_j \alpha_j L_J^{(2)} \hat{e}_j = - \sum_j f_j \hat{e}_j. \quad (11.20)$$

This equation reduces to linear algebra for the coefficient vector  $\alpha = (\alpha_1, \alpha_2, \dots)^T$  (finite number of entries),

$$A\alpha = b, \quad (11.21)$$

which may be solved if  $b$  is in the range of  $A$ , or alternatively if

$$-F_2 \in \text{Range of } L_J^{(2)}. \quad (11.22)$$

If  $-F_2$  is not in the Range of  $L_J^{(2)}$ , some terms cannot be eliminated. such terms are referred to as **resonant terms**. In the presence of a few resonant terms, we find

$$y' = Jy + F_2^R(y) + \tilde{F}_3(y) + \dots + \tilde{F}_{r-1}(y) + \mathcal{O}(|y|^r). \quad (11.23)$$

Here the superindex  $R$  denotes resonant terms. The quantities  $\tilde{F}_k$  denote homogeneous polynomials of degree  $k$  in the components of  $y$ .

## 11.3 Example: the Takens-Bogdanov normal form

Let's put all of this in practice.

**Example 18** *Suppose that*

$$J = \begin{pmatrix} 0 & 1 \\ 0 & 0 \end{pmatrix}. \quad (11.24)$$

*We've already listed the 6 possible second-order terms above. Another way of phrasing this is that  $H_2$  is six dimensional:*

$$H_2 = \text{span} \left\{ \begin{pmatrix} x^2 \\ 0 \end{pmatrix}, \begin{pmatrix} xy \\ 0 \end{pmatrix}, \begin{pmatrix} y^2 \\ 0 \end{pmatrix}, \begin{pmatrix} 0 \\ x^2 \end{pmatrix}, \begin{pmatrix} 0 \\ xy \end{pmatrix}, \begin{pmatrix} 0 \\ y^2 \end{pmatrix} \right\}. \quad (11.25)$$

*We'd like to determine what the range of  $L_J^{(2)}$  is. Recall that*

$$L_J^{(2)} h_2(x, y) = J h_2(x, y) - D h_2(x, y) J \begin{pmatrix} x \\ y \end{pmatrix}. \quad (11.26)$$

*Since this is a linear equation for  $h_2 \in H_2$ , let's examine what happens for the six different basis vectors:*

$$\begin{aligned} \begin{pmatrix} x^2 \\ 0 \end{pmatrix} : \quad L_J^{(2)} \begin{pmatrix} x^2 \\ 0 \end{pmatrix} &= \begin{pmatrix} 0 & 1 \\ 0 & 0 \end{pmatrix} \begin{pmatrix} x^2 \\ 0 \end{pmatrix} - \begin{pmatrix} 2x & 0 \\ 0 & 0 \end{pmatrix} \begin{pmatrix} 0 & 1 \\ 0 & 0 \end{pmatrix} \begin{pmatrix} x \\ y \end{pmatrix} \\ &= \begin{pmatrix} 0 & 0 \\ 0 & 0 \end{pmatrix} - \begin{pmatrix} 2x & 0 \\ 0 & 0 \end{pmatrix} \begin{pmatrix} y \\ 0 \end{pmatrix} \\ &= \begin{pmatrix} -2xy \\ 0 \end{pmatrix} = -2 \begin{pmatrix} xy \\ 0 \end{pmatrix}, \end{aligned} \quad (11.27)$$

$$\begin{pmatrix} xy \\ 0 \end{pmatrix} \quad L_J^{(2)} \begin{pmatrix} xy \\ 0 \end{pmatrix} = - \begin{pmatrix} y^2 \\ 0 \end{pmatrix}, \quad (11.28)$$

$$\begin{pmatrix} y^2 \\ 0 \end{pmatrix} \quad L_J^{(2)} \begin{pmatrix} y^2 \\ 0 \end{pmatrix} = \begin{pmatrix} 0 \\ 0 \end{pmatrix}, \quad (11.29)$$

$$\begin{pmatrix} 0 \\ x^2 \end{pmatrix} \quad L_J^{(2)} \begin{pmatrix} 0 \\ x^2 \end{pmatrix} = \begin{pmatrix} x^2 \\ 0 \end{pmatrix} - 2 \begin{pmatrix} 0 \\ xy \end{pmatrix}, \quad (11.30)$$

$$\begin{pmatrix} 0 \\ xy \end{pmatrix} \quad L_J^{(2)} \begin{pmatrix} 0 \\ xy \end{pmatrix} = \begin{pmatrix} xy \\ 0 \end{pmatrix} - \begin{pmatrix} 0 \\ y^2 \end{pmatrix}, \quad (11.31)$$

$$\begin{pmatrix} 0 \\ y^2 \end{pmatrix} \quad L_J^{(2)} \begin{pmatrix} 0 \\ y^2 \end{pmatrix} = - \begin{pmatrix} y^2 \\ 0 \end{pmatrix}. \quad (11.32)$$

*It follows immediately from (11.29) that not all of  $H_2$  will be in the range of  $L_J^{(2)}$ , since  $L_J^{(2)}$  has a kernel. We have that*

$$\begin{aligned} L_J^{(2)}(H_2) &= \text{span} \left\{ \begin{pmatrix} xy \\ 0 \end{pmatrix}, \begin{pmatrix} y^2 \\ 0 \end{pmatrix}, \begin{pmatrix} x^2 \\ 0 \end{pmatrix} - 2 \begin{pmatrix} 0 \\ xy \end{pmatrix}, \begin{pmatrix} xy \\ 0 \end{pmatrix} - \begin{pmatrix} 0 \\ y^2 \end{pmatrix}, \begin{pmatrix} y^2 \\ 0 \end{pmatrix} \right\} \\ &= \text{span} \left\{ \begin{pmatrix} xy \\ 0 \end{pmatrix}, \begin{pmatrix} y^2 \\ 0 \end{pmatrix}, \begin{pmatrix} x^2 \\ 0 \end{pmatrix} - 2 \begin{pmatrix} 0 \\ xy \end{pmatrix}, \begin{pmatrix} 0 \\ y^2 \end{pmatrix} \right\}. \end{aligned}$$

Thus the resonant quadratic terms span a two-dimensional space, since all the vectors that are in the span of  $L_J^{(2)}(H_2)$  may be eliminated.

We need to find two vectors that are not contained in this four-dimensional set. Two candidates are

$$\begin{pmatrix} 0 \\ x^2 \end{pmatrix} \quad \text{and} \quad \begin{pmatrix} x^2 \\ 0 \end{pmatrix}. \quad (11.33)$$

Thus, up to quadratic terms, the normal form for the specified  $J$  is can be written as

$$\begin{cases} x' = y + a_1 x^2 + \mathcal{O}(3), \\ y' = a_2 x^2 + \mathcal{O}(3), \end{cases} \quad (11.34)$$

where  $\mathcal{O}(3)$  denote cubic and higher-order terms. Clearly the choice of the two chosen vectors is not unique. Hence the normal form for the given  $J$  is not unique.

## 11.4 Cubic terms

Let's see what we can do about the third order terms. We already have

$$y' = Jy + F_2^R + \tilde{F}_3(y) + \mathcal{O}(4). \quad (11.35)$$

Let

$$y = z + h_3(z), \quad (11.36)$$

where (you guessed it)  $h_3(z)$  contains cubic terms only. Here's the big thing: we want to do something about the cubic terms, but it's not allowed to make the linear or quadratic terms any worse. What do we get?

$$\begin{aligned} z' + Dh_3(z)z' &= Jz + Jh_3(z) + F_2^R(z + h_3(z)) + \tilde{F}_3(z + h_3(z)) + \mathcal{O}(4) \\ \Rightarrow (I + Dh_3(z))z' &= Jz + F_2^R(z) + Jh_3(z) + \tilde{F}_3(z) + \mathcal{O}(4). \end{aligned} \quad (11.37)$$

We can ignore all the other terms since they end up being higher-than-third order. Marching along ...

$$\begin{aligned}
z' &= (I - Dh_3(z) + \mathcal{O}(6)) \left( Jz + Jh_3(z) + F_2^R(z + h_3(z)) + \tilde{F}_3(z + h_3(z)) + \mathcal{O}(4) \right) \\
&= Jz + F_2^R(z) - Dh_3(z)Jz + \tilde{F}_3(z) + Jh_3(z) + \mathcal{O}(4) \\
&= Jz + F_2^R(z) + L_J^{(3)}h_3(z) + \tilde{F}_3(z) + \mathcal{O}(4),
\end{aligned} \tag{11.38}$$

where the operator  $L_J^{(3)}$  is defined as before, see (11.16). Thus in order to eliminate cubic terms, we need to solve

$$L_J^{(3)}h_3(z) = -\tilde{F}_3(z), \tag{11.39}$$

which may be solved just like before: introduce a space  $H_3$  of vectors with cubic components (there's a few more than quadratic, you see where this is going), figure out what the range of the operator is, *etc.*

## 11.5 The Normal Form Theorem

In general we have the following theorem.

**Theorem 25 (The Normal Form Theorem)** *Using a sequence of analytic coordinate changes, we may transform*

$$x' = G(x),$$

where  $G$  is  $r$  times differentiable, to

$$y' = Jy + F_2^R(y) + F_3^R(y) + \dots + F_{r-1}^R(y) + \mathcal{O}(|y|^r), \tag{11.40}$$

where the super index denotes resonant terms.

Note that the structure of the normal form is **completely** determined by the linear part  $J$ . Also, the normal form transformation of order  $j$  does not affect the already obtained results at orders  $1, 2, \dots, j - 1$ .



# Chapter 12

## Bifurcations of fixed points of vector fields

In this chapter we examine the behavior near fixed points of continuous-time dynamical systems, especially as a function of changing parameters.

### 12.1 Preliminaries

Consider the autonomous system

$$y' = g(y, \lambda), \tag{12.1}$$

where  $y \in \mathbb{R}^n$ , and  $\lambda$  is a real parameter. Suppose that for a certain value of the parameter  $\lambda = \lambda_0$  there is a fixed point at  $y = y_0$ :

$$g(y_0, \lambda_0) = 0. \tag{12.2}$$

We want to answer two questions:

1. Is the fixed point stable or unstable?
2. How does this change (if it does) as  $\lambda$  is varied?

In general, **we will talk of a bifurcation if the behavior of a dynamical system, or some aspect of it, changes as one or more system parameters change.**

For sure, this is a pretty loose definition. But we want to be flexible (you live longer, that way): the change could be in the number of fixed points, in their dynamics, in the color of the trajectories, *etc.*

We know that hyperbolic fixed points are structurally stable<sup>1</sup> (*i.e.*), they remain hyperbolic under small changes in the parameters on which they depend continuously. Thus it

---

<sup>1</sup>Since hyperbolicity is determined by inequalities.

makes sense to focus our attention on non-hyperbolic fixed points. Let's start by considering the case of a zero eigenvalue.

Suppose that  $D_y g(y_0, \lambda_0)$  has a single zero eigenvalue. The behavior associated with the corresponding eigenspace is governed by the center manifold dynamics, which we can write as

$$x' = f(x, \mu), \quad (12.3)$$

where  $x \in \mathbb{R}$ ,  $\mu = \lambda - \lambda_0 \in \mathbb{R}$ . Further, by our assumptions

$$f(0, 0) = 0, \quad \frac{\partial f}{\partial x}(0, 0) = 0. \quad (12.4)$$

Let's start by looking at three specific examples.

**Example 19** Consider the equation

$$x' = \mu - x^2. \quad (12.5)$$

Thus here

$$f(x, \mu) = \mu - x^2, \quad (12.6)$$

and indeed

$$f(0, 0) = 0, \quad \frac{\partial f}{\partial x}(0, 0) = -2x|_{(x,\mu)=(0,0)} = 0. \quad (12.7)$$

The fixed points are given by

$$x^2 = \mu. \quad (12.8)$$

We immediately conclude that there are no fixed points for  $\mu < 0$  and two fixed points for  $\mu > 0$ . One of these fixed points is stable, the other is unstable. This is the canonical example of a **saddle-node** bifurcation: on one side of the bifurcation value, there are no fixed points. On the other side there are two, with different stability properties. This is illustrated in Figure 12.1.

**Example 20** Consider the equation

$$x' = \mu x - x^2. \quad (12.9)$$

Thus

$$f(x, \mu) = \mu x - x^2. \quad (12.10)$$

Then

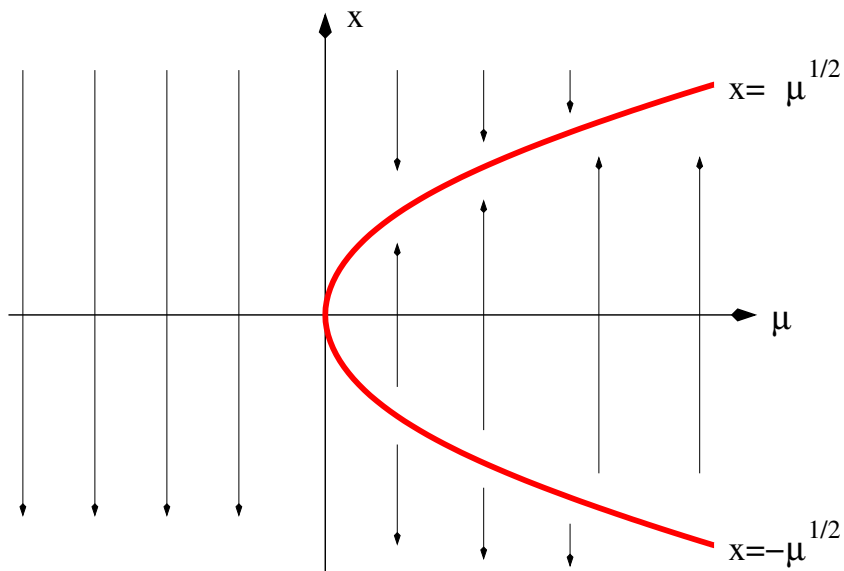


Figure 12.1: The bifurcation diagram for a saddle-node bifurcation.

$$f(0,0) = 0, \quad \frac{\partial f}{\partial x}(0,0) = \mu - 2x|_{(x,\mu)=(0,0)} = 0. \quad (12.11)$$

The fixed points are given by

$$x = 0 \quad \text{and} \quad x = \mu. \quad (12.12)$$

At  $\mu = 0$  the fixed points interchange stability properties. This is called a **transcritical bifurcation**. It is illustrated in Figure 12.2.

**Example 21** Consider the equation

$$x' = \mu x - x^3. \quad (12.13)$$

Thus here

$$f(x, \mu) = \mu x - x^3, \quad (12.14)$$

and again

$$f(0,0) = 0, \quad \frac{\partial f}{\partial x}(0,0) = \mu - 3x^2|_{(x,\mu)=(0,0)} = 0. \quad (12.15)$$

The fixed points are given by

$$x = 0 \quad \text{and} \quad x^2 = \mu. \quad (12.16)$$

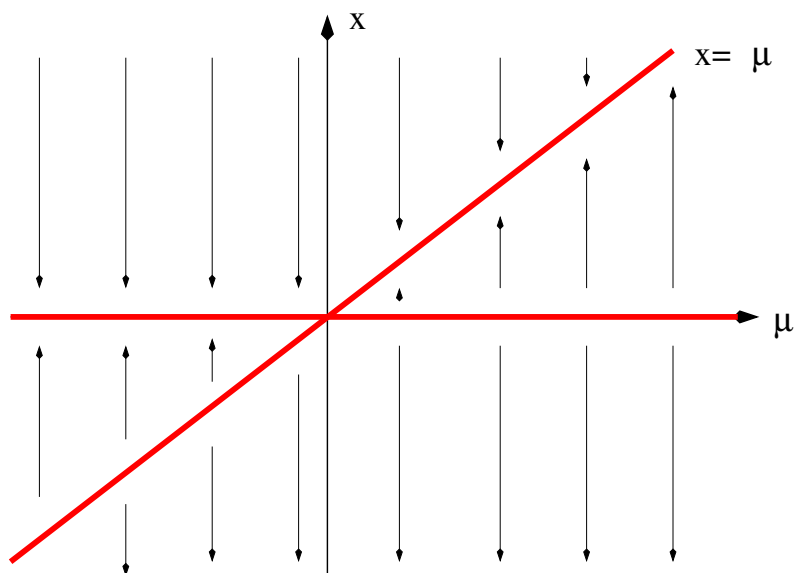


Figure 12.2: The bifurcation diagram for a transcritical bifurcation.

We conclude there is one fixed point for  $\mu < 0$  and three fixed points for  $\mu > 0$ . The original fixed point is stable, but it loses stability in the bifurcation, at which point two new fixed points are born. Both are stable. This is the canonical example of **pitchfork** bifurcation: on one side of the bifurcation value, there is one fixed point. On the other side there are three. The two new ones inherit the stability properties of the original fixed point. This is illustrated in Figure 12.3.

## 12.2 The saddle-node bifurcation

Let's investigate the saddle-node bifurcation in a lot more detail. Suppose we have

$$x' = f(x, \mu), \quad (12.17)$$

with  $x \in \mathbb{R}$  and  $\mu \in \mathbb{R}$ , so that

$$f(0, 0) = 0. \quad (12.18)$$

Thus the system has a fixed point at  $x = 0$  with bifurcation parameter  $\mu = 0$ . Furthermore, assume this fixed point is *not* hyperbolic:

$$\frac{\partial f}{\partial x}(0, 0) = 0. \quad (12.19)$$

A saddle-node bifurcation occurs when we (locally) have a curve of fixed points defined implicitly by

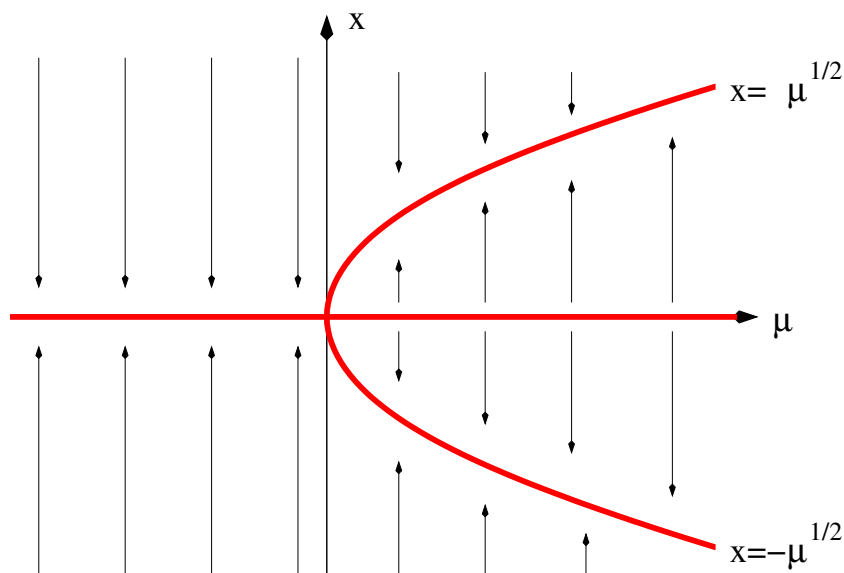


Figure 12.3: The bifurcation diagram for a pitchfork bifurcation.

$$\mu = \mu(x), \quad (12.20)$$

which is tangent to the line  $\mu = 0$ . In other words

$$\frac{d\mu}{dx}(0) = 0, \quad (12.21)$$

and it lies entirely on one side of this line:

$$\frac{d^2\mu}{dx^2}(0) \neq 0. \quad (12.22)$$

This implies that locally, near the bifurcation point, the picture looks like one of the two cases depicted in Figure 12.4. The picture on the left is that of a *supercritical* saddle-node bifurcation, implying that the fixed points exist for values of the parameter  $\mu$  greater than the bifurcation value  $\mu = 0$ . Similarly, the right case shows a *subcritical* bifurcation. It should be stated that there are two schools of thought on the nomenclature of bifurcations: one school uses the words *supercritical* and *subcritical* to differentiate stability properties. That is not the school we'll follow here<sup>2</sup>. We'll make a different choice, using these words only to indicate existence of fixed points.

<sup>2</sup>Frankly, I have no idea why they would do that. That is just absolutely a boneheaded thing to do. Something akin to barbarian times. It is so absurd, one can only question their sanity. It's like something from the middle ages. **We**, on the other hand, find ourselves squarely in the Renaissance. Clearly, it's the better way to go. And there's no choice. You're either with us, or against us. And you don't want to be against us. We can be vicious. Back to the course.

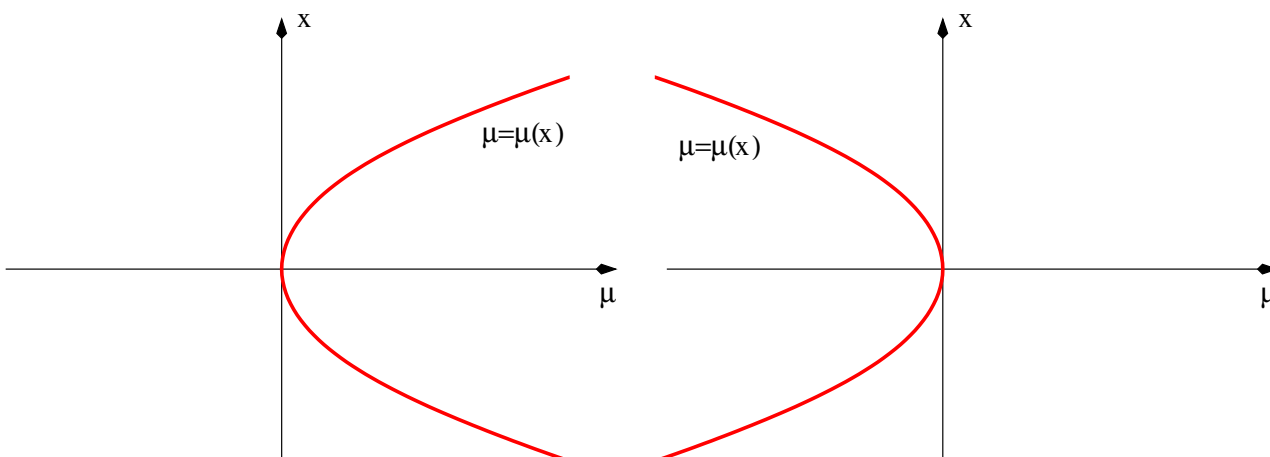


Figure 12.4: The fixed-point curves, locally near the bifurcation point for a (left) supercritical and (right) subcritical saddle-node bifurcation.

So, what are the conditions on  $f(x, \mu)$  for a saddle-node bifurcation to happen? We already have

$$f(0, 0) = 0, \quad (12.23)$$

and

$$\frac{\partial f}{\partial x}(0, 0) = 0. \quad (12.24)$$

By the implicit function theorem, if

$$\frac{\partial f}{\partial \mu}(0, 0) \neq 0, \quad (12.25)$$

we have that in a neighborhood of the bifurcation point  $\mu = \mu(x)$  solves

$$f(x, \mu(x)) = 0. \quad (12.26)$$

Taking a derivative with respect to  $x$ , we get

$$\frac{\partial f}{\partial x} + \frac{\partial f}{\partial \mu} \mu'(x) = 0. \quad (12.27)$$

Evaluating this at  $(0, 0)$ , we get  $\mu'(0) = 0$ , as desired. Taking another derivative,

$$\frac{\partial^2 f}{\partial x^2} + 2 \frac{\partial^2 f}{\partial x \partial \mu} \mu'(x) + \frac{\partial^2 f}{\partial \mu^2} \mu'^2(x) + \frac{\partial f}{\partial \mu} \mu''(x) = 0. \quad (12.28)$$

Again, we evaluate this at  $(0, 0)$  to get

$$\frac{\partial^2 f}{\partial x^2}(0,0) + \frac{\partial f}{\partial \mu}(0,0)\mu''(0) = 0 \Rightarrow \mu''(0) = -\frac{\partial^2 f/\partial x^2}{\partial f/\partial \mu}(0,0). \quad (12.29)$$

Thus  $\mu''(0) \neq 0$  provided

$$\frac{\partial^2 f}{\partial x^2}(0,0) \neq 0. \quad (12.30)$$

We can (and we will!) summarize the conditions on the right-hand side of the system to have a saddle-node bifurcation at  $(0,0)$ .

**Theorem 26** *The system*

$$x' = f(x, \mu) \quad (12.31)$$

*will undergo a saddle-node bifurcation of its fixed point at  $x = 0$  with bifurcation parameter  $\mu = 0$  if*

- $f(0,0) = 0$ ,
- $f_x(0,0) = 0$  (*this and the previous condition state that we have a nonhyperbolic fixed point at the bifurcation point*),
- $f_\mu(0,0) \neq 0$  (*thus the implicit function theorem may be used*),
- $f_{xx}(0,0) \neq 0$  (*the bifurcation curve lies on one side of the  $\mu = 0$  line*).

Let's put this theorem to work. In general we have

$$f(x, \mu) = ax + b\mu + cx^2 + dx\mu + e\mu^2 + \mathcal{O}(3). \quad (12.32)$$

Imposing the conditions for a saddle-node bifurcations, we get:

- $f_x(0,0) = a = 0$ ,
- $f_\mu(0,0) = b \neq 0$ ,
- $f_{xx}(0,0) = 2c \neq 0$ .

Thus,

$$f(x, \mu) = b\mu + cx^2 + dx\mu + e\mu^2 + \mathcal{O}(3). \quad (12.33)$$

What is the normal form for this system, near the bifurcation point? Consider the two-dimensional system

$$\begin{cases} x' = f(x, \mu) = b\mu + cx^2 + dx\mu + e\mu^2 + \mathcal{O}(3) \\ \mu' = 0 \end{cases}. \quad (12.34)$$

By using a time scaling, we can equate  $b = 1$ . Note that this may have an influence on whether the bifurcation is sub- or supercritical. Then the linear part of the above system is determined by the matrix

$$J = \begin{pmatrix} 0 & 1 \\ 0 & 0 \end{pmatrix}, \quad (12.35)$$

which gives rise to the Takens-Bogdanov normal form (see the previous chapter). We know that all terms of the form  $(x\mu, 0)^T$  and  $(\mu^2, 0)^T$  may be eliminated. This leads to the reduced form of the first equation as

$$x' = \mu + cx^2 + \mathcal{O}(3). \quad (12.36)$$

Up to a scaling on the  $x$  variable, this is the canonical form for the saddle-node bifurcation given in the previous section.

## 12.3 The transcritical bifurcation

In this section we give the same detailed treatment of the transcritical bifurcation that we just gave of the saddle-node bifurcation.

A transcritical bifurcation happens when, near the bifurcation point, there are two curves of fixed points for all values of the bifurcation parameter  $\mu$ , both passing through  $(0, 0)$ . Their stability properties change as we pass through this bifurcation point.

Again, consider

$$x' = f(x, \mu), \quad (12.37)$$

with  $(x, \mu) \in \mathbb{R} \times \mathbb{R}$ . As before, we require the existence of a nonhyperbolic fixed point at the bifurcation point:

$$f(0, 0) = 0, \quad \frac{\partial f}{\partial x}(0, 0) = 0. \quad (12.38)$$

To have a transcritical bifurcation we also need

$$\frac{\partial f}{\partial \mu}(0, 0) = 0. \quad (12.39)$$

Otherwise, by the implicit function theorem, there would exist a unique solution  $\mu = \mu(x)$  to  $f(x, \mu) = 0$ , violating the assumption of having two curves of fixed points.

We impose that  $x = 0$  is one of the two fixed points of the system, for all  $\mu$ . We let

$$x' = f(x, \mu) = xF(x, \mu), \quad (12.40)$$

where

$$F(x, \mu) = \begin{cases} f(x, \mu)/x & x \neq 0 \\ f_x(0, \mu) & x = 0 \end{cases}. \quad (12.41)$$

Notice that we could always accomplish this by a linear transformation on  $x$ , if necessary. We refer to  $x = 0$  as the trivial fixed point, and the other one as the (you guessed it) nontrivial fixed point. The reason for assuming the presence of a trivial fixed point is that many application systems have one, corresponding to the system being in its quiescent state.

Using the above,

$$F(0, 0) = \frac{\partial f}{\partial x}(0, 0) = 0. \quad (12.42)$$

Let us assume that

$$\frac{\partial F}{\partial \mu}(0, 0) = \frac{\partial^2 f}{\partial x \partial \mu}(0, 0) \neq 0. \quad (12.43)$$

By the implicit function theorem, there exists a unique  $\mu(x)$  such that

$$F(x, \mu(x)) = 0. \quad (12.44)$$

Taking a derivative

$$\frac{\partial F}{\partial x} + \frac{\partial F}{\partial \mu} \mu'(x) = 0 \quad \Rightarrow \quad \mu'(x) = -\frac{F_x}{F_\mu}. \quad (12.45)$$

We want  $\mu'(x)$  to be finite but not zero at the bifurcation point. Thus in addition we need

$$F_x(0, 0) = \frac{\partial^2 f}{\partial x^2}(0, 0) \neq 0. \quad (12.46)$$

We may summarize as before.

**Theorem 27** *The system*

$$x' = f(x, \mu) \quad (12.47)$$

*will undergo a transcritical bifurcation at  $x = 0$  with bifurcation parameter  $\mu = 0$  if*

- $f(0, 0) = 0$ ,
- $f_x(0, 0) = 0$  (*this and the previous condition state that we have a nonhyperbolic fixed point at the bifurcation point*),
- $f_\mu(0, 0) = 0$  (*thus the implicit function theorem cannot be used*),
- $f_{x\mu}(0, 0) \neq 0$ ,
- $f_{xx}(0, 0) \neq 0$ .

This collection of conditions ensures behavior near the bifurcation point depicted in Figure 12.5. Using a normal-form argument like for the saddle-node bifurcation, we can show that

$$x' = \mu x \pm x^2 + \mathcal{O}(3) \quad (12.48)$$

may be regarded as the canonical form of the transcritical bifurcation.

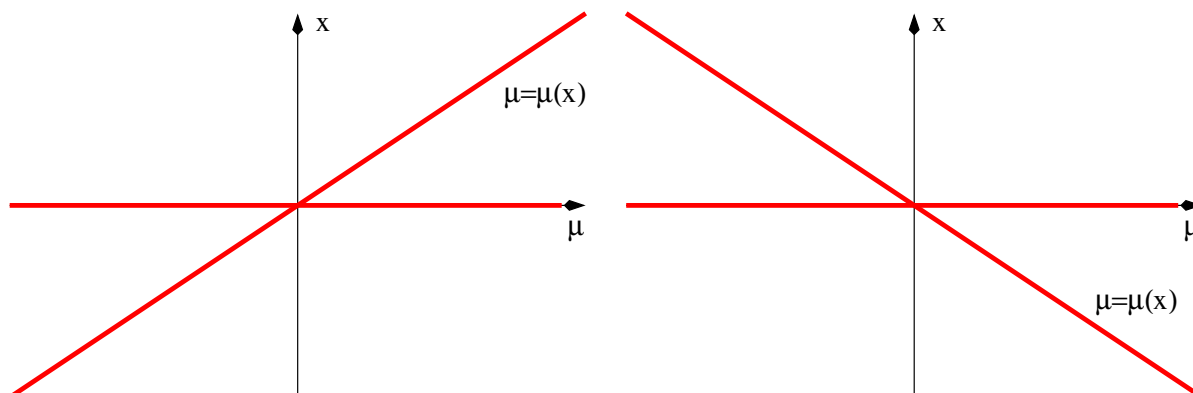


Figure 12.5: The fixed-point curves, locally near the bifurcation point for a transcritical bifurcation.

## 12.4 The pitchfork bifurcation

The discussion of the pitchfork bifurcation very much follows the same lines as that of the transcritical bifurcation. Oh, the anticipation!

A pitchfork is characterized by two curves of fixed points passing through the bifurcation point  $(x, \mu) = (0, 0)$ . One of these curves gives the “trivial” fixed point  $x = 0$ , while the other one (as in the case of a saddle-node bifurcation) lies entirely on one side of  $\mu = 0$ . Further, the  $x = 0$  curve of fixed points changes its stability upon going through the bifurcation. The stability of the nontrivial branches of fixed points is the same as that of the trivial fixed point in the region where it is the only fixed point.

Consider

$$x' = f(x, \mu), \quad (12.49)$$

with a nonhyperbolic fixed point at  $(0, 0)$ :

$$f(0, 0) = 0, \quad f_x(0, 0) = 0. \quad (12.50)$$

As for the transcritical bifurcation, we want more than one curve of fixed points through the origin, implying we cannot allow the implicit function theorem to be applicable:

$$f_\mu(0, 0) = 0. \quad (12.51)$$

Next, we impose that  $x = 0$  is a curve of fixed points, for all values of the bifurcation parameter  $\mu = 0$ . Then  $f(x, \mu)$  can be written as

$$x' = f(x, \mu) = xF(x, \mu), \quad (12.52)$$

so that

$$F(x, \mu) = \begin{cases} f(x, \mu)/x & x \neq 0 \\ f_x(0, \mu) & x = 0 \end{cases}. \quad (12.53)$$

To have a second curve of fixed points, we need

$$F(0, 0) = 0, \quad \text{and} \quad F_\mu(0, 0) \neq 0 \quad (12.54)$$

so that by the implicit function theorem we have that there exists a curve

$$\mu = \mu(x) \quad (12.55)$$

which solves

$$F(x, \mu(x)) = 0. \quad (12.56)$$

Next, we impose conditions on this curve of fixed points to satisfy our earlier assumptions. We want this curve of fixed points to be tangent to the  $\mu = 0$ , and only lie on one side of it. Thus

$$\mu'(0) = 0, \quad (12.57)$$

and

$$\mu''(0) \neq 0, \quad (12.58)$$

as for the saddle-node bifurcation. You see where we're going with this:

$$\mu'(x) = -\frac{F_x}{F_\mu} \Rightarrow \mu'(0) = -\frac{f_{xx}(0, 0)}{f_{x\mu}(0, 0)} = 0. \quad (12.59)$$

Thus we need

$$f_{xx}(0, 0) = 0. \quad (12.60)$$

Next, since

$$F_x + f_\mu \mu' = 0 \Rightarrow F_{xx} + 2F_{x\mu} \mu' + F_{\mu\mu} \mu'^2 + F_\mu \mu'' = 0. \quad (12.61)$$

Evaluating this at the bifurcation points, we find

$$F_{xx}(0, 0) + F_{\mu}(0, 0)\mu''(0) = 0, \quad (12.62)$$

from which it follows that

$$\mu''(0) = -\frac{F_{xx}(0, 0)}{F_{\mu}(0, 0)} = -\frac{f_{xxx}(0, 0)}{f_{x\mu}(0, 0)}, \quad (12.63)$$

implying that we need

$$f_{xxx}(0, 0) \neq 0. \quad (12.64)$$

Summarizing, we get the following theorem.

**Theorem 28** *The system*

$$x' = f(x, \mu) \quad (12.65)$$

*will undergo a pitchfork bifurcation at  $x = 0$  at bifurcation parameter  $\mu = 0$  if*

- $f(0, 0) = 0$ ,
- $f_x(0, 0) = 0$  (*this and the previous condition state that we have a nonhyperbolic fixed point at the bifurcation point*),
- $f_{\mu}(0, 0) = 0$  (*thus the implicit function theorem cannot be used*),
- $f_{xx}(0, 0) = 0$ ,
- $f_{x\mu}(0, 0) \neq 0$ ,
- $f_{xxx}(0, 0) \neq 0$ .

Locally, near the bifurcation point this results in one of two scenarios, both of which are illustrated in Figure 12.6. Further, as before,

$$x' = \mu x \pm x^3 \quad (12.66)$$

may be regarded as the normal form of the pitchfork bifurcation.

## 12.5 The Hopf bifurcation

The Hopf bifurcation is our first example of a bifurcation where we are dealing with a fixed point that is nonhyperbolic at the bifurcation point that has a center manifold associated with it that is more than one dimensional<sup>3</sup>. Specifically, we consider the case where the center subspace is characterized by two complex conjugate imaginary eigenvalues. In order to understand how generic a Hopf bifurcation truly is, we start by investigating the normal form of a reduced system with two such imaginary eigenvalues.

---

<sup>3</sup>Holy run-on sentence, Batman! With a footnote to boot!

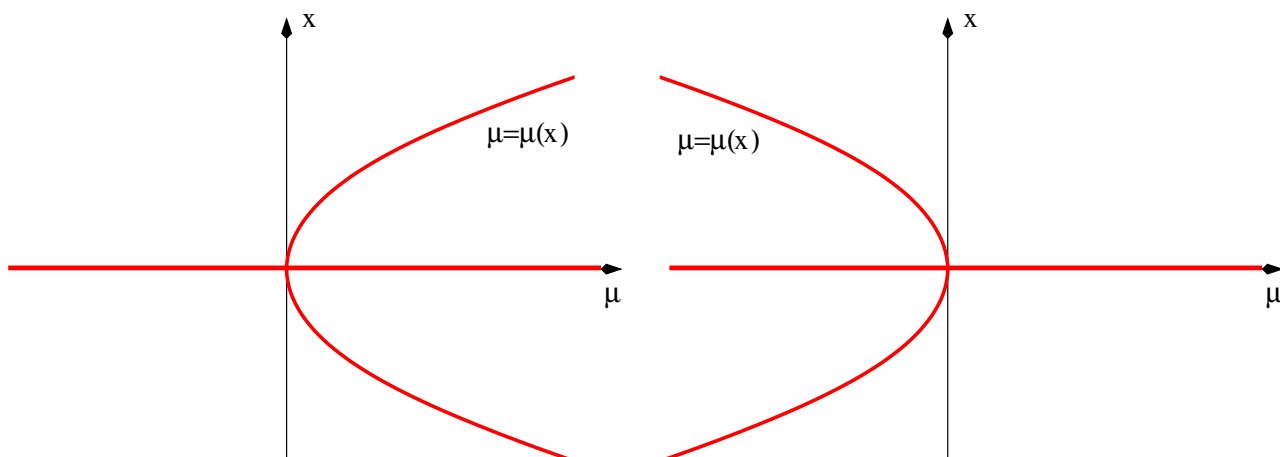


Figure 12.6: The fixed-point curves, locally near the bifurcation point for a pitchfork bifurcation. A supercritical bifurcation is shown on the left, a subcritical one on the right.

## 1. Preparation steps and complexification

Consider the system

$$x' = f(x, \mu), \quad (12.67)$$

with  $x \in \mathbb{R}^2$  and  $\mu \in \mathbb{R}$ . Further, we assume that at  $\mu = 0$ , the Jacobian  $D_x f(x, \mu)|_{(0,0)}$  has two purely imaginary eigenvalues

$$\lambda(0) = \pm i\omega(0), \quad (12.68)$$

where the zero argument corresponds to the value of  $\mu$ . Under rather generic conditions, for small  $\mu \neq 0$  we have

$$\lambda(\mu) = \text{Re}\lambda(\mu) \pm i\omega(\mu). \quad (12.69)$$

After a linear transformation, the Jacobian may be written as

$$D_x f(0, \mu) = \begin{pmatrix} \text{Re}\lambda(\mu) & -\omega(\mu) \\ \omega(\mu) & \text{Re}\lambda(\mu) \end{pmatrix}, \quad (12.70)$$

which is nothing but the real Jordan form of the matrix. We have also assumed that for  $\mu$  sufficiently small  $x = 0$  is a fixed point.

Our dynamical system is rewritten as

$$\begin{cases} x' = \text{Re}\lambda(\mu)x - \omega(\mu)y + f_1(x, y, \mu) \\ y' = \omega(\mu)x + \text{Re}\lambda(\mu)y + f_2(x, y, \mu) \end{cases}, \quad (12.71)$$

from which it follows that

$$\begin{aligned}
(x + iy)' &= \operatorname{Re}\lambda(\mu)x - \omega(\mu)y + f_1(x, y, \mu) + i(\omega(\mu)x + \operatorname{Re}\lambda(\mu)y + f_2(x, y, \mu)) \\
\Rightarrow &= \lambda(\mu)x + i\lambda(\mu)y + f_1(x, y, \mu) + if_2(x, y, \mu) \\
\Rightarrow & z' = \lambda(\mu)z + F(z, \bar{z}, \mu),
\end{aligned} \tag{12.72}$$

where  $z = x + iy$ ,  $\bar{z} = x - iy$ , and the last equality defines  $F(z, \bar{z}, \mu)$ . We take (12.72) as our starting point. We now reduce it to normal form.

## 2. Second-order terms

Let

$$z = \hat{z} + h_2(\hat{z}, \hat{\bar{z}}), \tag{12.73}$$

where  $h_2(\hat{z}, \hat{\bar{z}})$  is quadratic in its arguments. We rewrite the system (12.72) as

$$z' = \lambda(\mu)z + F_2(\hat{z}, \hat{\bar{z}}, \mu) + F_3(\hat{z}, \hat{\bar{z}}, \mu) + \dots, \tag{12.74}$$

where each  $F_k$  is a homogeneous polynomial of degree  $k$ . The result of our near-identity transformation is

$$\hat{z}' + \frac{\partial h_2}{\partial \hat{z}} \hat{z}' + \frac{\partial h_2}{\partial \hat{\bar{z}}} \hat{\bar{z}}' = \lambda(\mu)(\hat{z} + h_2(\hat{z}, \hat{\bar{z}})) + F_2(\hat{z}, \hat{\bar{z}}) + \mathcal{O}(3). \tag{12.75}$$

In what follows, we drop the  $\hat{\cdot}$ 's to ease up on notation. We get

$$z' \left( 1 + \frac{\partial h_2}{\partial z} \right) + \frac{\partial h_2}{\partial \bar{z}} \bar{z}' = \lambda(\mu)z + \lambda(\mu)h_2(z, \bar{z}) + F_2(z, \bar{z}) + \mathcal{O}(3). \tag{12.76}$$

Of course, the complex conjugate of this equation also holds:

$$\bar{z}' \left( 1 + \frac{\partial \bar{h}_2}{\partial \bar{z}} \right) + \frac{\partial \bar{h}_2}{\partial z} z' = \bar{\lambda}(\mu)\bar{z} + \bar{\lambda}(\mu)\bar{h}_2(z, \bar{z}) + \bar{F}_2(z, \bar{z}) + \mathcal{O}(3). \tag{12.77}$$

Keeping only linear terms in  $z$  and  $\bar{z}$ , we find that

$$\bar{z}' = \bar{\lambda}(\mu)\bar{z} + \mathcal{O}(2). \tag{12.78}$$

Using this in (12.76), we get

$$\begin{aligned}
& z' \left( 1 + \frac{\partial h_2}{\partial z} \right) + \frac{\partial h_2}{\partial \bar{z}} \bar{\lambda}(\mu) \bar{z} = \lambda(\mu) z + \lambda(\mu) h_2(z, \bar{z}) + F_2(z, \bar{z}) + \mathcal{O}(3) \\
\Rightarrow & z' = \left( 1 + \frac{\partial h_2}{\partial z} \right)^{-1} \left( \lambda(\mu) z + \lambda(\mu) h_2(z, \bar{z}) + F_2(z, \bar{z}) - \frac{\partial h_2}{\partial \bar{z}} \bar{\lambda}(\mu) \bar{z} \right) + \mathcal{O}(3) \\
\Rightarrow & z' = \left( 1 - \frac{\partial h_2}{\partial z} \right) \left( \lambda(\mu) z + \lambda(\mu) h_2(z, \bar{z}) + F_2(z, \bar{z}) - \frac{\partial h_2}{\partial \bar{z}} \bar{\lambda}(\mu) \bar{z} \right) + \mathcal{O}(3) \\
\Rightarrow & z' = \lambda(\mu) z + \left( \lambda(\mu) h_2(z, \bar{z}) + F_2(z, \bar{z}) - \frac{\partial h_2}{\partial \bar{z}} \bar{\lambda}(\mu) \bar{z} - \frac{\partial h_2}{\partial z} \lambda z \right) + \mathcal{O}(3). \quad (12.79)
\end{aligned}$$

Can we choose  $h_2$  so that the second-order terms vanish:

$$\lambda(\mu) h_2(z, \bar{z}) + F_2(z, \bar{z}) = \frac{\partial h_2}{\partial \bar{z}} \bar{\lambda}(\mu) \bar{z} + \frac{\partial h_2}{\partial z} \lambda z? \quad (12.80)$$

If we can accomplish this, the first correction to the linear behavior will be cubic!

There are three potential second-order terms:

$$z^2, \bar{z}^2, z\bar{z}. \quad (12.81)$$

We need to check whether these are in the range of the operator  $L^{(2)}$ :

$$L^{(2)} h_2 = \lambda(\mu) h_2 - \frac{\partial h_2}{\partial \bar{z}} \bar{\lambda}(\mu) \bar{z} - \frac{\partial h_2}{\partial z} \lambda z. \quad (12.82)$$

We have:

- $L^{(2)} z^2 = \lambda(\mu) z^2 - \lambda(\mu) z 2z = -\lambda(\mu) z^2,$
- $L^{(2)} \bar{z}^2 = \lambda(\mu) \bar{z}^2 - \bar{\lambda}(\mu) 2\bar{z}^2 = \bar{z}^2(\lambda(\mu) - 2\bar{\lambda}(\mu)).$  Note that the coefficient of the right-hand side is nonzero near the bifurcation point.
- $L^{(2)} z\bar{z} = \lambda(\mu) z\bar{z} - \lambda(\mu) z\bar{z} - \bar{\lambda}(\mu) \bar{z}z = -\bar{\lambda}(\mu) z\bar{z}.$

We see that  $L^{(2)}$  is diagonal in this basis and, indeed, all second-order terms may be eliminated. Thus, after the near-identity transformation, we have

$$z' = \lambda(\mu) z + F_3(z, \bar{z}, \mu) + \mathcal{O}(4). \quad (12.83)$$

### 3. Third-order terms

Well, can we be equally successful with the third-order terms? Maybe we can, if we want it enough: death to the third-order terms! Define a new near-identity transformation, to be applied to (12.83):

$$z = \hat{z} + h_3(\hat{z}, \hat{\bar{z}}). \quad (12.84)$$

After substitution we get (dropping the hats; it's too warm as it is)

$$\begin{aligned}
z' &= \left(1 + \frac{\partial h_3}{\partial z}\right)^{-1} \left(\lambda z + \lambda h_3 + F_3 - \frac{\partial h_3}{\partial \bar{z}} \bar{z}'\right) + \mathcal{O}(4) \\
&= \left(1 - \frac{\partial h_3}{\partial z}\right) \left(\lambda z + \lambda h_3 + F_3 - \frac{\partial h_3}{\partial \bar{z}} \bar{\lambda} \bar{z}\right) + \mathcal{O}(4) \\
&= \lambda z + \left(\lambda h_3 - \frac{\partial h_3}{\partial \bar{z}} \bar{\lambda} \bar{z} - \frac{\partial h_3}{\partial z} \lambda z + F_3\right) + \mathcal{O}(4).
\end{aligned} \tag{12.85}$$

Thus, again, we have to examine the operator

$$L^{(3)}h_3 = \lambda h_3 - \bar{\lambda} \bar{z} \frac{\partial h_3}{\partial \bar{z}} - \lambda z \frac{\partial h_3}{\partial z}. \tag{12.86}$$

Since  $F_3$  consists of a linear combination of terms of the form

$$z^3, z^2 \bar{z}, z \bar{z}^2, \bar{z}^3, \tag{12.87}$$

we examine how many of these terms are in the range of the operator.

- $z^3$ :  $L^{(3)}z^3 = -2\lambda z^3$ ,
- $z^2 \bar{z}$ :  $L^{(3)}z^2 \bar{z} = -z^2 \bar{z}(\lambda + \bar{\lambda})$ . Note that this coefficient is zero at the bifurcation point, since  $\lambda(0) = i\omega(0)$  there.
- $z \bar{z}^2$ :  $L^{(3)}z \bar{z}^2 = -2\bar{\lambda} z \bar{z}^2$ ,
- $\bar{z}^3$ :  $L^{(3)}\bar{z}^3 = (\lambda - 3\bar{\lambda})\bar{z}^3$ .

We see that all of the cubic terms are in the range of  $L^{(3)}$  at the bifurcation point, except the second one. Thus the  $z^2 \bar{z}$  term cannot be eliminated, and it needs to be retained in the normal form. Thus, up to cubic terms, we find the normal form to be

$$z' = \lambda(\mu)z + c(\mu)z^2 \bar{z} + \mathcal{O}(4). \tag{12.88}$$

#### 4. General discussion of the normal form

What can we say about the terms at any order? At each order, we obtain an operator of the form

$$Lh = \lambda h - \lambda z \frac{\partial h}{\partial z} - \bar{\lambda} \bar{z} \frac{\partial h}{\partial \bar{z}}. \tag{12.89}$$

If we let

$$h = z^n \bar{z}^m, \tag{12.90}$$

we get

$$Lz^n \bar{z}^m = z^n \bar{z}^m (\lambda - n\lambda - m\bar{\lambda}). \quad (12.91)$$

At  $\mu = 0$ ,  $\bar{\lambda} = -\lambda$ , thus if

$$1 - n + m = 0, \quad (12.92)$$

then the  $(n, m)$ -term cannot be eliminated. This is not possible if  $m + n$  is even, because then  $m - n = m + n - 2n$  is also even. Thus all terms of even order can always be eliminated. Our normal form is thus

$$z' = \lambda(\mu)z + c(\mu)z^2 \bar{z} + \mathcal{O}(5), \quad (12.93)$$

valid in some neighborhood of the bifurcation point  $(x, y, \mu) = (0, 0, 0)$ . In Cartesian coordinates, we get

$$\begin{aligned} x' + iy' &= (\alpha + i\omega)(x + iy) + (a + ib)(x + iy)^2(x - iy) + \mathcal{O}(5) \\ \Rightarrow \begin{cases} x' &= \alpha x - \omega y + (ax - by)(x^2 + y^2) + \mathcal{O}(5) \\ y' &= \omega x + \alpha y + (bx + ay)(x^2 + y^2) + \mathcal{O}(5) \end{cases}, \end{aligned} \quad (12.94)$$

where  $\alpha = \operatorname{Re}(\lambda)(\mu)$ , and  $c(\mu) = a + ib$ . Perhaps it is more transparent to write this in polar coordinates:

$$\begin{aligned} &(re^{i\theta})' = \lambda(\mu)re^{i\theta} + c(\mu)r^3e^{i\theta} + \mathcal{O}(5) \\ \Rightarrow r'e^{i\theta} + ir\theta'e^{i\theta} &= \lambda(\mu)re^{i\theta} + c(\mu)r^3e^{i\theta} + \mathcal{O}(5) \\ \Rightarrow r' + ir\theta' &= \lambda(\mu)r + c(\mu)r^3 + \mathcal{O}(5) \\ \Rightarrow \begin{cases} r' &= \alpha r + ar^3 + \mathcal{O}(5) \\ \theta' &= \omega + br^2 + \mathcal{O}(4) \end{cases}. \end{aligned} \quad (12.95)$$

## 5. Discussion of the Hopf bifurcation

Now that we have established this normal form, we can use it to study the Hopf bifurcation. We have

$$\begin{cases} r' &= \alpha(\mu)r + a(\mu)r^3 + \mathcal{O}(5) \\ \theta' &= \omega(\mu) + b(\mu)r^2 + \mathcal{O}(4) \end{cases}. \quad (12.96)$$

Since we are interested in the behavior near the bifurcation point  $(r, \mu) = (0, 0)$ , we may expand the normal form around  $\mu = 0$ :

$$\begin{cases} r' &= (\alpha(0) + \mu\alpha'(0) + \dots)r + (a(0) + \mu a'(0) + \dots)r^3 + \mathcal{O}(5) \\ \theta' &= \omega(0) + \mu\omega'(0) + \dots + (b(0) + \mu b'(0) + \dots)r^2 + \mathcal{O}(4) \end{cases}, \quad (12.97)$$

which may be simplified as

$$\begin{cases} r' &= \alpha'(0)\mu r + a(0)r^3 + \dots \\ \theta' &= \omega(0) + \omega'(0)\mu + b(0)r^2 + \dots \end{cases}, \quad (12.98)$$

since, by assumption,  $\alpha(0) = 0$ . Note that we are ignoring higher-order terms in  $\mu$ . Thus we end up studying the truncated normal form

$$\begin{cases} r' &= \alpha'(0)\mu r + a(0)r^3 \\ \theta' &= \omega(0) + \omega'(0)\mu + b(0)r^2 \end{cases}, \quad (12.99)$$

or

$$\begin{cases} r' &= d\mu r + ar^3 \\ \theta' &= \omega + c\mu + br^2 \end{cases}, \quad (12.100)$$

where we have simplified the notation a little, by introducing new constants.

If  $r' = 0$  but  $\theta' \neq 0$ , then it appears we have found a periodic orbit. This is easily done:

$$d\mu r + ar^3 = 0 \quad \Rightarrow \quad r = \sqrt{\frac{-d\mu}{a}}, \quad (12.101)$$

and we have discarded the zero solution. Then

$$\begin{aligned} \theta' &= \omega + c\mu - \frac{bd\mu}{a} \\ &= \omega + (c - bd/a)\mu \\ \Rightarrow \quad \theta &= \theta_0 + [\omega + (c - bd/a)\mu]t, \end{aligned} \quad (12.102)$$

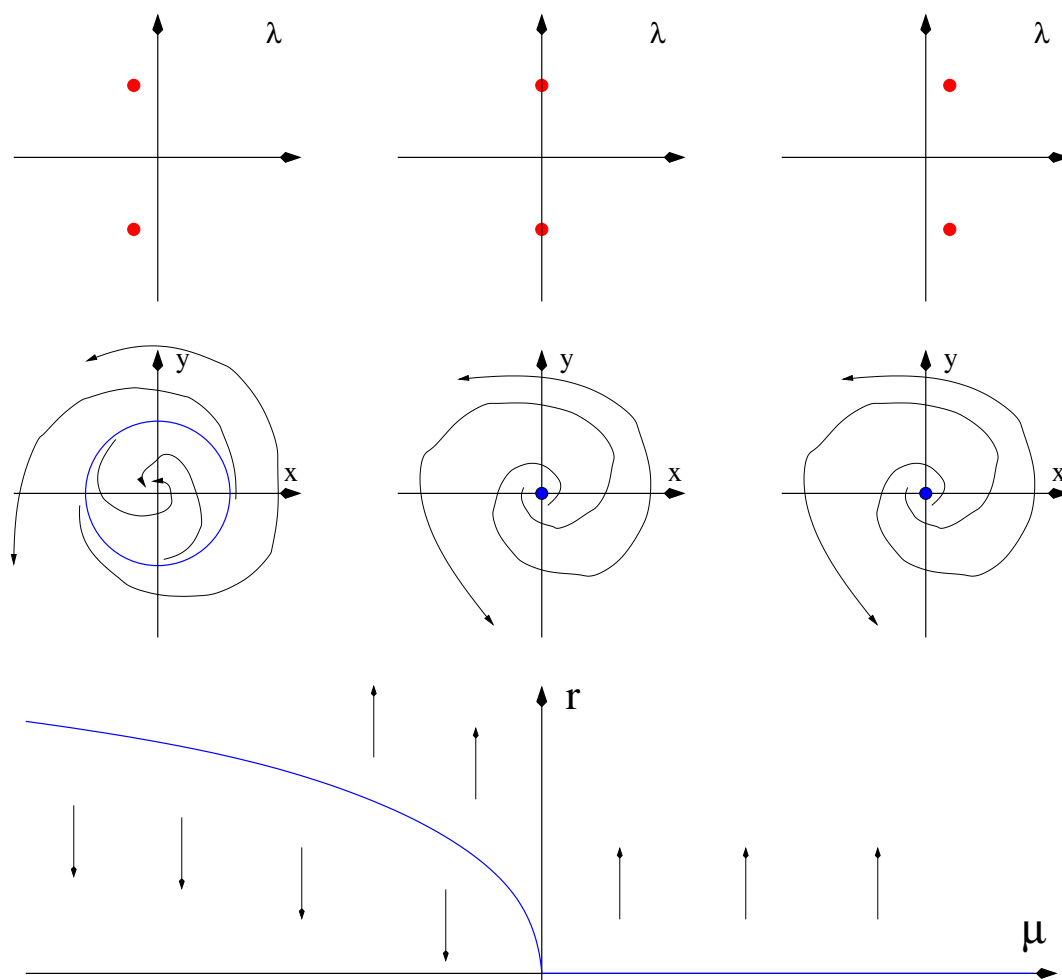
which is nonconstant near  $\mu = 0$ . Thus we have a periodic orbit if  $d\mu/a < 0$ . Next, we investigate the stability of this periodic orbit using a Poincaré map technique, which really just means we're using the equation for  $r'$  as a function of  $r$ .

There are four different cases to consider.

**Case 1.**  $d > 0, a > 0$  In this case, the periodic orbit exists for  $\mu < 0$ . Various things are illustrated in Figure 12.7. The first row shows the  $\lambda$  eigenvalue plane, and the location of the eigenvalues in it. The second row displays the  $(x, y)$  phase plane, while the last row summarizes. We see that in this case, an unstable periodic orbit for  $\mu < 0$  shrinks to a point at  $\mu = 0$ . For  $\mu > 0$  an unstable spiral point exists.

**Case 2.**  $d > 0, a < 0$  In this case, the periodic orbit exists for  $\mu > 0$ . Various things are illustrated in Figure 12.8, using the same layout as before. We see that in this case, a stable periodic orbit is born out of a stable spiral point as  $\mu$  passes through the bifurcation value.

**Case 3.**  $d < 0, a > 0$  In this case, the periodic orbit exists for  $\mu > 0$ , as illustrated in Figure 12.9. We see that in this case, an unstable periodic orbit is born out of an unstable spiral point as  $\mu$  passes through the bifurcation value.

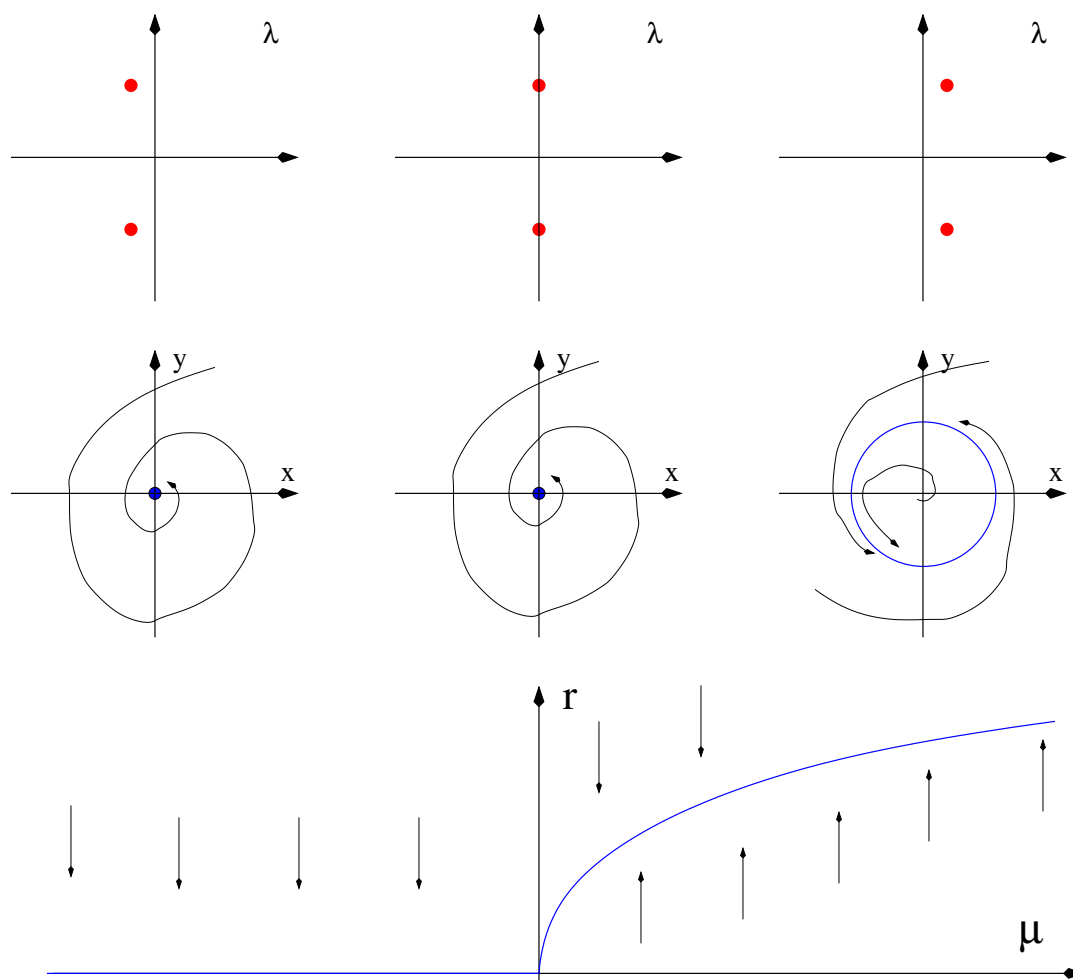
Figure 12.7: The Hopf bifurcation with  $a > 0$ ,  $d > 0$ .

**Case 4.**  $d < 0$ ,  $a < 0$  In this case, the periodic orbit exists for  $\mu < 0$ , as illustrated in Figure 12.10. We see that in this case, a stable periodic orbit degenerates to a stable spiral point as  $\mu$  passes through the bifurcation value.

For all cases, the stability of the periodic orbit is determined by  $a$ : if  $a < 0$  then the orbit is stable. Otherwise it is unstable. Next, we prove that the higher-order terms have no effect on the Hopf bifurcation.

**Theorem 29** *For  $\mu$  sufficiently small, one of the four cases described above holds.*

**Proof.** First, consider the truncated form

Figure 12.8: The Hopf bifurcation with  $a < 0$ ,  $d > 0$ .

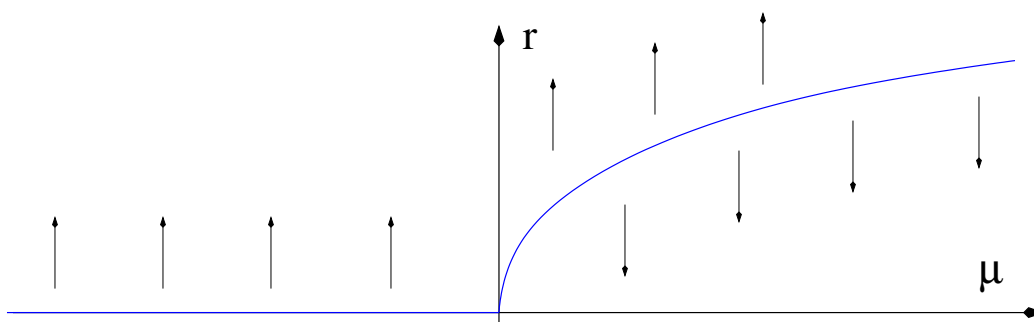
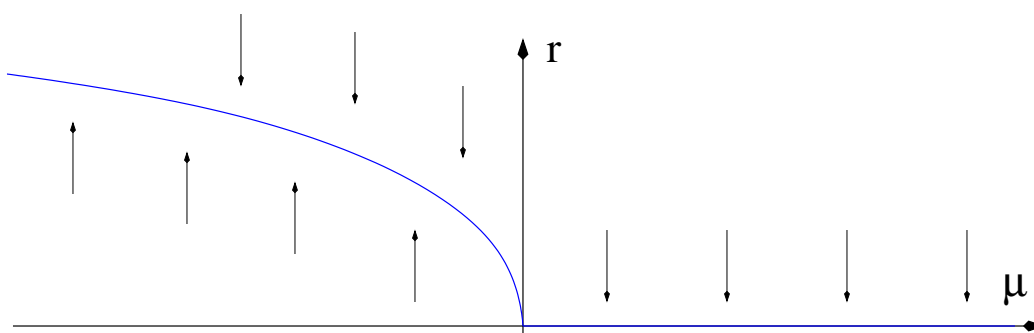
$$\begin{cases} r' = d\mu r + ar^3 \\ \theta' = \omega + c\mu + br^2 \end{cases}, \quad (12.103)$$

with the  $a < 0$ ,  $d > 0$  case. Then the periodic orbit exists for  $\mu > 0$  and is stable there.

For  $\mu$  sufficiently small and positive, consider the annulus

$$A = \{(r, \theta) | r_1 \leq r \leq r_2\}, \quad (12.104)$$

with  $0 < r_1 \leq \sqrt{-d\mu/a} < r_2$ . We see that  $A$  is positively invariant. Since it contains no fixed points, it must contain a periodic orbit, by Poincaré-Bendixson. We already knew this. The nice part is that we can use this argument also for the case where the higher-order terms are included. By letting  $\mu$  and  $r$  be sufficiently small,  $A$  (now a smaller region) is still positively invariant, thus a periodic orbit still exists in it, by Poincaré-Bendixson.

Figure 12.9: The Hopf bifurcation with  $a > 0$ ,  $d < 0$ .Figure 12.10: The Hopf bifurcation with  $a < 0$ ,  $d > 0$ .

The other cases proceed in a similar fashion. ■

**Remark.** For specific systems, we need to figure out what  $a$  and  $d$  are. Here  $d = \alpha'(0)$  is relatively easy. But determining  $a$  is much more involved.



# Chapter 13

## Bifurcations in maps

In this chapter we provide a brief introduction to some of the most important bifurcation phenomena that occur in discrete-time systems.

### 13.1 The period-doubling bifurcation

We'll study this important bifurcation by way of an example, making generalizing statements as we proceed.

Consider the discrete equation

$$x_{n+1} = f(x_n) = -x - \mu x + x^3, \quad (13.1)$$

where  $x \in \mathbb{R}$  and  $\mu \in \mathbb{R}$ . Note that there exists a nonhyperbolic fixed point at  $(x, \mu) = (0, 0)$ :

$$f(0, 0) = 0, \quad \frac{\partial f}{\partial x}(0, 0) = -1 - \mu + 3x^2|_{(0,0)} = -1. \quad (13.2)$$

All fixed points are determined by the equation

$$\begin{aligned} & -x - \mu x + x^3 = x \\ \Rightarrow & -2x - \mu x + x^3 = 0 \\ \Rightarrow & x = 0 \quad \text{or} \quad -2 - \mu + x^2 = 0 \\ \Rightarrow & x = 0 \quad \text{or} \quad x^2 = 2 + \mu. \end{aligned} \quad (13.3)$$

The second (nontrivial) branch of fixed points exists for  $\mu > -2$ , but does not pass through the bifurcation point. A plot of the fixed point branches is shown in Figure 13.1. The question is: what's going on at the bifurcation point  $(0, 0)$  (if anything) and what is happening at  $\mu = -2$  that causes the birth of two new fixed points?

Let's examine the stability of these different fixed points. We have

$$\frac{\partial f}{\partial x} = -1 - \mu + 3x^2. \quad (13.4)$$

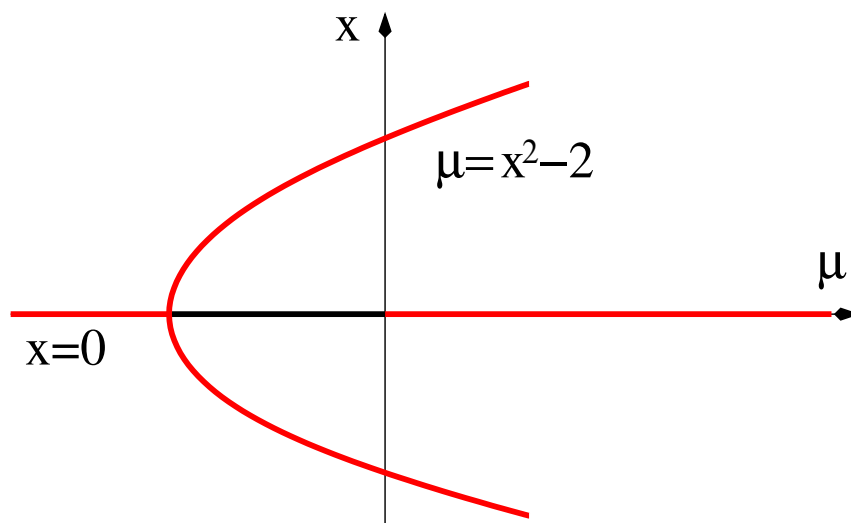


Figure 13.1: The different fixed-point branches of the map  $x_{n+1} = f(x_n) = -x - \mu x + x^3$ . The red branches are unstable.

- **The trivial fixed points**  $x = 0$ : Then  $f_x = -1 - \mu$ , and the fixed point  $x = 0$  is stable if  $|-1 - \mu| < 1$ :

$$\begin{aligned} \Rightarrow & \quad -1 - \mu < 1 \quad \text{and} \quad -1 - \mu > -1 \\ \Rightarrow & \quad \mu > -2 \quad \text{and} \quad \mu < 0. \end{aligned} \tag{13.5}$$

Thus  $x = 0$  if  $\mu \in (-2, 0)$ . The fixed point is nonhyperbolic at the endpoints of this interval.

- **The nontrivial fixed points**  $x^2 = 2 + \mu$ : Then

$$\frac{\partial f}{\partial x} = -1 - \mu + 3(\mu + 2) = 2\mu + 5. \tag{13.6}$$

Since for these fixed points to exist we need  $\mu > -2$ , it follows that they are unstable whenever they exist.

The main question remains: for  $-2 < \mu < 0$  we have a stable fixed point: nearby trajectories are drawn to it. It is spellbinding. What happens to the system when  $\mu$  passes through the origin? Is there anything else that trajectories get drawn to now that the trivial fixed lost its stability? We just learned it's not the nontrivial fixed point. Is there anything else? Oh despair of apocalyptic proportions!

Consider the second iterate of  $f(x)$ :

$$\begin{aligned}
f^2(x, \mu) &= -(-x - \mu x + x^3) - \mu(-x - \mu x + x^3) + (-x - \mu x + x^3)^3 \\
&= (-x - \mu x + x^3) (-1 - \mu + (-x - \mu x + x^3)^2) \\
&= (-x - \mu x + x^3) (-1 - \mu + x^2 + \mu^2 x^2 + 2\mu x^2 + x^6 - 2x^4 - 2\mu x^4). \quad (13.7)
\end{aligned}$$

As before,  $(0, 0)$  is a nonhyperbolic fixed point (check this):

$$f^2(0, 0) = 0, \quad \frac{\partial f^2}{\partial x}(0, 0) = 0. \quad (13.8)$$

Approximately, we have

$$f^2(x, \mu) = x + 2\mu x + \mu^2 x - 2x^3 + \mathcal{O}(4), \quad (13.9)$$

where  $\mathcal{O}(4)$  denotes terms that are of fourth degree in any combination of  $\mu$  and  $x$ . The approximate fixed points are given by

$$\begin{aligned}
& \text{and} & x = 0 & \text{(of course),} & (13.10) \\
& & 0 = 2\mu + \mu^2 - 2x^2 + \dots \\
& \Rightarrow & 2x^2 = 2\mu + \mu^2 + \dots \\
& \Rightarrow & x^2 = \mu + \frac{1}{2}\mu^2 + \dots \\
& \Rightarrow & x^2 \approx \mu + \dots & (13.11)
\end{aligned}$$

The stability of this period-two orbit is determined by

$$\begin{aligned}
\lambda &= f'(\sqrt{\mu})f'(-\sqrt{\mu}) \\
&= (-1 - \mu + 3\mu)(-1 - \mu + 3\mu) \\
&= (-1 + 2\mu)^2. \quad (13.12)
\end{aligned}$$

Stability requires  $|\lambda| < 1$ , which implies

$$|-1 + 2\mu| < 1 \quad \Rightarrow \quad -1 < -1 + 2\mu < 1 \quad \Rightarrow \quad 0 < \mu < 1. \quad (13.13)$$

This leads to the bifurcation diagram of Figure 13.2.

We see that at  $\mu = 0$  the stable fixed point gives way to a stable periodic orbit of period 2. This is called a **period-doubling bifurcation**. In general for maps, as here, an eigenvalue  $\lambda = -1$  is a sign of a period-doubling bifurcation.

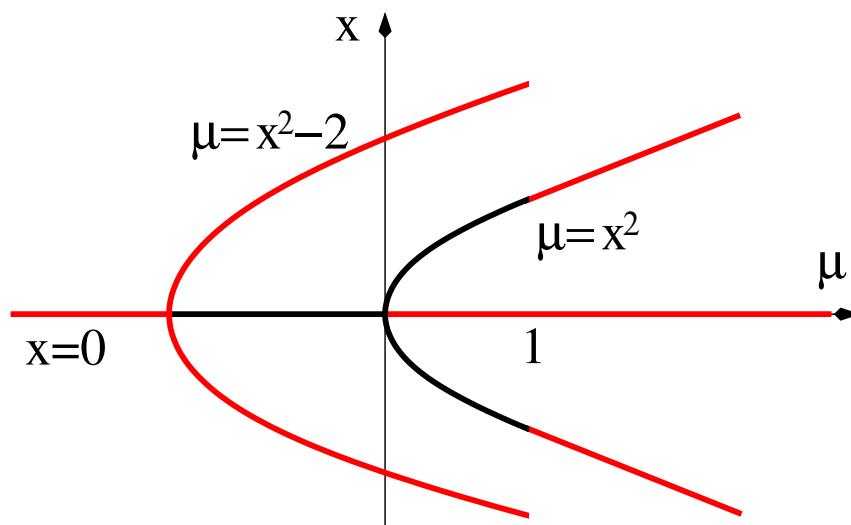


Figure 13.2: The different fixed-point branches of the map  $x_{n+1} = f(x_n) = -x - \mu x + x^3$ . Also indicated is the location of the points of the period two orbit. The red branches are unstable.

## 13.2 The logistic map

For the sake of argument, we continue working with a single example. We'll switch over to the celebrated logistic map:

$$x_{n+1} = \mu x_n(1 - x_n) = f(x_n). \quad (13.14)$$

We wish to examine how the dynamics of this map changes as the bifurcation parameter  $\mu$  increases, starting from  $\mu = 0$ .

### 1. Fixed points

The fixed points are given by

$$x = 0 \quad \text{and} \quad x = 1 - \frac{1}{\mu} = \frac{\mu - 1}{\mu}. \quad (13.15)$$

The stability of these fixed points is determined by

$$f'(x) = \mu(1 - 2x), \quad (13.16)$$

which gives the following results.

- $x = 0$ : here  $f'(0) = \mu$ . Thus  $x = 0$  is stable if  $\mu < 1$  and unstable for  $\mu > 1$ . At  $\mu = 1$ ,  $f'(0) = 1$  and the fixed point is nonhyperbolic. Presumably  $(x, \mu) = (0, 1)$  is a bifurcation point.

- $x = (\mu - 1)/\mu$ : here  $f'((\mu - 1)/\mu) = 2 - \mu$ . Thus  $x = (\mu - 1)/\mu$  is stable if  $\mu \in (1, 3)$  and unstable for  $\mu < 1$  or  $\mu > 3$ . Thus we confirm that  $(x, \mu) = (0, 1)$  is a bifurcation point. In addition it appears that  $(x, \mu) = (2/3, 3)$  is a bifurcation point too.

The bifurcation diagram reflecting our current knowledge is shown in Figure 13.3. As announced there is a (transcritical) bifurcation at  $(x, \mu) = (0, 1)$  where the fixed points switch stability properties. Note that for the nontrivial fixed point  $f'(2/3) = -1$ , which leads us to believe<sup>1</sup> that there might be a period-doubling bifurcation at  $(x, \mu) = (2/3, 3)$ . We'll confirm this in what follows.

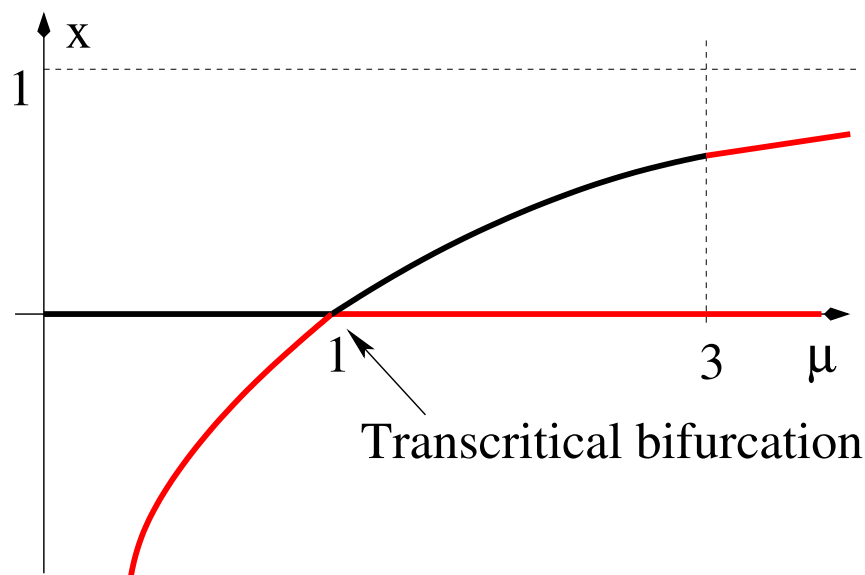


Figure 13.3: The bifurcation diagram for the logistic map, reflecting the dynamics near the fixed points. The red branches are unstable.

We can understand this bifurcation diagram by looking at the map directly. For  $0 < \mu < 1$  the situation is depicted in Figure 13.4. Here the parabola defining the map and the bisectrix intersect only at the origin. The derivative at this fixed point is positive and less than one: the familiar cobweb diagram converges monotone to the fixed point, from both directions.

As  $\mu$  increases, the tangent at the origin becomes steeper, exceeding slope 1 for  $\mu > 1$ . At this value the origin loses its stability, as the cobweb diagram diverges from the fixed point from both sides. On the upper side, it now converges to  $x = (\mu - 1)/\mu$ , the newly born fixed point. For  $\mu < 2$  the fixed point is on the left of the maximum of the parabola, and the slope of the tangent is positive. As a consequence, the cobweb diagram converges to the fixed point in a monotone way. This set-up is shown in Figure 13.5

For  $2 < \mu < 3$ , the fixed point is on the right of the maximum of the parabola, and the slope of the tangent is negative. Its slope is less than 1, in absolute value. Thus the

<sup>1</sup>We're gullible.

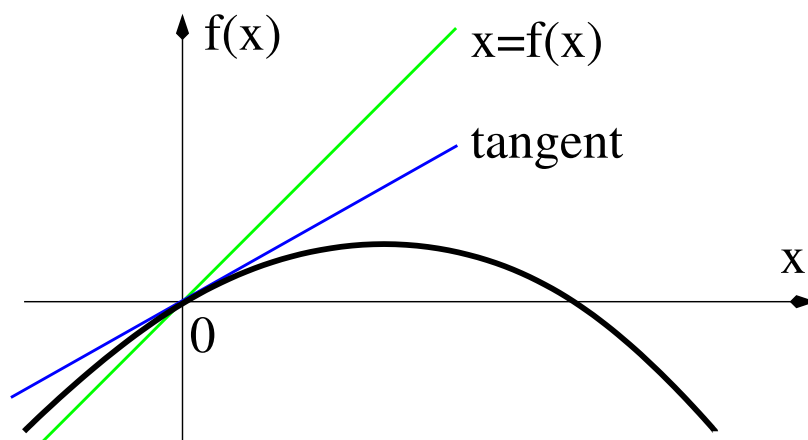


Figure 13.4: The logistic map  $f(x) = \mu x(1 - x)$  and the first bisectrix for  $0 < \mu < 1$ .

fixed point is still stable, but due to the negative slope the cobweb diagram now displays oscillatory convergence to the fixed point. This situation is depicted in Figure 13.6. As  $\mu$  approaches  $\mu = 3$ , the tangent line approaches slope  $-1$ , and the convergence becomes slower, failing at  $\mu = 2$ .

## 2. Period-two orbits

At  $\mu = 3$  a period-two orbit is born, as we'll see now. Such an orbit is a fixed point of the map  $f^2(x)$ . With  $f(x) = \mu x(1 - x)$ , we have

$$\begin{aligned}
 f^2(x) &= \mu^2 x(1 - x)(1 - \mu x(1 - x)) \\
 &= x(\mu^2 - \mu^2 x)(1 - \mu x + \mu x^2) \\
 &= \mu x(-\mu x^3 + 2\mu x^2 - (1 + \mu)x + 1).
 \end{aligned} \tag{13.17}$$

This is a quartic equation, but we do know two of its roots: the fixed points of  $f(x)$  must be solutions, since they are (trivial) period two orbits. Indeed, factoring out  $x$  and  $x - 1 + 1/\mu$ , we get (check this!)

$$\mu^2 x^2 - \mu^2 x - \mu x + \mu + 1 = 0, \tag{13.18}$$

resulting in

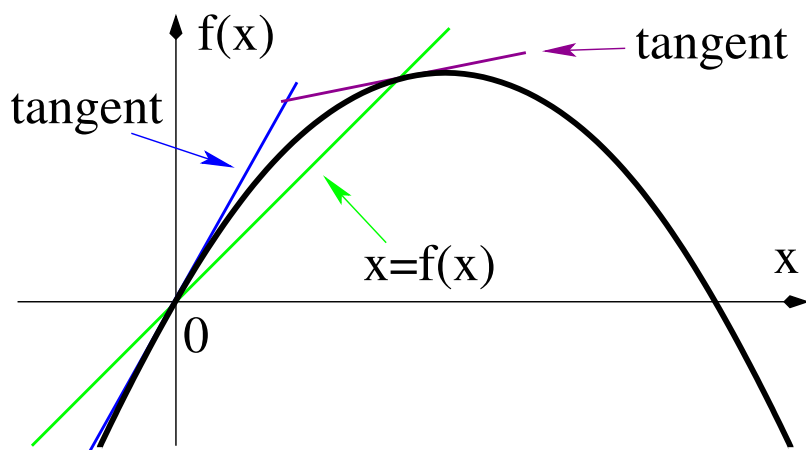


Figure 13.5: The logistic map  $f(x) = \mu x(1 - x)$  and the first bisectrix for  $1 < \mu < 2$ .

$$\begin{aligned}
 x &= \frac{\mu + \mu^2 \pm \sqrt{(\mu + \mu^2)^2 - 4\mu^2(1 + \mu)}}{2\mu^2} \\
 &= \frac{1 + \mu \pm \sqrt{\mu^2 - 2\mu - 3}}{2\mu} \\
 &= \frac{1 + \mu \pm \sqrt{(\mu + 1)(\mu - 3)}}{2\mu} = p, q,
 \end{aligned} \tag{13.19}$$

where the last equation defined  $p$  and  $q$ , corresponding to the  $+$  and  $-$ , respectively. The values  $p$  and  $q$  give rise to one period-two orbit:

$$f(p) = q, \quad f(q) = p. \tag{13.20}$$

From the product in the square root, it is clear that this period-two orbit is born at  $\mu = 3$ , *i.e.*, right when the nontrivial fixed point loses its stability. Indeed, at  $\mu = 3$  we have

$$p, q = \frac{4 \pm 0}{6} = \frac{2}{3}, \tag{13.21}$$

which is the value of the nontrivial fixed point at  $\mu = 3$ . The stability of the period-two orbit is governed by

$$\begin{aligned}
 \lambda &= f'(p)f'(q) \\
 &= \mu^2(1 - 2p)(1 - 2q) \\
 &= \mu^2(1 - 2(p + q) + 4pq).
 \end{aligned} \tag{13.22}$$

We know that  $p + q = 1 + 1/\mu$  and  $pq = (\mu + 1)/\mu^2$ . Thus

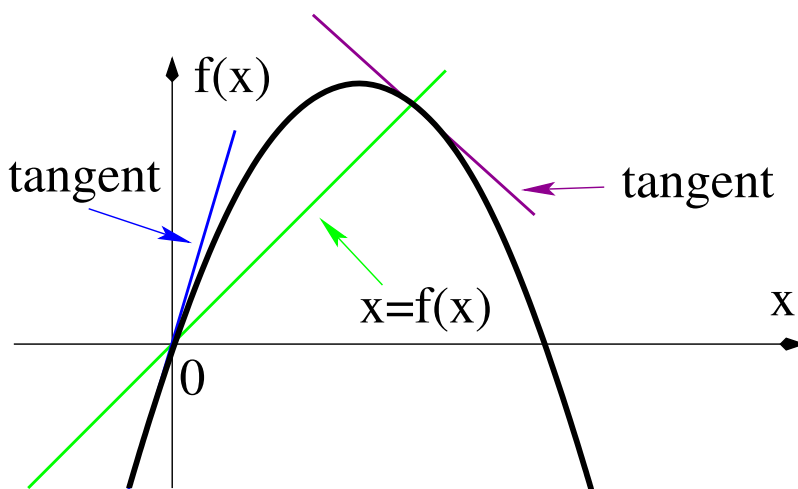


Figure 13.6: The logistic map  $f(x) = \mu x(1 - x)$  and the first bisectrix for  $2 < \mu < 3$ .

$$\begin{aligned}
 \lambda &= \mu^2 \left( 1 - 2\frac{1+\mu}{\mu} + 4\frac{1+\mu}{\mu^2} \right) \\
 &= \mu^2 - 2\mu(1+\mu) + 4(1+\mu) \\
 &= \mu^2 - 2\mu^2 - 2\mu + 4\mu + 4 \\
 &= -\mu^2 + 2\mu + 4 \\
 &= -(\mu - 1 + \sqrt{5})(\mu - 1 - \sqrt{5}). \tag{13.23}
 \end{aligned}$$

At  $\mu = 3$ ,  $\lambda = 1$ . Further,  $\lambda$  decreases for increasing  $\mu > 3$ . Thus the question is: “for what value of  $\lambda > 1 + \sqrt{5} \approx 3.2$  do we have  $\lambda = -1$ ”? This is easily answered: we need

$$\begin{aligned}
 &-\mu^2 + 2\mu + 4 = -1 \\
 \Rightarrow &-\mu^2 + 2\mu + 5 = 0 \\
 \Rightarrow &\mu = 1 \pm \sqrt{6}. \tag{13.24}
 \end{aligned}$$

Clearly, we need to use the + sign, resulting in  $\lambda = -1$  when  $\mu = 1 + \sqrt{6} \approx 3.45$ . Thus, the period two orbit loses stability and undergoes its own period-doubling bifurcation at  $\mu = 1 + \sqrt{6}$ . The summary of our bifurcation diagram thus far is shown in Figure 13.7.

### 3. Beyond period-two orbits: superstable orbits

The period-doubling sequence continues, giving rise to a sequence of period doublings<sup>2</sup>:

<sup>2</sup>A shakespearean sentence, to say the least!

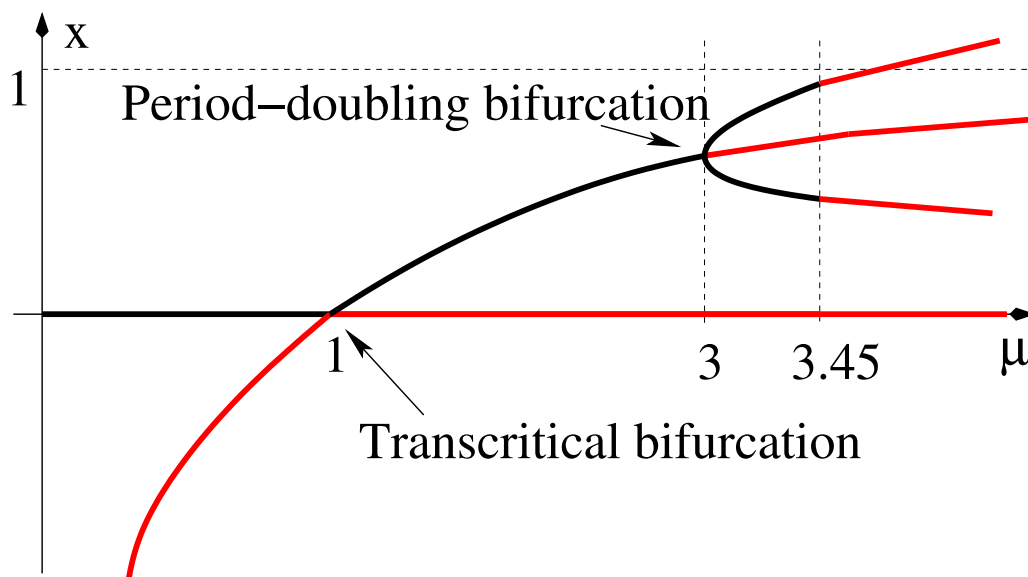


Figure 13.7: The bifurcation diagram for the logistic map  $f(x) = \mu x(1 - x)$  displaying the fixed points and the period two orbit. Red segments denote unstable fixed points/orbits.

$$1 \rightarrow 2 \rightarrow 4 \rightarrow 8 \rightarrow \dots \quad (13.25)$$

One finds that the stability intervals for successive orbits are increasingly smaller. A cartoon of the resulting bifurcation diagram is shown in Figure 13.8.

Let's try to characterize this. We call an orbit **superstable** if  $\lambda = 0$ . For this to happen, the graph of the map of which the orbit is a fixed point should have a horizontal tangent at the fixed point. For our period orbits of successively larger periods, this amounts to investigating for which values of  $\mu$  the first bisectrix intersects the graph of  $f^{2^n}$  at the fixed point which is simultaneously a local extremum of  $f^{2^n}$ . The following table is obtained.

period	$\mu_{\text{superstable}}$
1	2
2	$1 + \sqrt{5} \approx 3.2$
4	$\vdots$
$\vdots$	$\vdots$
4096	3.5699456
$\vdots$	$\vdots$
$2^\infty$	3.569956

It appears that the numbers in this table are converging geometrically. Indeed: if this is the case then there are  $c$  and  $\mu_\infty$  such that asymptotically

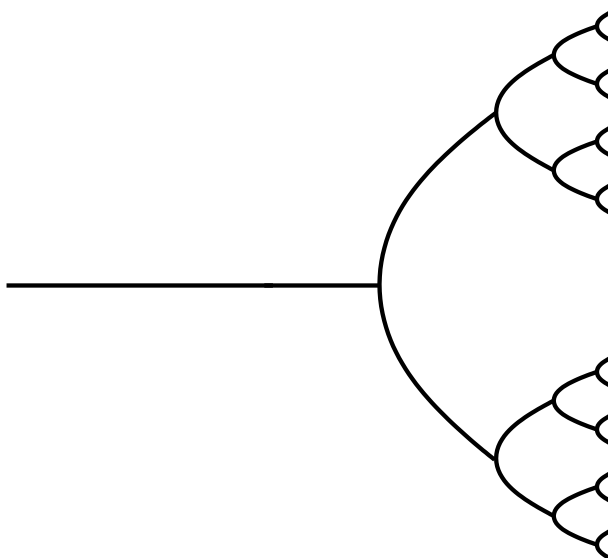


Figure 13.8: A cartoon for the bifurcation diagram for the logistic map  $f(x) = \mu x(1 - x)$  displaying the fixed points and several period  $2^n$  orbits. Only stable orbits are shown.

$$\begin{aligned}
 & \mu_n = \mu_\infty + c\delta^{-n} \\
 \Rightarrow & \mu_{n+1} = \mu_\infty + c\delta^{-n-1} \\
 \Rightarrow & \frac{\mu_{n+1} - \mu_n}{\mu_n - \mu_{n-1}} = \frac{c\delta^{-n-1} - c\delta^{-n}}{c\delta^{-n} - c\delta^{-n+1}} \\
 & = \frac{1}{\delta} \frac{\delta^{-n} - \delta^{-n+1}}{\delta^{-n} - \delta^{-n+1}} \\
 & = \frac{1}{\delta}.
 \end{aligned} \tag{13.26}$$

This gives the geometrical convergence rate. Using the results in the table (including some extra lines you figure out), you<sup>3</sup> find

$$\delta = 4.669201660910\dots \tag{13.27}$$

This is known as the **Feigenbaum** constant. Amazingly, it appears to be a universal constant: the same number occurs in the period-doubling sequences of all one-dimensional maps that have such a period-doubling cascade.

Further, Sarkovskii proved that in all such maps, the existence of a period-three orbit for a certain value of the bifurcation parameter  $\mu$  implies the existence of orbit with any other period, for that value of  $\mu$ . Having orbits of arbitrarily large periods is a well-established

---

<sup>3</sup>In the Feigenbaum sense.

hallmark of chaos. Because of this, the periodic-doubling cascade is known as the period-doubling route to chaos. The universality that Feigenbaum found can to some extent be understood in the context of **renormalization** theory, which we now briefly discuss.

### 13.3 Renormalization theory: an introduction

Let's consider our map at the superstable fixed point. For the logistic map, this occurs at  $\mu = 2$ , displayed in Figure 13.9. Next we consider the superstable orbit of period two, which gives rise to two points  $p$  and  $q$ , at which  $f^2(x)$  has a horizontal tangent. This is shown in Figure 13.10.

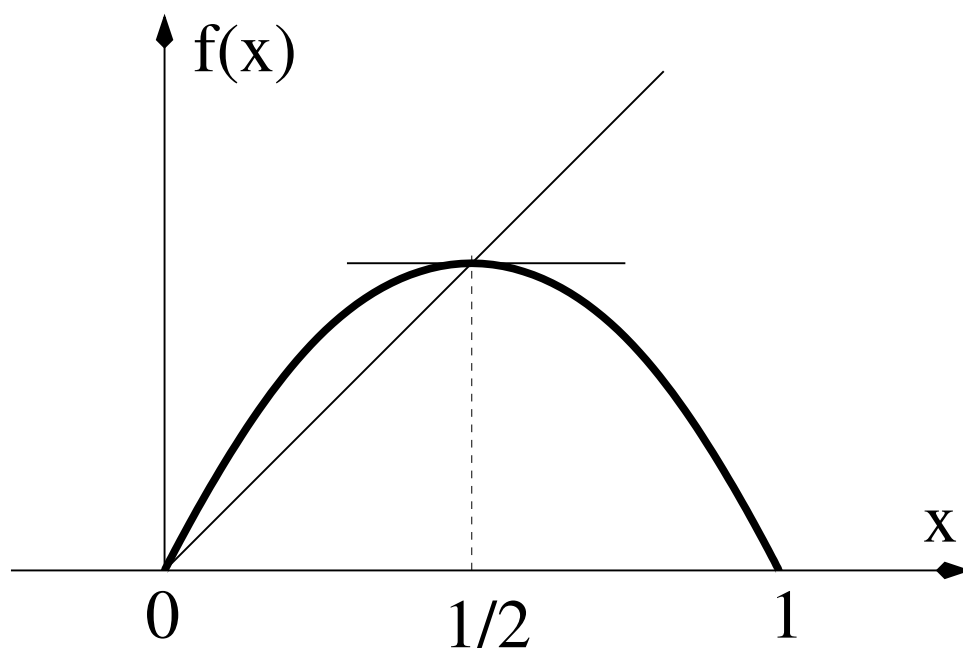


Figure 13.9: The logistic map with  $\mu = 2$ , corresponding to a superstable fixed point.

The main idea is that, up to a scaling<sup>4</sup>, the behavior in the blue box of Figure 13.10 is similar to that of the original Figure 13.9. This motivates the consideration of a **renormalization operator** which maps maps to maps:

$$R[f](x) = \alpha f^2\left(\frac{x}{\alpha}\right), \quad (13.28)$$

where  $\alpha < 0$  is the scaling factor. How do we understand the behavior of such an operator? Do this end we first look at a simpler example.

**Example 22** Consider the operator

<sup>4</sup>With negative scaling factor, to take care of the up-down.

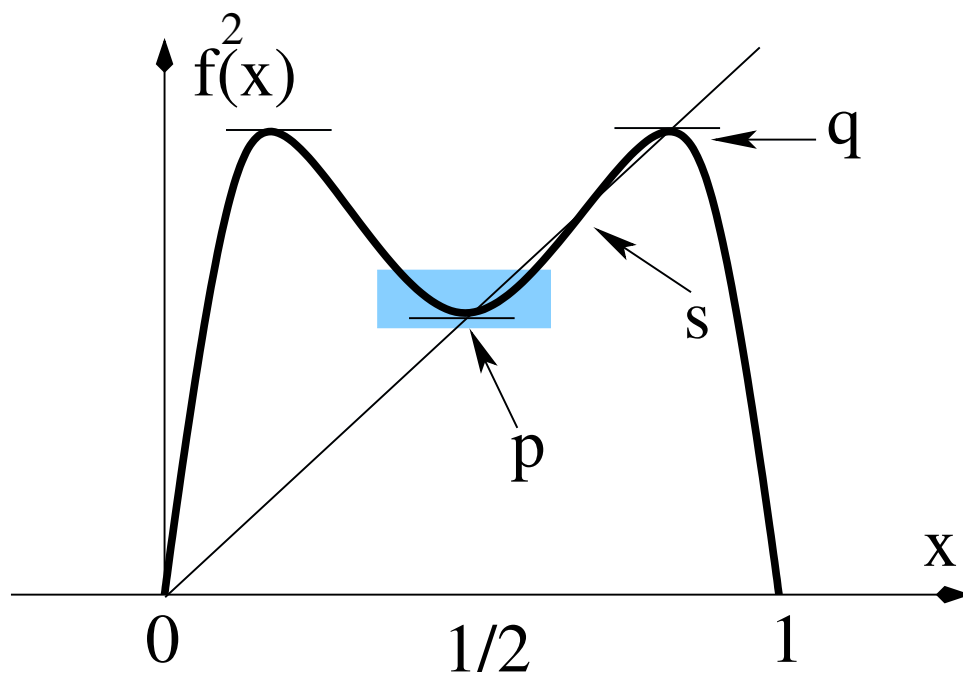


Figure 13.10: The second iterate of the logistic map with  $\mu = 1 + \sqrt{5}$ , for which the period-two orbit is superstable. Here  $s$  corresponds to the fixed point of  $f$ , which is now unstable. The points  $p$  and  $q$  constitute the period-two orbit.

$$S[f](x) = 4f\left(\frac{x}{2}\right). \quad (13.29)$$

Suppose that  $f(x)$  has a Taylor expansion:

$$f(x) = a_0 + a_1x + a_2x^2 + a_3x^3 + \dots \quad (13.30)$$

We may think of  $f(x)$  as an element of an infinite-dimensional space, specified by the infinite-dimensional vector  $(a_0, a_1, a_2, \dots)$ . Then  $S$  becomes an operator on this space. We have

$$\begin{aligned} S[a_0 + a_1x + a_2x^2 + a_3x^3 + \dots] &= 4\left(a_0 + a_1\frac{x}{2} + a_2\frac{x^2}{4} + a_3\frac{x^3}{8} + \dots\right) \\ &= 4a_0 + 2a_1x + a_2x^2 + \frac{a_3}{2}x^3 + \frac{a_4}{2^2}x^4 + \dots \end{aligned} \quad (13.31)$$

It follows that  $S$  has the following action on the vector  $(a_0, a_1, a_2, \dots)$ :

$$S : (a_0, a_1, a_2, \dots) \rightarrow (4a_0, 2a_1, a_2, a_3/2, a_4/2^2, \dots). \quad (13.32)$$

Notice that  $f(x) \equiv 0$  is a fixed point of  $S$ . Examining the stability of  $S$  near this fixed point, we have that

$$\begin{aligned}
 W^U &= \{(a_0, a_1, 0, 0, \dots)\}, \\
 W^S &= \{(0, 0, 0, a_3, a_4, \dots)\}, \\
 W^C &= \{(0, 0, a_2, 0, 0, \dots)\}.
 \end{aligned}
 \tag{13.33}$$

We see that all maps of the form

$$F(x) = a_2 x^2 \tag{13.34}$$

are fixed points of  $S$ . Furthermore, if higher-order terms are added to  $F(x)$  the map converges to  $F(x)$  as the number of iterations of  $S$  increases.

The phase space near the fixed point  $F(x)$  may be conceptualized as shown in Figure 13.11. We see that under the action of  $S$ , all maps approach  $F(x)$  along a codimension 3 stable manifold  $W^S$  at a rate of  $1/2$ , whereas they diverge from  $F(x)$  along a two-dimensional unstable manifold  $W^U$  with rate 2. The fixed point  $F(x)$  itself is not isolated, and there exists a one-dimensional center manifold.

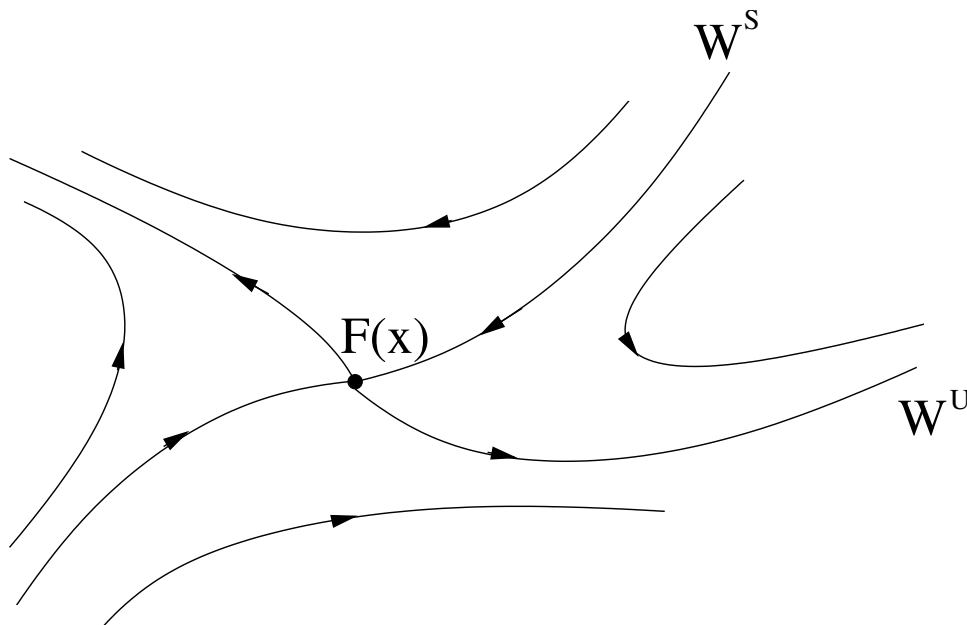


Figure 13.11: A cartoon of the “dynamics” of the operator  $S$  on the function space with (non-isolated) fixed point  $F(x)$ .

It follows that if we start with maps  $f(x)$  which do not have any linear or constant terms, then up to an overall scaling factor (due to the center manifold), the action of  $S$  results in a universal map, independent of the remaining specifics of the original starting map. This universal map is approached at a constant geometric rate.

Let's return to the original problem. We are considering the operator  $R$  defined by

$$R[f](x) = \alpha f^2\left(\frac{x}{\alpha}\right), \quad (13.35)$$

and we anticipate that the action of  $R$  is asymptotically (for large  $n$ ) equivalent with mapping the value  $\mu_n$  corresponding to the superstable orbit of period  $2^n$  to that of  $\mu_{n+1}$ , corresponding to the superstable orbit of period  $2^{n+1}$ . As for the example, let

$$f(x) = a_0 + a_1x + a_2x^2 + \dots \quad (13.36)$$

Then

$$\begin{aligned} R[f](x) &= \alpha f\left(f\left(\frac{x}{\alpha}\right)\right) \\ &= \alpha f\left(a_0 + a_1\frac{x}{\alpha} + a_2\frac{x^2}{\alpha^2} + \dots\right) \\ &= \alpha \left( a_0 + a_1 \left( a_0 + a_1\frac{x}{\alpha} + a_2\frac{x^2}{\alpha^2} + \dots \right) + a_2 \left( a_0 + a_1\frac{x}{\alpha} + a_2\frac{x^2}{\alpha^2} + \dots \right)^2 + \dots \right). \end{aligned} \quad (13.37)$$

Thus we find the following mappings:

$$a_0 \rightarrow \alpha a_0 (1 + a_1 + a_2 a_0 + a_3 a_0^2 + \dots), \quad (13.38)$$

$$a_1 \rightarrow a_1 (a_1 + 2a_0 a_2 + 3a_0 a_3 + \dots), \quad (13.39)$$

$$a_2 \rightarrow \frac{a_2}{\alpha} (a_1 + 2a_2 a_0 + a_1^2 + \dots), \quad (13.40)$$

and so on. Lanford, using a computer-assisted proof, was able to prove the following theorem.

**Theorem 30** *The operator  $R$  has a fixed point, given by*

$$G(x) = 1 + 0x - 1.52763x^2 + 0.104815x^4 + \dots, \quad (13.41)$$

*with corresponding  $\alpha = -2.5029078$ . Here the first two coefficients correspond to a center manifold, and any other choice could have been made.*

The existence of  $G(x)$  as a fixed point of  $R$  implies many properties. For instance, it follows that  $G(x)$  has periodic orbits of all periods of the form  $2^n$ . Indeed: first, note that  $G(x)$  has a positive fixed point, since it is basically a concave down parabola. Let's call this fixed point  $x^*$ :

$$G(x^*) = x^*. \quad (13.42)$$

Expressing that  $G(x)$  is a fixed point of  $R$ , and evaluating the result at  $x^*$ , we have

$$\begin{aligned}
& G(x^*) = \alpha G^2\left(\frac{x^*}{\alpha}\right) \\
\Rightarrow & \quad x^* = \alpha G^2\left(\frac{x^*}{\alpha}\right) \\
\Rightarrow & \quad \frac{x^*}{\alpha} = G^2\left(\frac{x^*}{\alpha}\right), \tag{13.43}
\end{aligned}$$

so that  $x^*/\alpha$  is on a period-two orbit. Iterating with  $R$ , we get

$$\begin{aligned}
& R[G(x)] = R\left[\alpha G^2\left(\frac{x}{\alpha}\right)\right] \\
\Rightarrow & \quad G(x) = \alpha \alpha G^2\left(\frac{1}{\alpha} \alpha G^2\left(\frac{x}{\alpha^2}\right)\right) \\
& \quad = \alpha^2 G^4\left(\frac{x}{\alpha^2}\right) \\
\Rightarrow & \quad x^* = \alpha^2 G^4\left(\frac{x^*}{\alpha^2}\right) \\
\Rightarrow & \quad \frac{x^*}{\alpha^2} = G^4\left(\frac{x^*}{\alpha^2}\right), \tag{13.44}
\end{aligned}$$

and  $x^*/\alpha^2$  is on a period-four orbit. Similarly, by induction, you can establish that  $x^*/\alpha^n$  is on a period  $2^n$  orbit.

Near  $G(x)$ , the dynamics of  $R$  on the phase space is like that of Figure 13.11, but with a one-dimensional unstable manifold  $W^U$  and (as before) a codimension-three stable manifold  $W^S$ . Recall that there exists a two-dimensional center manifold specifying the constant and linear terms of  $G(x)$ . Thus, if we put ourselves on  $W^S$ , the universal fixed point  $G(x)$  is approached at a universal geometric rate, given by the largest eigenvalue inside the unit circle. This rate is

$$1/\delta = 1/4.669201660910\dots \tag{13.45}$$

The unstable direction occurs if we are not careful about where we zoom in: most zooms will diverge from the fixed point. This is easily visualized: if you were to use a mouse to successively zoom, it is necessary to re-center continuously to keep the fixed point as the focus of the operation. Successive zoom without re-centering will quickly lose the fixed point.

This rudimentary normalization picture gives an indication of the universality of period-doubling bifurcations in one-dimensional maps. Similar renormalization approaches may be used (see MacKay and others) to explain the universality that is observed in the break-up of KAM tori, period-doubling in symplectic maps, *etc.*